



ORNL/Sub/86-17498/1

**OAK RIDGE
NATIONAL
LABORATORY**

MARTIN MARIETTA

**Development and Proof-Testing of
Advanced Absorption Refrigeration
Cycle Concepts**

Report on Phases I and IA

Robert J. Modahl
Floyd C. Hayes

MANAGED BY
MARTIN MARIETTA ENERGY SYSTEMS, INC.
FOR THE UNITED STATES
DEPARTMENT OF ENERGY

This report has been reproduced directly from the best available copy.

Available to DOE and DOE contractors from the Office of Scientific and Technical Information, P.O. Box 62, Oak Ridge, TN 37831; prices available from (615) 576-8401, FTS 626-8401.

Available to the public from the National Technical Information Service, U.S. Department of Commerce, 5285 Port Royal Rd., Springfield, VA 22161.

This report was prepared as an account of work sponsored by an agency of the United States Government. Neither the United States Government nor any agency thereof, nor any of their employees, makes any warranty, express or implied, or assumes any legal liability or responsibility for the accuracy, completeness, or usefulness of any information, apparatus, product, or process disclosed, or represents that its use would not infringe privately owned rights. Reference herein to any specific commercial product, process, or service by trade name, trademark, manufacturer, or otherwise, does not necessarily constitute or imply its endorsement, recommendation, or favoring by the United States Government or any agency thereof. The views and opinions of authors expressed herein do not necessarily state or reflect those of the United States Government or any agency thereof.

ORNL/Sub/86-17498/1

**DEVELOPMENT AND PROOF-TESTING OF
ADVANCED ABSORPTION REFRIGERATION CYCLE CONCEPTS**

REPORT ON PHASES I AND IA

**Robert J. Modahl
Floyd C. Hayes**

Published March 1992

Report prepared by

THE TRANE COMPANY
Applied Unitary/Refrigeration Systems Division
Commercial Systems Group
3600 Pammel Creek Road
La Crosse, WI 54601
under Subcontract 86X-17498C

for

OAK RIDGE NATIONAL LABORATORY
P.O. Box 2008
Oak Ridge, Tennessee 37831-6285
managed by
MARTIN MARIETTA ENERGY SYSTEMS, INC.
for the
U.S. DEPARTMENT OF ENERGY
under Contract DE-AC05-84OR21400

CONTENTS

LIST OF FIGURES	v
LIST OF TABLES	vii
ABSTRACT	ix
I. INTRODUCTION AND SUMMARY	1
II. PRELIMINARY SCREENING OF ADVANCED CYCLE CONCEPTS	3
A. Single Effect (with Liquid/Liquid Heat Exchange)	5
B. Double (or Multiple) Effect	5
C. Generator Heat Exchange/Absorber Heat Exchange	6
D. Absorber/Generator Heat Exchange	7
E. Absorber/Generator Heat Exchange Combined with Generator Heat Exchange and Absorber Heat Exchange	8
F. Regenerative Cycles	9
G. Resorption/Desorption Cycles	10
III. FLUIDS	13
IV. COMPUTER MODELING	15
V. CYCLE/FLUID COMBINATIONS	21
A. Combinations ABS1, ABS2, ABS3, and ABS21	21
B. Combinations ABS4, ABS5, ABS12, and ABS15	26
C. Combinations ABS13 and ABS16	28
D. Combinations ABS6A and ABS6B	36
E. Combinations ABS14 and ABS17	36
F. Combinations ABS18, ABS19, and ABS20	41
G. Combinations ABS7A and ABS7B	51
H. Combination ABS8	55
I. Combination ABS9	55
J. Combinations ABS10A and ABS10B	60
K. Combination ABS11	65
VI. SELECTION OF PREFERRED CYCLE/FLUID COMBINATIONS	69
VII. PRELIMINARY SYSTEM DESIGNS AND INSTALLED COST ESTIMATES	75
VIII. USER ECONOMICS	77
IX. CONCLUSIONS	83

LIST OF FIGURES

Fig. 1. Conventional single-effect absorption cycle	3
Fig. 2. Double-effect generator/common-condenser cycle	6
Fig. 3. Generator heat exchange/absorber heat exchange	7
Fig. 4. Absorber/generator heat exchange	8
Fig. 5. Regenerative cycle	9
Fig. 6. Double-effect evaporation employing resorption/desorption cycle	11
Fig. 7. Double-effect generator with resorption/desorption cycle	12
Fig. 8. Flow chart for computer models	19
Fig. 9. (a) Circuit schematic and (b) pressure-temperature-composition chart of generator heat exchange/absorber heat exchange	22
Fig. 10. (a) Circuit schematic and (b) pressure-temperature-composition chart of generator heat exchange/absorber heat exchange and absorber/ generator heat exchange	27
Fig. 11. (a) Circuit schematic and (b) pressure-temperature-composition chart of generator heat exchange/absorber heat exchange, absorber/generator heat exchange, and absorbent recirculation	33
Fig. 12. (a) Circuit schematic and (b) pressure-temperature-composition chart of generator heat exchange/absorber heat exchange, absorber/generator heat exchange, and regeneration (1-stage)	37
Fig. 13. (a) Circuit schematic and (b) pressure-temperature-composition chart of generator heat exchange/absorber heat exchange, absorber/generator heat exchange, and regeneration (2-stage)	39
Fig. 14. (a) Circuit schematic and (b) pressure-temperature-composition chart of generator heat exchange/absorber heat exchange, absorber/generator heat exchange, absorber recirculation, and regeneration	42
Fig. 15. (a) Circuit schematic and (b) pressure-temperature-composition chart of generator heat exchange/absorber heat exchange, absorber/generator heat exchange, and resorption/desorption circuit for evaporator/condenser	45
Fig. 16. (a) Circuit schematic and (b) pressure-temperature-composition chart of generator heat exchange/absorber heat exchange, absorber/generator heat exchange, absorbent recirculation, and resorption/desorption circuit for evaporator/condenser	46
Fig. 17. (a) Circuit schematic and (b) pressure-temperature-composition chart of generator heat exchange/absorber heat exchange, absorber/generator heat exchange, regeneration, absorbent recirculation, and resorption/ desorption circuit for evaporator/condenser	47
Fig. 18. (a) Circuit schematic and (b) pressure-temperature-composition chart of generator heat exchange/absorber heat exchange, absorber/generator heat exchange, and flash regeneration	52
Fig. 19. (a) Circuit schematic and (b) pressure-temperature-composition chart of double-effect generator with cascaded evaporator/absorber	56
Fig. 20. (a) Circuit schematic and (b) pressure-temperature-composition chart of double evaporator with resorption/desorption circuit	58
Fig. 21. Pressure-temperature-composition chart of double-effect generator with resorption/ desorption circuit	60

LIST OF FIGURES (continued)

Fig. 22. Pressure-temperature-composition chart of double-effect generator with regeneration	61
Fig. 23. (a) Circuit schematic and (b) pressure-temperature-composition chart of double-effect generator with generator heat exchange/absorber heat exchange	66
Fig. 24. (a) Simple payback period and (b) internal rate of return obtained from parametric study	80

LIST OF TABLES

Table 1. Types of advanced cycles	4
Table 2. Fluid properties	13
Table 3. Nomenclature for example computer model description	15
Table 4. Computer model output for ABS1 (refer to Fig. 9)	23
Table 5. Computer model output for ABS2 (refer to Fig. 9)	24
Table 6. Computer model output for ABS3 (refer to Fig. 9)	25
Table 7. Computer model output for ABS21 (refer to Fig. 9)	26
Table 8. Computer model output for ABS4 (refer to Fig. 10)	29
Table 9. Computer model output for ABS5 (refer to Fig. 10)	30
Table 10. Computer model output for ABS12 (refer to Fig. 10)	31
Table 11. Computer model output for ABS15 (refer to Fig. 10)	32
Table 12. Computer model output for ABS13 (refer to Fig. 11)	34
Table 13. Computer model output for ABS16 (refer to Fig. 11)	35
Table 14. Computer model output for ABS6B (refer to Fig. 13)	38
Table 15. Computer model output for ABS6A (refer to Fig. 13)	40
Table 16. Computer model output for ABS14 (refer to Fig. 14)	43
Table 17. Computer model output for ABS17 (refer to Fig. 14)	44
Table 18. Computer model output for ABS18 (refer to Fig. 15)	48
Table 19. Computer model output for ABS19 (refer to Fig. 16)	49
Table 20. Computer model output for ABS20 (refer to Fig. 17)	50
Table 21. Computer model output for ABS7A (refer to Fig. 18)	53
Table 22. Computer model output for ABS7B (refer to Fig. 18)	54
Table 23. Computer model output for ABS8 (refer to Fig. 19)	57
Table 24. Computer model output for ABS9 (refer to Fig. 20)	59
Table 25. Computer output for ABS10A (refer to Fig. 21)	62
Table 26. Computer output for ABS10B (refer to Fig. 22)	64
Table 27. Computer output for ABS11 (refer to Fig. 23)	67
Table 28. Cycle/fluid combinations	70
Table 29. Computer model results	71
Table 30. Definition of penalty points	72
Table 31. Ranking of cycle/fluid combinations	73
Table 32. Summary of preliminary system performance and installed cost	76
Table 33. Results of user economics analysis	78
Table 34. Summary of trace runs	81

ABSTRACT

The overall objectives of this project are to evaluate, develop, and proof-test advanced absorption refrigeration cycles that are applicable to residential and commercial heat pumps for space conditioning. The heat pump system is to be direct-fired with natural gas and is to use absorption working fluids whose properties are known. Target coefficients of performance (COPs) are 1.6 at 47°F and 1.2 at 17°F in the heating mode, and 0.7 at 95°F in the cooling mode, including the effect of flue losses.

The project is divided into three phases. Phase I entailed the analytical evaluation of advanced cycles and included the selection of preferred concepts for further development. Phase II involves the development and testing of critical components and of a complete laboratory breadboard version of the selected system. Phase III calls for the development of a prototype unit and is contingent on the successful completion of Phase II. This report covers Phase I work on the project.

In Phase I, 24 advanced absorption cycle/fluid combinations were evaluated, and computer models were developed to predict system performance. COP, theoretical pump power, and internal heat exchange were calculated for each system, and these calculations were used as indicators of operating and installed costs in order to rank the relative promise of each system. The highest ranking systems involve the cycle concepts of absorber/generator heat exchange, generator heat exchange/absorber heat exchange, regeneration, and resorption/desorption, in combination with the $\text{NH}_3/\text{H}_2\text{O}/\text{LiBr}$ ternary absorption fluid mixture or with the $\text{NH}_3/\text{H}_2\text{O}$ binary solution.

The user economic analysis concludes that the gas-fired absorption heat pump can be an attractive alternative in the commercial market, especially in areas which have high heating loads. The economic analysis shows simple payback and internal rate of return to be about the same for a highly complicated advanced cycle using the ternary solution and for a relatively simple advanced cycle using the binary solution when compared to a conventional gas boiler and air-cooled reciprocating compressor chiller. Therefore, the simpler cycle, which involves absorber heat exchange, absorber/generator heat exchange, and generator heat exchange using $\text{NH}_3/\text{H}_2\text{O}$, was chosen for initial breadboard testing in Phase II. Consideration of the $\text{NH}_3/\text{H}_2\text{O}/\text{LiBr}$ ternary and other advanced cycle features, which offer the potential of higher COP at a higher first cost, was postponed until a later date.

Compared to the conventional, electric air-conditioner/gas boiler system used as the reference system in this study, the gas-fired advanced absorption cycle heat pump accomplishes the U.S. Department of Energy's (DOE) goal of conserving energy and provides much more balanced loads for both electric and gas utilities.

Based upon these conclusions, the recommendation was made to proceed to Phase II, the laboratory breadboard proof-of-concept.

I. INTRODUCTION AND SUMMARY

The overall objectives of this project are to evaluate, develop, and proof-test advanced absorption refrigeration cycles that are applicable to residential and commercial heat pumps for space conditioning. The heat pump system is to be direct-fired with natural gas and is to use working fluids whose properties are known. Target COPs are 1.6 at 47°F and 1.2 at 17°F in the heating mode, and 0.7 at 95°F in the cooling mode, including the effect of flue losses.

This report covers the work completed in Phases I and IA of the project. The objectives of this work were to analytically evaluate advanced absorption heat pump concepts and to select a preferred concept for breadboard demonstration in Phase II.

The work steps in Phases I and IA of the project included:

- Select cycle/fluid combinations to be evaluated.
- Develop fluid property subroutines and add to computer data files.
- Develop computer models of selected cycle/fluid combinations.
- Conduct preliminary cycle analyses.
- Select preferred concepts for further analysis.
- Estimate hardware costs.
- Study user economics.
- Select preferred system for Phase II demonstration.

The selection of cycle/fluid combinations for detailed evaluation was based on the results of a literature review and of a simplified "ideal" cycle analysis. The cycle concepts selected for detailed analysis included double-effect cycles, generator heat exchange/absorber heat exchange, absorber/generator heat exchange, regenerative cycles, and resorption/desorption cycles. Fluids were restricted to combinations whose properties were reasonably well known and whose corrosion and stability characteristics were thought to be reasonably good in the region of interest. These included the binary combinations $\text{NH}_3/\text{H}_2\text{O}$, R22/DMETEG, R123a/ETFE, and $\text{LiBr}/\text{H}_2\text{O}$, and the ternary combinations $\text{NH}_3/\text{H}_2\text{O}/\text{LiBr}$, $\text{CH}_3\text{NH}_2/\text{H}_2\text{O}/\text{LiBr}$, and $\text{CH}_3\text{OH}/\text{LiBr}/\text{ZnBr}_2$.

A total of 24 cycle/fluid combinations were evaluated in preliminary computer calculations. These results indicated that project efficiency goals can be attained, especially with ternary fluid systems. Based on these results, five combinations were selected for further analysis, which included preliminary design for a 155-ton application, hardware cost estimates, and user economics studies.

User economics studies were based on an apartment building application. Design capacity was 155 tons cooling. This application was chosen for its relatively high heating/cooling load ratio; it is the type of application in which the absorption heat pump is expected to compare most favorably with conventional equipment. Results of this study showed that the best absorption heat pumps offer a 2.2-year payback and 37% internal rate of return (IRR) compared with a reciprocating chiller/gas

boiler for an installation in Chicago, Illinois. Other conclusions from the user economics study were as follows:

- Annual electricity usage for the absorption systems was about the same as for the reference system, because the pumps running year-round offset the lower electricity usage during the summer.
- Annual electricity costs were slightly lower for the absorption systems because of lower demand charges.
- The savings in gas during the winter more than offset the cost of gas used for air-conditioning during the summer.
- Annual operating cost savings for the absorption system were primarily attributable to lower gas usage.

The cycle selected for breadboard demonstration in Phase II includes generator heat exchange/absorber heat exchange, absorber/generator heat exchange, regeneration, and resorption/desorption. The preferred fluid is the ternary $\text{NH}_3/\text{H}_2\text{O}/\text{LiBr}$.

II. PRELIMINARY SCREENING OF ADVANCED CYCLE CONCEPTS

The advanced cycle concepts considered in this investigation were primarily obtained from an extensive literature survey. The concepts selected for more detailed evaluation were based on a simplified analysis described in this section of the report.

In the preliminary screening of advanced cycle concepts, simplified Duhring plots were used, such as the one shown in Figure 1.

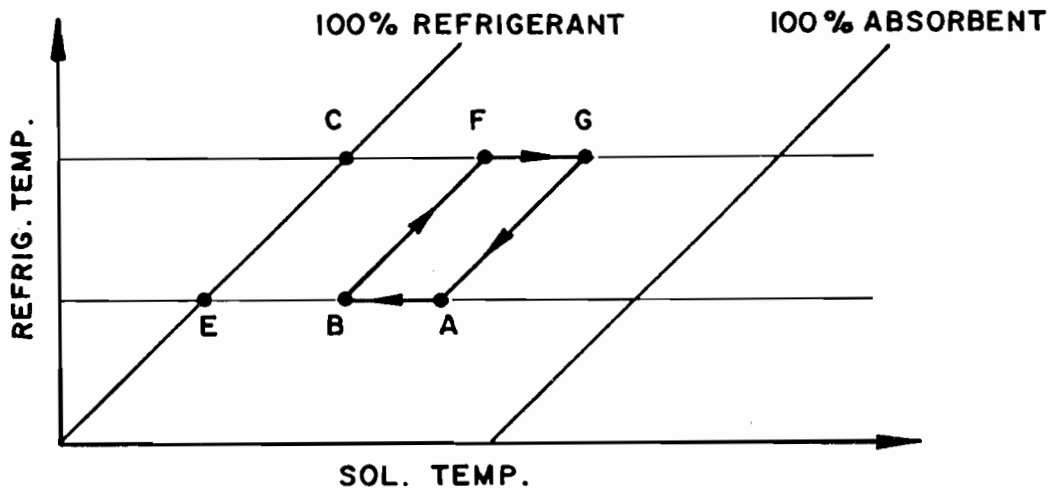


Fig. 1. Conventional single-effect absorption cycle.

Basically, the simplification introduced is that all lines of constant concentration will appear as 45° lines when plotted as refrigerant temperature vs. solution temperature, although real fluids depart from this simplification to varying degrees. In the final evaluation of advanced cycles, real fluid properties were used.

Table 1 summarizes the basic cycle alternatives that were considered, alone or in combination, to achieve the project goals. This table also shows the approximate ideal COPs for the concepts. A discussion of the concepts and of the method of calculating the ideal COPs follows.

Table 1. Types of advanced cycles

		Ideal COP	
		Cooling	Heating
Single effect (with liquid/liquid heat exchange)		1.0	2.0
Double (or multiple) effect	n=2	2.0	3.0
	n=3	3.0	4.0
Generator heat exchange/ absorber heat exchange		$\frac{1}{1-\epsilon}$	$\frac{2-\epsilon}{1-\epsilon}$
	$\epsilon=1/3$	1.5	2.5
Absorber/generator heat exchange		$\frac{1}{1-\delta}$	$\frac{2-\delta}{1-\delta}$
Binary	$\delta=1/4$	1.33	2.33
Ternary	$\delta=1/2$	2.0	3.0
Absorber/generator heat exchange combined with generator heat exchange/absorber heat exchange		$\frac{1}{(1-\delta)(1-\epsilon_1)}$	$1+\frac{1}{(1-\delta)(1-\epsilon_1)}$
Binary	$d=1/4$ $\epsilon_1=1/3$	2.0	3.0
Ternary	$\delta=1/2$ $\epsilon_1=1/3$	3.0	4.0
Regenerative cycles		$(\frac{1}{1-\delta})+(\frac{n-1}{n})$	$1+(\frac{1}{1-\delta})+(\frac{n-1}{n})$
Binary	$\delta=1/4$ n=2	1.83	2.83
	n=3	2.0	3.0
Ternary	$\delta=1/2$ n=2	2.5	3.5
	n=3	2.67	3.67

Table 1. (continued)

			Ideal COP	
			Cooling	Heating
with generator heat exchange			$(\frac{1}{1-\epsilon})(\frac{1}{1-\delta})+(\frac{n-1}{n})$	$1+(\frac{1}{1-\epsilon})(\frac{1}{1-\delta})+(\frac{n-1}{n})$
Absorber heat exchange	Binary	$\delta=1/4, \epsilon_1=1/3, n=2$	2.75	3.75
		$n=3$	3.0	4.0
	Ternary	$\delta=1/2, \epsilon_1=1/3, n=2$	3.75	4.75
		$n=3$	4.0	5.0
Resorption/desorption cycles				
with double evaporation			2.0	3.0
with double effect generator			2-x	3-x
For X=1/2			1.5	2.5

A. SINGLE EFFECT (WITH LIQUID/LIQUID HEAT EXCHANGE)

The conventional single-effect absorption cycle is illustrated in Figure 1. External heat is added in the generator F-G to boil off the refrigerant. The refrigerant is condensed at C and evaporated at E with external heat input. The evaporated refrigerant is absorbed back into the solution in the absorber A-B. Heat input is conserved by transferring heat from the strong solution to the weak solution, so that the only external heat input is at F-G.

Each unit of refrigerant vaporized at F-G provides one unit of cooling at E. Thus, the ideal cooling COP is 1. Similarly, in the heating mode, each unit vaporized at F-G provides one unit of heating at C and one unit at A-B. Thus, the ideal heating COP is 2.

B. DOUBLE (OR MULTIPLE) EFFECT

The most widely known advanced absorption cycles are double-effect cycles. There are several types of double-effect cycles, with the most common being double-effect generator/common condenser, double-effect generator/common absorber, and double evaporation. If the solution properties permit the use of double-effect cycles, ideal cooling COPs twice as large as those of the conventional single-effect cycle can be obtained.

A double-effect generator/common condenser cycle is shown in Figure 2.

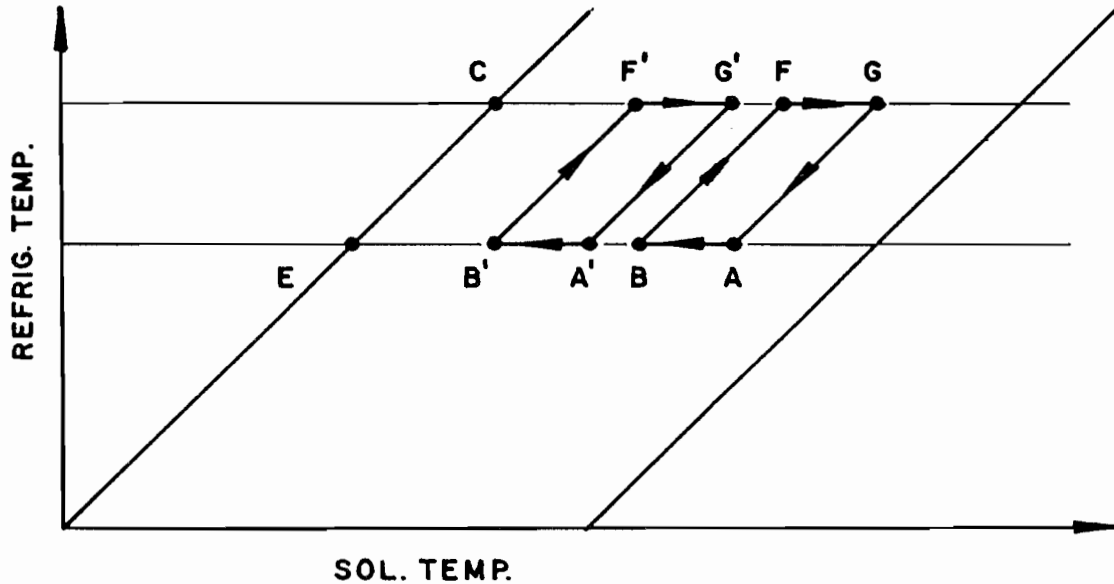


Fig. 2. Double-effect generator/common-condenser cycle.

One unit of refrigerant is produced in the first-stage generator, F-G, as before, using an external source of heat. Another unit of refrigerant then is produced in the second-stage generator, F'-G', using heat from the first-stage absorber. Thus, for one unit of heat input, two units of cooling are produced, resulting in an ideal cooling COP of 2. The corresponding ideal heating COP is 3.

The concept illustrated in Figure 2 can be extended to three or more effects if the solution field is wide enough, in which case the ideal cooling COP equals the number of effects.

C. GENERATOR HEAT EXCHANGE/ABSORBER HEAT EXCHANGE

Efficiency improvements can be made on the conventional single-effect cycle without the complication of double-effect machines. The simplest improvements are generator heat exchange and absorber heat exchange. The effects are illustrated in Figure 3.

Basically, this concept reduces losses associated with temperature differences in the liquid/liquid heat exchanger of the conventional cycle. As shown in Figure 1, a significant temperature difference exists between the strong solution G-A and the weak solution B-F throughout the length of the heat exchanger. Cycle efficiency can be improved by using heat from the highest-temperature strong solution (G-G') to boil off refrigerant in the first part of the generator (F-F'). The maximum fraction, ϵ , of generator heat that can be supplied in this manner is about 1/3 for the NH₃/H₂O binary, which has a high ratio of refrigerant latent heat to solution specific heat. For fluids with a low ratio of refrigerant latent heat to solution specific heat, the ratio may be in the range of 3/5; but these fluids usually are not the best absorption fluids for other reasons. Liquid/liquid heat exchange in this case is between the strong solution (G'-A) and the weak solution (B'-F), but in this ideal case the

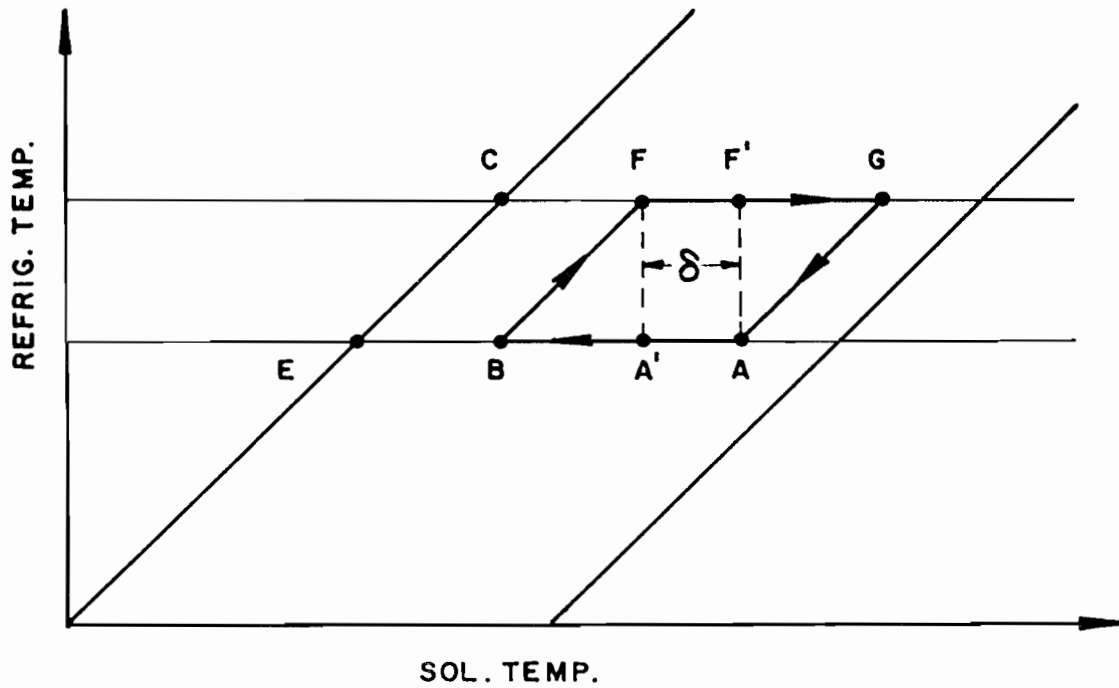


Fig. 4. Absorber/generator heat exchange.

as high as 1/2 for ternary fluids. The simplified relation for the ideal cooling COP is

$$COP_c = \frac{1}{1-\delta} .$$

For binary fluid, $\delta = 1/4$: $COP_c = 1.33$. For ternary fluid, $\delta = 1/2$: $COP_c = 2.0$.

E. ABSORBER/GENERATOR HEAT EXCHANGE COMBINED WITH GENERATOR HEAT EXCHANGE AND ABSORBER HEAT EXCHANGE

Generator heat exchange and absorber heat exchange can be utilized with other single- and double-effect efficiency improvement concepts. An attractive combination is to combine them with absorber/generator heat exchange. The resulting simplified relation for the ideal cooling COP is as follows:

$$COP_c = \frac{1}{(1-\delta)(1-\epsilon)} ,$$

where

$q_{ex} + \delta + \epsilon = 1$,
 q_{ex} = fraction of generator heat supplied externally,

δ = maximum fraction of generator heat supplied by absorber,
 ϵ = maximum fraction of generator heat supplied by strong solution (generator heat exchange),
 $\epsilon_1 = \frac{\epsilon}{q_{ex} + \epsilon}$.

For binary fluid, $\delta = 1/4$, $\epsilon_1 = 1/3$: $COP_c = 2$.

For ternary fluid, $\delta = 1/2$, $\epsilon_1 = 1/3$: $COP_c = 3$.

F. REGENERATIVE CYCLES

Regenerative processes use vapor transfer at one or more intermediate pressures (refrigerant temperatures) to achieve a larger overlap of absorber/generator heat exchange.

Figure 5 shows a possible regenerative cycle with one intermediate pressure compared with the one-step absorber/generator heat exchange cycle FGAB with overlap δ .

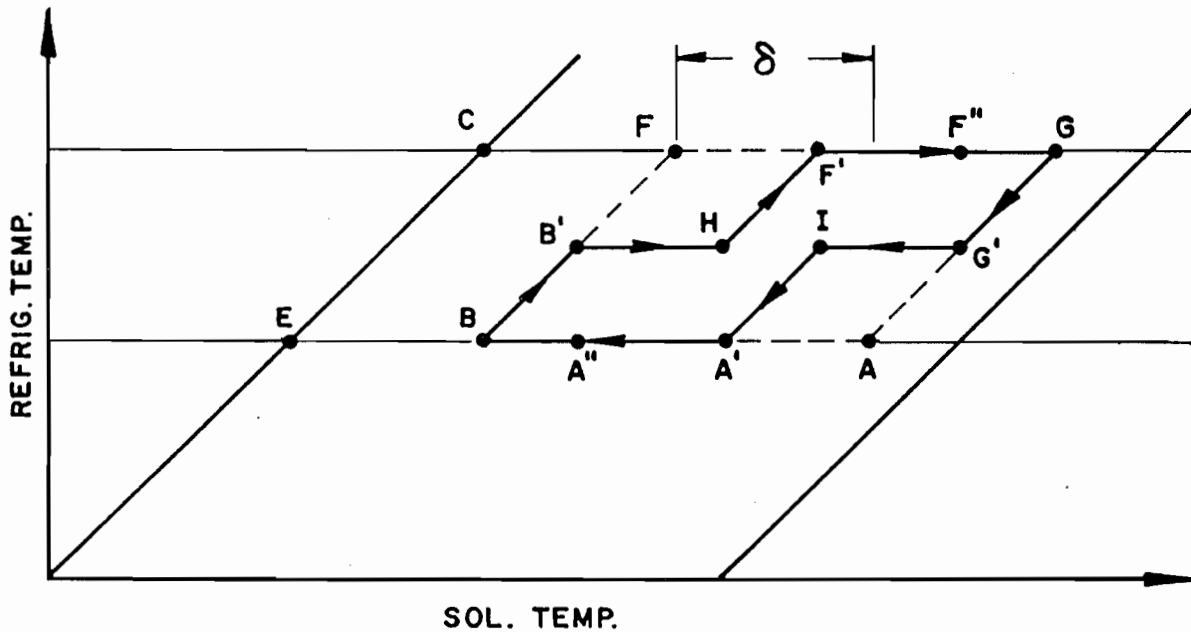


Fig. 5. Regenerative cycle.

In this cycle, vapor is generated at intermediate pressure between B' and H using absorber heat A'-A". The vapor is absorbed at intermediate pressure between G' and I, and the absorber heat is used in the high-pressure generator between F' and F". As Figure 5 shows for the example chosen, the fraction of generator heat supplied by absorber heat exchange has increased from 1/2 for the one-step process to 3/5 for the two-step process. The simplified analysis yields the following expression for the ideal cooling COP:

$$\text{COP}_c = \frac{1}{1-\delta} + \frac{n-1}{n} ,$$

where

n = number of pressure levels at which vapor is generated ($n=1$ for conventional cycle),
 δ = maximum fraction of generator heat supplied by absorber, for $n=1$.

If generator heat exchange and absorber heat exchange are also utilized,

$$\text{COP}_c = \left(\frac{1}{1-\epsilon_1}\right)\left(\frac{1}{1-\delta}\right) + \left(\frac{n-1}{n}\right) .$$

Typical values for binary and ternary fluids are shown in Table 1.

G. RESORPTION/DESORPTION CYCLES

A resorption/desorption cycle is defined as a cycle in which the flow is the opposite of that in the conventional absorber/generator cycle. In the resorption/desorption cycle, refrigerant is desorbed (generated) at the low pressure and resorbed (absorbed) at the high pressure, just the reverse of the conventional absorber/generator cycle.

The resorption/desorption cycle can be used in combination with a conventional absorber/generator cycle in a variety of ways. The combined effects might range from a double-effect machine to a system with reduced operating pressures. Three examples follow that illustrate the benefits of resorption/desorption cycles:

1. Double-Effect Evaporator Cycle

The resorption/desorption cycle allows double-effect evaporation to be achieved. For example, in the double-effect evaporation cycle shown in Figure 6, one unit of refrigerant is generated with external heat in the generator/absorber loop FGAB, producing one unit of cooling at ϵ .

The refrigerant evaporated at ϵ is resorbed at A'-B' of the resorption/desorption loop and desorbed at F'-G', producing a second unit of cooling and thus allowing an ideal cooling COP of 2 to be attained. The refrigerant desorbed at F'-G' is absorbed at A-B. Thus, the resorption/desorption cycle in this case is crucial to allow double-effect evaporation to be achieved at the same temperature.

2. Double-Effect Generator with Resorption/Desorption Cycle

Another application of resorption/desorption cycles lies in achieving intermediate COPs if the solution stability and refrigerant vapor pressure do not allow the benefits of a full double-effect cycle to be attained. This concept is illustrated in the double-effect generator cycle

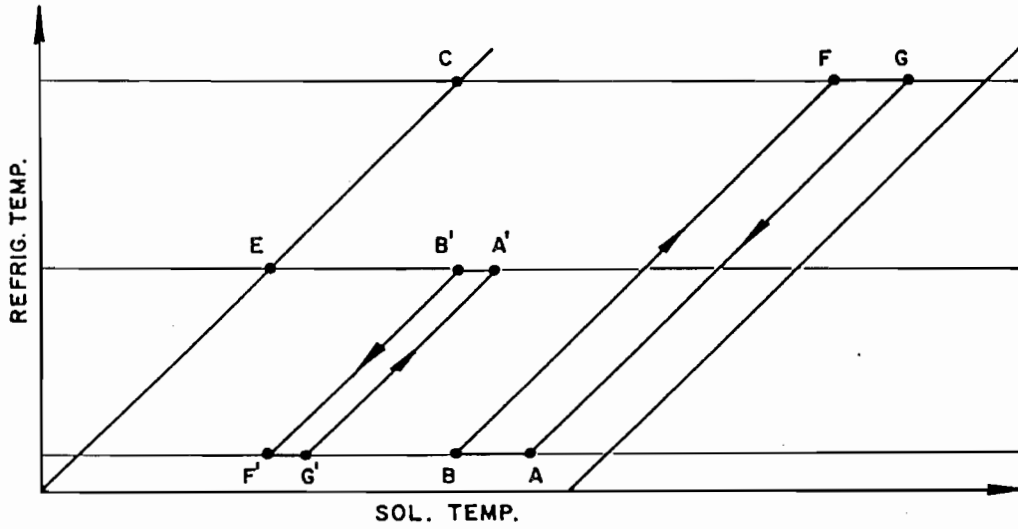


Fig. 6. Double-effect evaporation employing resorption/desorption cycle.

shown in Figure 7.

One unit of refrigerant is boiled off in the first-stage generator F_1 - G_1 using an external source of heat, but a fraction of this refrigerant, x , is resorbed at high pressure in a resorber cycle PQRS, while the rest goes to the first-stage condenser C1.

Another unit of refrigerant is boiled off in the second-stage generator F_2 - G_2 using heat from the first-stage condenser C1 and the resorption process P-Q. This refrigerant is condensed in the second-stage condenser C2. Part of the heat from the second-stage condenser is used to generate vapor at R-S in the low-pressure section of the resorption cycle. This vapor, as well as vapor from the evaporator E, is absorbed at A-B.

The simplified expression for the ideal cooling COP of this cycle is

$$COP_c = 2-x ,$$

where x is the fraction of refrigerant generated in the first-stage generator that is resorbed in the resorption/desorption cycle. Because this refrigerant provides no useful cooling effect, the ideal COP of the cycle is less than 2, even though it is a double-effect cycle.

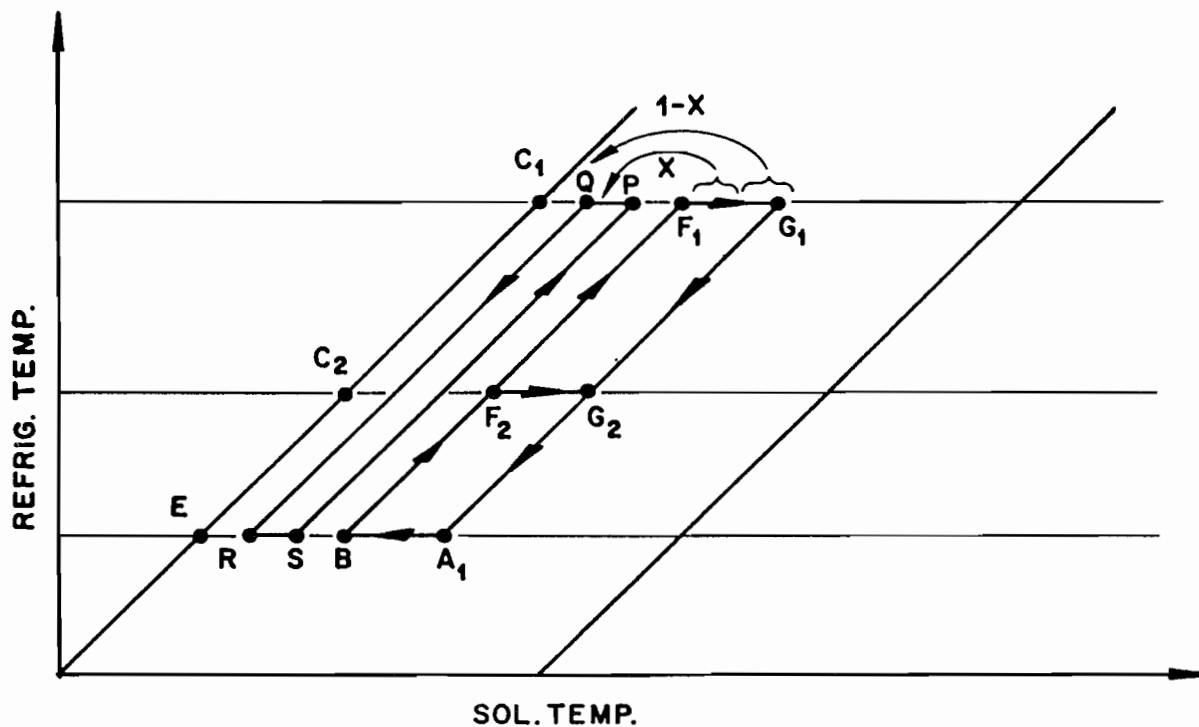


Fig. 7. Double-effect generator with resorption/desorption cycle.

3. Resorption/Desorption Circuit Substituted for Evaporator/Condenser Circuit

A final example of the application of a resorption/desorption circuit entails replacing the conventional condenser/evaporator circuitry of the system. This would not affect an ideal cycle COP, but it would lower the operating pressure of the system and might reduce auxiliary power and system cost.

The primary purpose for discussing these examples is to clarify terminology and to develop a first-order summary of the efficiency potential of the various cycle concepts. Many variations and combinations of these concepts can be formed. Although it was not possible to consider every variation and combination in this investigation, a representative number of them were evaluated using real fluids and representative design conditions.

While one normally first thinks of double- or multiple-effect cycles when considering advanced absorption concepts, Table 1 shows that there are a number of alternatives for achieving high efficiencies. Choosing a cycle must therefore include consideration of other factors, including system cost and complexity, manufacturability, reliability, and auxiliary power requirements.

III. FLUIDS

The fluid mixtures considered in this investigation are listed in Table 2. Initially, the selection of fluids was based on binary mixtures whose properties were reasonably well known and whose stability and corrosion characteristics were thought to be reasonably good in the region of interest. The list of fluids was later expanded to include ternary mixtures when it was determined that binary mixtures showed marginal prospects for achieving project efficiency goals. This expansion, however, introduces more uncertainty into property data and stability/corrosion characteristics and thus will require that more consideration be given to these uncertainties in Phase II of the program.

Table 2. Fluid properties

<u>Mixture</u>	<u>Data Source</u>
NH ₃ /H ₂ O	Macriss, R. H. et al., <i>Physical and Thermodynamic Properties of Ammonia-Water Mixtures</i> , Research Bulletin 34, prepared for the American Gas Association (AGA), Chicago: Institute of Gas Technology (IGT), September 1964.
R22/DMETEG	Macriss, R. A., and D. Mason, <i>Physical and Thermodynamic Properties of New Refrigerant-Absorbent Pairs</i> , Project ZB-85 Final Report, prepared for the Air Conditioning and Prime Mover Research Committee of the AGA, Chicago: IGT, October 1964.
R123a/ETFE	Murphy, K. P. et al., <i>Development of a Residential Gas-Fired Absorption Heat Pump—Physical and Thermodynamic Properties of R123a/ETFE, System Development and Testing and Economic Analysis</i> , ORNL/Sub/79-24610/4, Oak Ridge, Tennessee: Oak Ridge National Laboratory (ORNL), Martin Marietta Energy Systems, Inc., August 1985.
LiBr/H ₂ O	McNeely, L. A., "Thermodynamic Properties of Aqueous Solutions of Lithium Bromide," <i>ASHRAE Trans.</i> 85, 413 (1979).
NH ₃ /H ₂ O/LiBr CH ₃ NH ₂ /H ₂ O/LiBr	Radermacher, R., "Working Substance Combinations For Absorption Heat Pumps," Dissertation, University of Munich, January 1981.
CH ₃ OH/LiBr/ZnBr ₂	Aker, J. E., R. G. Squires, and L. E. Albright, "An Evaluation of Alcohol-Salt Mixtures as Absorption Refrigeration Solutions," <i>ASHRAE Trans.</i> 71 (Pt. 1), 14 (1965).

Curve-fit equations were developed for the fluid properties needed for computer modeling work on each fluid pair. Coefficients for the curve-fit equations were determined by log-mean-square fit of the source data.

IV. COMPUTER MODELING

Steady-state computer models were developed for selected cycle/fluid combinations. Modeling involved writing energy balances, flow balances, concentration balances, and transfer rate equations for the various components of the system. This resulted in the need to simultaneously solve 23 to 54 equations for each cycle in order to determine conditions throughout the system. The sets of nonlinear equations were solved using Newton's method and Gaussian elimination.

In order to demonstrate the development of the modeling equations, an example is given for the ammonia/water cycle that is shown in Figure 10. This figure illustrates a simple absorption cycle incorporating generator heat exchange/absorber heat exchange and absorber/generator heat exchange. Four types of equations—energy balance, flow balance, concentration balance, and transfer rate—may be written for each component.

The following equations and assumptions were developed for the cycle represented by Figure 10. The nomenclature for the variables is given in Table 3.

Table 3. Nomenclature for example computer model description

Variable	Definition
Q_{abs}	Rate of Heat Removal from Absorber
Q_{gen}	Rate of Heat Input into Generator
Q_{rect}	Rate of Heat Removal from Rectifier
Q_{cond}	Rate of Heat Removal from Condenser
Q_{evap}	Rate of Heat Addition at Evaporator
M_N	Mass Flow Rate at Point "N"
X_N	Liquid Refrigerant Concentration at Point "N"
Y_N	Vapor Refrigerant Concentration at Point "N"
T_N	Temperature of Fluid at Point "N"
H_N	Enthalpy of Fluid at Point "N"
EFFABS	Absorber Efficiency
SHTM	Degree of Superheat Entering Condenser
FRACMR	Fractional Minimum Reflux
DYHYO	$Y_H - Y_O$, NH_3 /Mix Specified Entering Rectifier Condition
EFFHXZ	Effectiveness of Refrigerant Vapor/Liquid Heat Exchanger

Mass Transfer Rate: $X_E - X_L = (X_{E_{sat}} - X_K) \cdot \text{EFFAAB}$

Heat Transfer Rate: $T_F = T_L - 2$

Assumption: F = Saturated liquid

ABSORBER EQUATIONS

Energy balance: $Q_{abs} = (M_L \cdot H_L) - (M_F \cdot H_F) + (M_U \cdot H_U)$

Mass balance: $M_E = M_L + M_U$

Concentration balance: $M_E \cdot X_E = M_L \cdot X_L + M_U \cdot Y_U$

ABSORBER/GENERATOR HEAT EXCHANGE EQUATIONS

Energy balance: $(M_K \cdot H_K) + (M_V \cdot H_V) - (M_L \cdot H_L) = (M_O \cdot H_O) + (M_S \cdot H_S) - (M_G \cdot H_G)$

Mass balance: $M_G = M_S + M_O$
 $M_L = M_K + M_V$
 $M_D = M_U + M_V$

Concentration balance: $(M_G \cdot X_G) = (M_O \cdot X_O) + (M_S \cdot Y_S)$
 $(M_L \cdot X_L) = (M_K \cdot Y_K) + (M_V \cdot Y_V)$

Assumptions: L = Saturated liquid
O = Saturated liquid
S = Vapor saturated
 $T_S = T_O$

GENERAL EQUATIONS

Energy balance: $Q_{gen} = (M_T \cdot H_T) + (M_K \cdot H_K) - (M_O \cdot H_O) - (M_P \cdot H_P)$
 $T_H = T_O + 10$

Mass balance: $M_O + M_P = M_T + M_K$

Concentration

balance: $(M_O \cdot X_O) + (M_P \cdot X_P) = (M_K \cdot X_K) + (M_T \cdot X_T)$

Assumptions: K = Saturated liquid at absorber pressure

J = Saturated liquid at generator pressure

T = Superheated vapor at $T_O + 10$

$$Y_T = Y_S = Y_O$$

RECTIFIER EQUATIONS

Energy balance: $Q_{\text{rect}} = (M_H \cdot H_H) - (M_M \cdot H_M) - (M_I \cdot H_I)$

Flow balance: $M_M = M_H - M_I$

Heat transfer rate: $T_M = TMSTAT + SHTM$

Reflux requirement: $\frac{M_I}{M_H} = (Y_Q - Y_A)(X_Q - X_A) \cdot \text{FRACMR}$

Entering rectifier condition: $Y_H = Y_O + DYHYO$

Assumptions: I = Saturated Liquid

M = Superheated Vapor

CONDENSER EQUATIONS

Energy balance: $Q_{\text{cond}} = M_A \cdot (H_M - H_A)$

Assumption: A = Saturated liquid

HEAT EXCHANGER NO. 2 EQUATIONS

Energy balance: $H_A - H_B = H_D - H_C$

Heat transfer rate: $T_D = T_C + (T_A - T_C) \cdot \text{EFFHX2}$

EVAPORATOR EQUATIONS

Energy balance:

$$Q_{\text{evap}} = M_C \cdot (H_C - H_B)$$

Assumption: C = Saturated vapor

The input parameters for each model consist of refrigerant flow rate and concentration, saturated condensing and evaporating temperatures, generator and absorber fluid leaving temperatures, fractional minimum reflux and entering rectifier concentration differences, the efficiencies of the absorber and the refrigerant vapor/liquid heat exchanger, and the degree of refrigerant superheat entering the condenser. Output consists of the thermodynamic properties and the flow rates at each designated point in the cycle, all external and internal heat transfers, and the COP. The flow chart in Figure 8 shows the solution procedure followed in the program.

All other computer models were developed in a similar manner. The primary changes in each model include defining a new equation subroutine (EQNS) and modifying the input and output to match the assumptions and desired results.

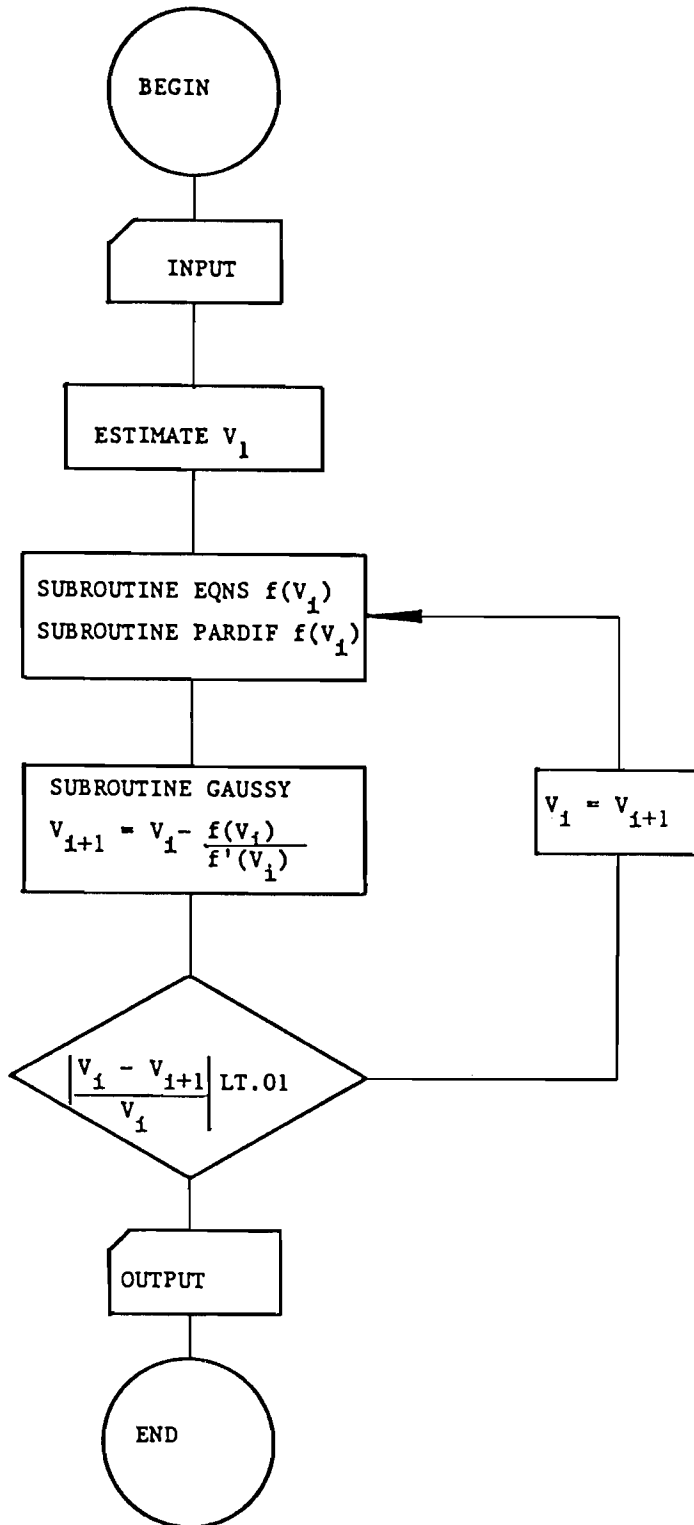


Fig. 8. Flow chart for computer models.

V. CYCLE/FLUID COMBINATIONS

This section describes the 24 cycle/fluid combinations that were selected for more detailed evaluation. Outputs from the computer models also are given, and the conditions to which the computed results apply are listed below. The latter were selected to be representative of conditions that might be experienced in an air-cooled unit at the heating rating point of 47/43/70 and at the cooling rating point of 80/67/95.

- Maximum solution temperature = 400°F
- Minimum absorber solution temperature = 110°F
- Minimum internal heat exchanger approach temperature = 10°F
- Condenser saturation temperature = 120°F (130–110 for resorber type)
- Evaporator saturation temperature = 37°F (25–43 for desorber type)

A. COMBINATIONS ABS1, ABS2, ABS3, AND ABS21

These combinations all utilize the concept of the generator heat exchange/absorber heat exchange cycle. Combinations ABS1, ABS2, ABS3, and ABS21 incorporate the fluids $\text{NH}_3/\text{H}_2\text{O}$, R22/DMETEG, R123a/ETFE, and $\text{CH}_3\text{OH}/\text{LiBr}/\text{ZnBr}_2$, respectively.

Figure 9 shows the cycle on the $\text{NH}_3/\text{H}_2\text{O}$ equilibrium diagram along with a flow chart. Refrigerant A is generated at O-J by direct burner-heat input and by heat recovered in generator heat exchange. The latter is recovered from the strong solution at J-N, and the refrigerant is evaporated at C and is absorbed at K-E. Absorber heat exchange occurs between K-E and E-G, and sensible liquid/liquid heat exchange occurs between N-K and G-O.

Computer model outputs for ABS1, ABS2, ABS3, and ABS21 are shown in Tables 4, 5, 6, and 7, respectively. Several points should be noted. The first is that the fluids R22/DMETEG (ABS2) and $\text{CH}_3\text{OH}/\text{LiBr}/\text{ZnBr}_2$ (ABS21) do not require a rectifier because adequate separation can be achieved in the generator. Second, slightly higher COPs are achieved with the fluids R22/DMETEG and R123a/ETFE than with $\text{NH}_3/\text{H}_2\text{O}$. These higher COPs are attributable primarily to the fact that R22 and R123a have significantly lower latent-heat/specific-heat ratios than NH_3 , which allows a greater fraction of the generator heat to be supplied from the sensible heat in the strong solution. On the other hand, a slightly lower COP is achieved with $\text{CH}_3\text{OH}/\text{LiBr}/\text{ZnBr}_2$ because of its higher latent-heat/specific-heat ratio and because the maximum generator temperature is limited by stability concerns. Finally, the COP advantage of the fluids with lower latent-heat/specific-heat ratios is offset by the significantly higher sensible heat transfer required between the high side and low side. This offset is reflected in the absorber heat exchange and generator heat exchange values listed in the tables and results in larger heat exchangers and higher product costs.

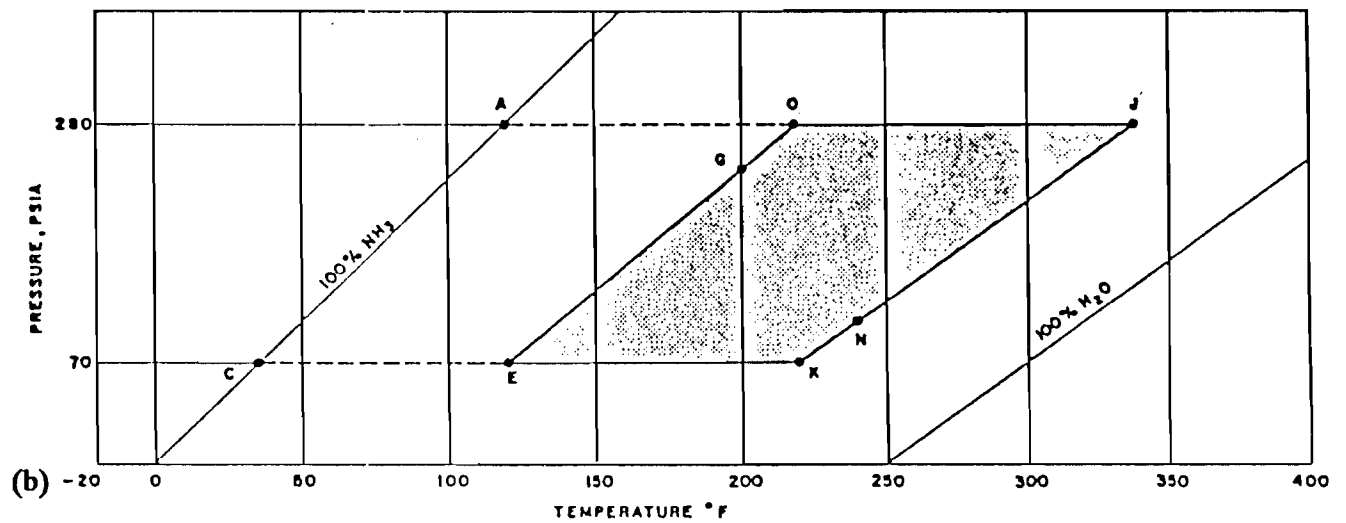
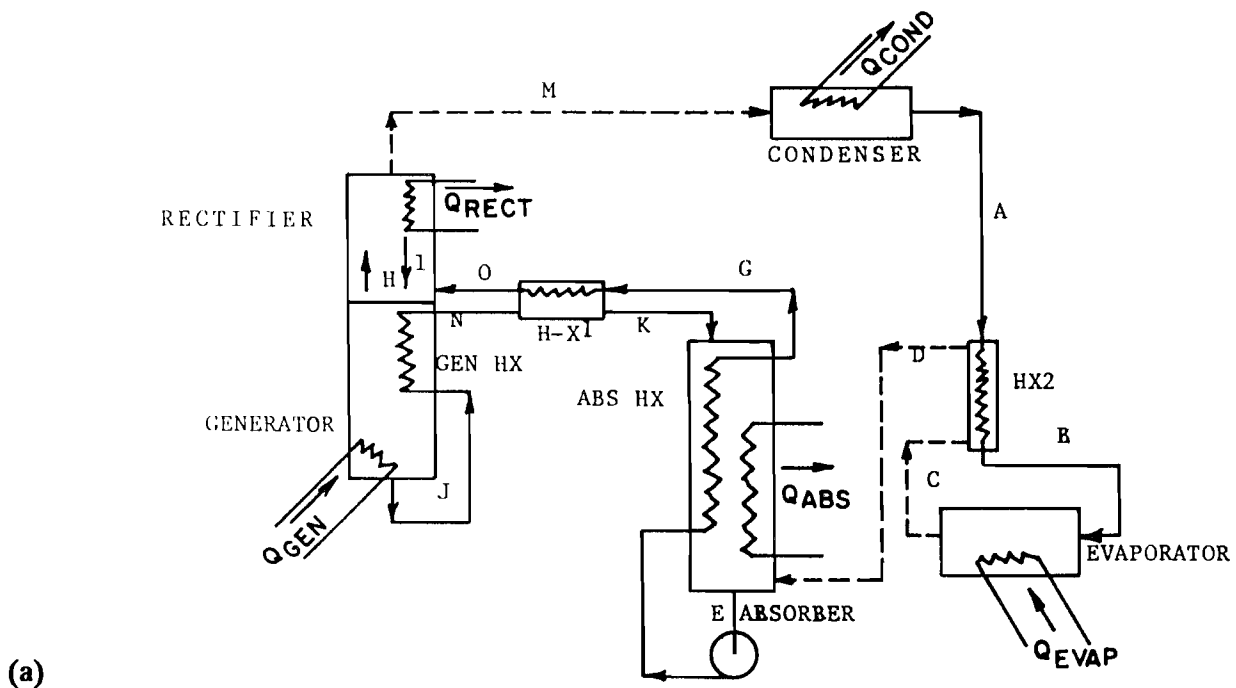


Fig. 9. (a) Circuit schematic and (b) pressure-temperature-composition chart of generator heat exchange/absorber heat exchange.

Table 4. Computer model output for ABS1 (refer to Fig. 9)

Fluid: NH₃/H₂O
 Basis: 12,000 Btu/h evaporator input

Point	Pressure (psia)	Temp. (°F)	Flow (lbm/h)	Concen. (NH ₃ /mix)	H (Btu/lb)
A	286.5	120.0	24.9	0.998	101.0
B	286.5	89.2	24.9	0.998	64.5
C	68.9	37.0	24.9	0.998	546.1
D	68.9	110.0	24.9	0.998	582.6
E	68.9	110.0	72.5	0.447	-24.5
G	286.5	211.9	72.5	0.447	91.1
H	286.5	229.2	27.1	0.995	650.3
I	286.5	208.7	2.2	0.458	87.4
J	286.5	332.0	47.7	0.157	267.7
K	68.9	222.0	47.6	0.157	150.6
M	286.5	160.0	24.9	0.998	579.0
N	286.5	222.9	47.6	0.157	151.5
O	286.5	212.4	72.5	0.447	91.7

External Heat Transfer, Btu/h

Absorber	18,000
Generator	17,950
Rectifier	2,960
Condenser	11,900
Evaporator	12,000

Internal Heat Transfer, Btu/h

Abs. heat exch.	8,400
Gen. heat exch.	5,500
HX1	50
HX2	900

COP (thermodynamic), heating 1.67

Table 5. Computer model output for ABS2 (refer to Fig. 9)

Fluid: R22/DMETEG
 Basis: 12,000 Btu/h evaporator input

Point	Pressure (psia)	Temp. (°F)	Flow (lbm/h)	Concen. (R22/mix)	H (Btu/lb)
A	276.4	120.0	160.0	1.000	14.4
B	276.4	80.2	160.0	1.000	1.8
C	78.8	37.0	160.0	1.000	76.5
D	78.8	109.2	160.0	1.000	89.0
E	78.8	110.0	456.0	0.428	-4.7
G	276.4	214.0	456.0	0.428	40.3
J	276.4	343.0	296.0	0.119	110.9
K	78.8	224.4	296.0	0.119	56.9
M	276.4	235.0	160.0	1.000	106.5
N	276.4	224.8	296.0	0.119	57.1
O	276.4	214.3	456.0	0.428	40.4
P	276.4	235.0	160.0	1.000	106.6

External Heat Transfer, Btu/h

Absorber	12,600
Generator	15,500
Condenser	14,700
Evaporator	12,000

Internal Heat Transfer, Btu/h

Abs. heat exch.	19,200
Gen. heat exch.	15,800
HX1	0
HX2	2,100

COP (thermodynamic), heating 1.77

Table 6. Computer model output for ABS3 (refer to Fig. 9)

Fluid: R123a/ETFE
 Basis: 12,000 Btu/h evaporator input

Point	Pressure (psia)	Temp. (°F)	Flow (lbm/h)	Concen. (R123a/mix)	H (Btu/lb)
A	28.9	120.0	166.7	0.998	39.5
B	28.9	72.8	166.7	0.998	27.6
C	4.9	37.0	166.7	0.998	100.0
D	4.9	115.8	166.7	0.998	111.9
E	4.9	110.0	490.0	0.393	34.6
G	28.9	186.8	490.0	0.393	66.0
H	28.9	219.1	181.7	0.956	122.6
I	28.9	198.8	15.0	0.464	67.8
J	28.9	306.0	323.3	0.081	142.1
K	4.9	191.7	323.3	0.081	84.2
M	28.9	160.0	166.7	0.998	116.8
N	28.9	225.9	323.3	0.081	100.9
O	28.9	214.5	490.0	0.393	77.5

External Heat Transfer, Btu/h

Absorber	13,500
Generator	16,200
Rectifier	1,700
Condenser	12,800
Evaporator	12,000

Internal Heat Transfer, Btu/h

Abs. heat exch.	15,300
Gen. heat exch.	13,300
HX1	5,300
HX2	2,000

COP (thermodynamic), heating 1.75

Table 7. Computer model output for ABS21 (refer to Fig. 9)

Fluid: CH₃OH/LiBr/ZnBr₂
 Basis: 12,000 Btu/h evaporator input

Point	Pressure (psia)	Temp. (°F)	Flow (lbm/h)	Concen. (CH ₃ OH/mix)
A	40	120	25.5	1.0
B	40	83	25.5	1.0
C	6	37	25.5	1.0
E	6	110	216.5	0.4
G	40	153	216.5	0.4
O	40	198	216.5	0.4
J	40	250	191.0	0.32
K	6	163	191.0	0.32
M	40	208	191.0	0.32

External Heat Transfer, Btu/h

Absorber	15,600
Generator	18,300
Condenser	13,300
Evaporator	12,000

Internal Heat Transfer, Btu/h

Abs. heat exch.	4,300
Gen. heat exch.	2,900
Liquid/liquid heat exch.	3,100
Vapor/liquid heat exch.	600

COP (thermodynamic), heating 1.58

B. COMBINATIONS ABS4, ABS5, ABS12, AND ABS15

Cycle features for these combinations include generator heat exchange/absorber heat exchange and absorber/generator heat exchange. The combinations ABS4, ABS5, ABS12, and ABS15 utilize the fluids NH₃/H₂O, R22/DMETEG, NH₃/H₂O/LiBr, and CH₃NH₂/H₂O/LiBr, respectively.

In this cycle, the maximum generator temperatures have been increased to achieve an overlap in temperatures between the high end of the absorber and the low end of the generator, thus allowing absorber/generator heat exchange, as shown in Figure 10.

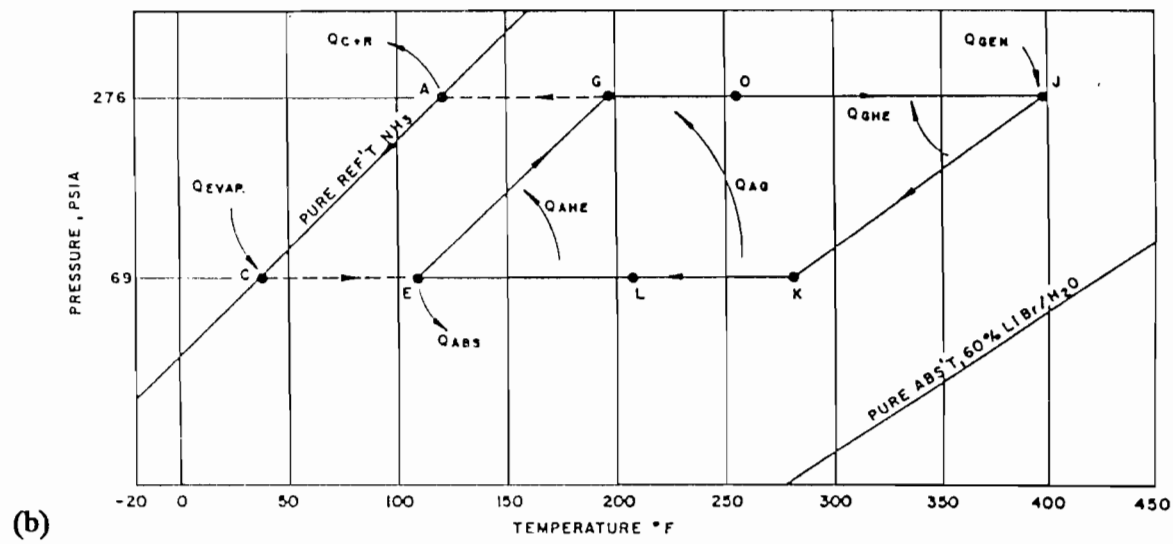
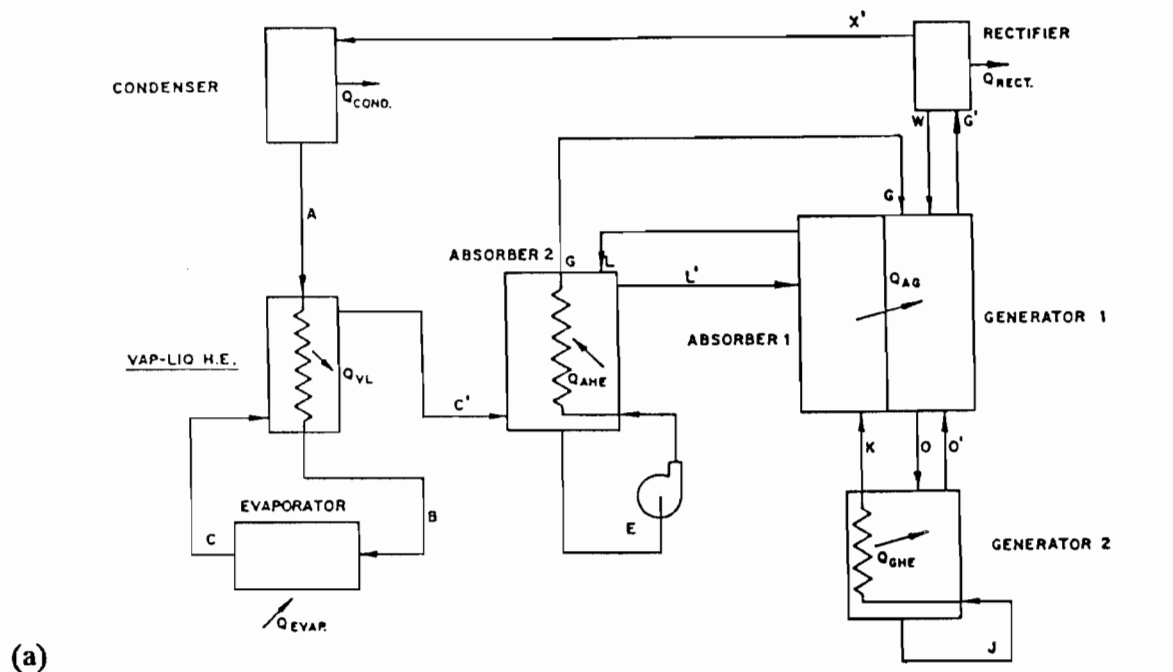


Fig. 10. (a) Circuit schematic and (b) pressure-temperature-composition chart of generator heat exchange/absorber heat exchange and absorber/generator heat exchange.

Absorber/generator heat exchange occurs between K-L and G-O. The rest of the cycle is basically the same as the cycle shown in Figure 9.

Output from the computer model calculations for ABS4, ABS5, ABS12, and ABS15 is shown in Tables 8, 9, 10, and 11, respectively. For the binary fluids operating at the same maximum generator temperature, Tables 8 and 9 show a slight efficiency advantage of the R22/DMETEG fluid over $\text{NH}_3/\text{H}_2\text{O}$. This is a carry-over from the advantage of a lower latent-heat/specific-heat ratio in generator heat exchange/absorber heat exchange.

Table 10 shows that there is a significant COP improvement when the ternary $\text{NH}_3/\text{H}_2\text{O}/\text{LiBr}$ is substituted for the binary $\text{NH}_3/\text{H}_2\text{O}$. Adding the lithium bromide to the $\text{NH}_3/\text{H}_2\text{O}$ lowers the vapor pressure of the solution. This allows operation at higher generator temperatures and thus increases the overlap for absorber/generator heat exchange. The $\text{NH}_3/\text{H}_2\text{O}$ system (Table 8) is limited to a maximum generator temperature of 380°F, at which point the concentration of ammonia in the solution is 6.5%. Operation at higher temperatures is not deemed practical because of the difficulty of separation beyond 6.5%. The ternary system, on the other hand, is operated at the imposed stability limit of 400°F, at which point the concentration of ammonia in the solution was 13%, a considerably easier separation (Table 10).

It is evident when comparing Tables 8 and 10 that the vapor pressures of ammonia in the condenser are different, although the condensing temperatures are the same. This difference arises from the different sources of data used for the $\text{NH}_3/\text{H}_2\text{O}$ and $\text{NH}_3/\text{H}_2\text{O}/\text{LiBr}$ properties. It is not expected to have much effect on the performance comparisons.

Table 11 shows that an alternate ternary fluid, $\text{CH}_3\text{NH}_2/\text{H}_2\text{O}/\text{LiBr}$, also exhibits higher efficiencies than those of the binary fluids, although not as high as that of $\text{NH}_3/\text{H}_2\text{O}/\text{LiBr}$.

C. COMBINATIONS ABS13 AND ABS16

These combinations also utilize generator heat exchange/absorber heat exchange and absorber/generator heat exchange. Absorbent recirculation is added to maximize the amount of absorber/generator heat exchange that can be achieved. Combinations ABS13 and ABS16 utilize the ternary fluids $\text{NH}_3/\text{H}_2\text{O}/\text{LiBr}$ and $\text{CH}_3\text{NH}_2/\text{H}_2\text{O}/\text{LiBr}$, respectively.

The previous cycle (Figure 10) shows a temperature rise in the low end of the generator (G-O) that is smaller than the temperature drop in the high end of the absorber (K-L) during absorber/generator heat exchange. This smaller rise is caused primarily by the fact that the specific heat of the strong solution entering the absorber is less than that of the weak solution entering the generator. Absorber/generator heat exchange can be improved by increasing the circulation rate in the high end of the absorber by absorbent recirculation until the temperature differences at both ends of the counterflow heat exchanger are approximately the same, as shown in Figure 11. As a result, the COPs of the $\text{NH}_3/\text{H}_2\text{O}/\text{LiBr}$ and $\text{CH}_3\text{NH}_2/\text{H}_2\text{O}/\text{LiBr}$ systems are increased from 2.08 to 2.19 and from 1.87 to 2.09, respectively (Tables 12 and 13).

Table 8. Computer model output for ABS4 (refer to Fig. 10)

Fluid: NH₃/H₂O
 Basis: 12,000 Btu/h evaporator input

Point	Pressure (psia)	Temp. (°F)	Flow (lbm/h)	Concen. (NH ₃ /mix)	H (Btu/lb)
A	286.5	120.0	24.9	0.998	101.0
B	286.5	89.2	24.9	0.998	64.5
C	68.9	37.0	24.9	0.998	546.1
D	68.9	37.0	24.9	0.998	582.6
E	68.9	110.0	61.5	0.442	-24.4
G	286.5	214.0	61.5	0.442	93.5
H	286.5	224.1	27.4	0.945	650.5
I	286.5	230.4	2.5	0.395	114.4
J	286.5	380.0	36.6	0.065	344.9
K	68.9	266.2	36.6	0.065	219.7
L	68.9	224.0	40.6	0.153	153.7
M	286.5	160.1	24.9	0.998	579.1
O	286.5	232.9	48.1	0.388	117.8
S	286.5	232.9	5.2	0.940	655.9

External Heat Transfer, Btu/h

Absorber	12,750
Generator	15,930
Rectifier	3,090
Condenser	11,900
Evaporator	12,000

Internal Heat Transfer, Btu/h

Abs. heat exch.	7,270
Gen. heat exch.	4,610
Abs./Gen. heat exch.	4,060
HX2	920

COP (thermodynamic), heating 1.74

Table 9. Computer model output for ABS5 (refer to Fig. 10)

Fluid: R22/DMETEG
 Basis: 12,000 Btu/h evaporator input

Point	Pressure (psia)	Temp. (°F)	Flow (lbm/h)	Concen. (R22/mix)	H (Btu/lb)
A	276.4	120.0	162.2	1.000	14.4
B	276.4	83.5	162.2	1.000	2.8
C	78.8	37.0	162.2	1.000	76.5
D	78.8	103.4	162.2	1.000	88.0
E	78.8	110.0	433.0	0.427	-4.7
G	276.4	214.8	433.0	0.427	40.7
J	276.4	380.0	270.8	0.083	129.4
K	78.8	254.5	270.8	0.083	72.2
L	78.8	224.8	282.2	0.118	57.1
M	276.4	234.3	162.2	1.000	106.4
O	276.4	226.2	403.8	0.384	46.9
S	276.4	226.2	29.2	1.000	104.7

External Heat Transfer, Btu/h

Absorber	11,840
Generator	14,800
Condenser	14,900
Evaporator	12,000

Internal Heat Transfer, Btu/h

Abs. heat exch.	19,600
Gen. heat exch.	15,600
Abs./Gen. heat exch.	4,400
HX2	1,900

COP (thermodynamic), heating 1.81

Table 10. Computer model output for ABS12 (refer to Fig. 10)

Fluid: NH₃/H₂O/LiBr
 Basis: 12,000 Btu/h evaporator input

Point	Pressure (psia)	Temp. (°F)	Flow (lbm/h)	Concen. (NH ₃ /mix)	Enthalpy (Btu/lb)
A	276	120	24.9	1.0	497
E	69	110	80.2	0.4	164
G	276	198	80.2	0.4	229
J	276	400	55.3	0.13	287
K	69	283	55.3	0.13	218
I	276	---	0.6	0.6	418
D	69	110	24.9	1.0	980
H	276	198	25.5	0.991	996

External Heat Transfer, Btu/h

Absorber	10,500
Generator	11,200
Condenser + rectifier	12,700
Evaporator	12,000

Internal Heat Transfer, Btu/h

Abs. heat exch.	5,200
Gen. heat exch.	3,800
Abs./Gen. heat exch.	7,600
Vapor/liquid heat exch.	900

COP (thermodynamic), heating 2.08

Table 11. Computer model output for ABS15 (refer to Fig. 10)

Fluid: CH₃NH₂/H₂O/LiBr
 Basis: 12,000 Btu/h evaporator input

Point	Pressure (psia)	Temp. (°F)	Flow (lbm/h)	Concen. (CH ₃ NH ₂ /mix)	Enthalpy (Btu/lb)
A	112	120	38.8	1.0	276
E	22	110	88.6	0.463	108
G	112	197	88.6	0.463	167
J	112	400	49.7	0.045	261
K	22	296	49.7	0.045	209
I	112	---	3.5	0.68	222
D	22	110	38.8	1.0	587
H	112	197	42.6	0.981	642

External Heat Transfer, Btu/h

Absorber	10,100
Generator	13,800
Condenser + rectifier	15,700
Evaporator	12,000

Internal Heat Transfer, Btu/h

Abs. heat exch.	5,300
Gen. heat exch.	2,600
Abs./Gen. heat exch.	8,300
Vapor/liquid heat exch.	900

COP (thermodynamic), heating 1.87

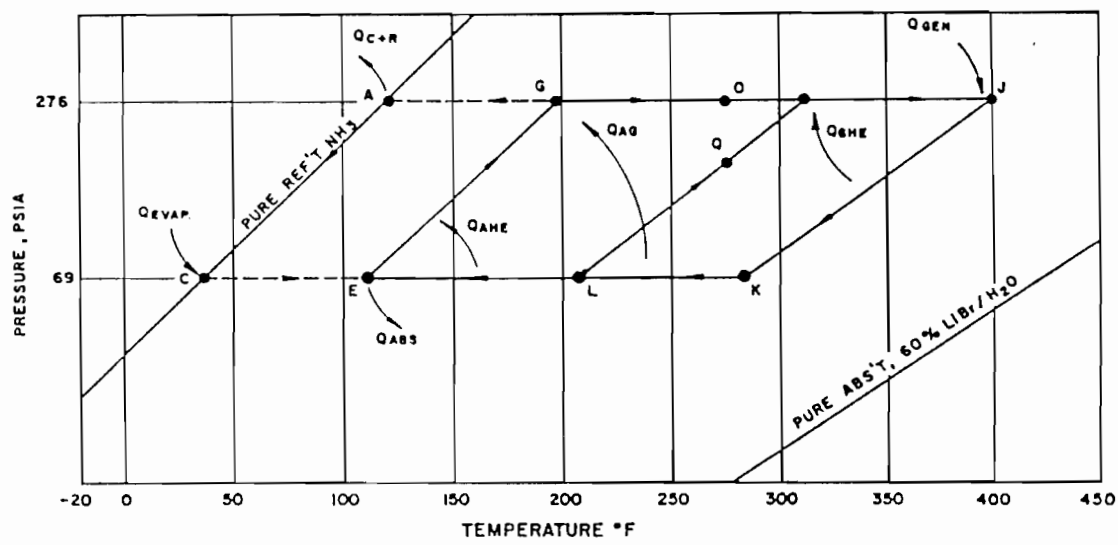
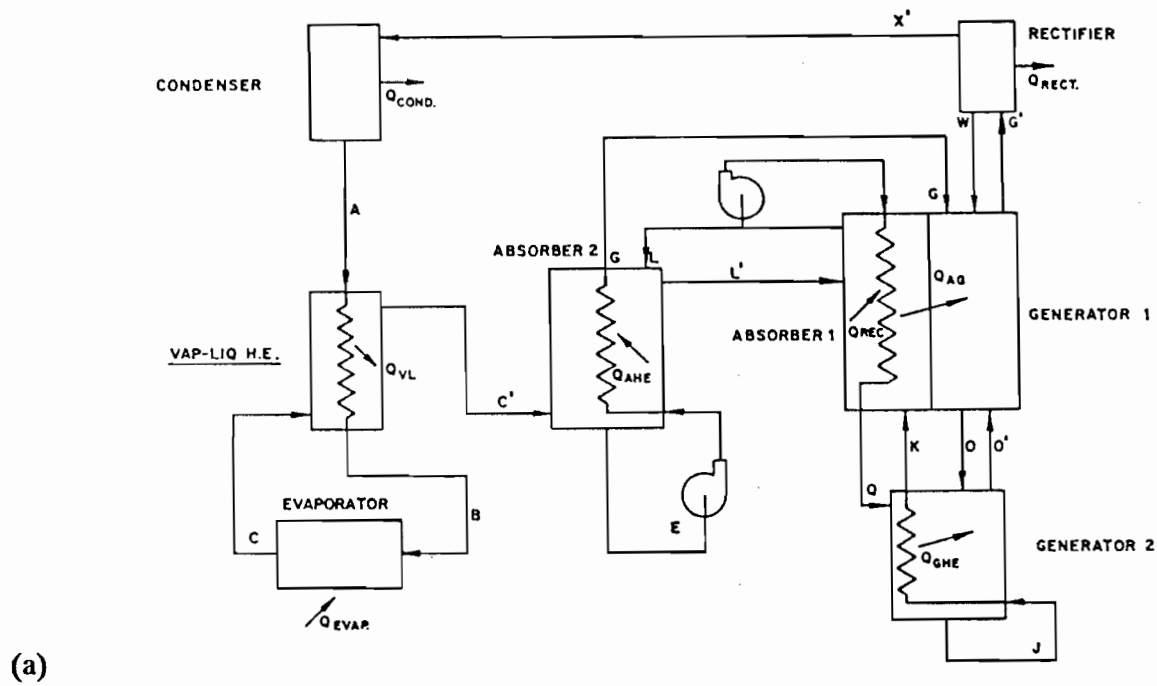


Fig. 11. (a) Circuit schematic and (b) pressure-temperature-composition chart of generator heat exchange/absorber heat exchange, absorber/generator heat exchange, and absorbent recirculation.

Table 12. Computer model output for ABS13 (refer to Fig. 11)

Fluid: NH₃/H₂O/LiBr
 Basis: 12,000 Btu/h evaporator input

Point	Pressure (psia)	Temp. (°F)	Flow (lbm/h)	Concen. (NH ₃ /mix)	Enthalpy (Btu/lb)
A	276	120	24.9	1.0	497
E	69	110	73.4	0.4	164
G	276	198	73.4	0.4	229
J	276	400	67.7	0.13	287
K	69	283	67.7	0.13	218
W	276	---	0.6	0.60	418
C	69	110	24.9	1.0	980
G	276	198	25.5	0.991	996

External Heat Transfer, Btu/h

Absorber	9,400
Generator	10,100
Condenser + rectifier	12,700
Evaporator	12,000

Internal Heat Transfer, Btu/h

Abs. heat exch.	4,800
Gen. heat exch.	4,600
Abs./Gen. heat exch.	8,500
Vapor/liquid heat exch.	900
Abs. recycle heat exch.	800

COP (thermodynamic), heating 2.19

Table 13. Computer model output for ABS16 (refer to Fig. 11)

Fluid: $\text{CH}_3\text{NH}_2/\text{H}_2\text{O}/\text{LiBr}$
 Basis: 12,000 Btu/h evaporator input

Point	Pressure (psia)	Temp. (°F)	Flow (lbm/h)	Concen. ($\text{CH}_3\text{NH}_2/\text{mix}$)	Enthalpy (Btu/lb)
A	112	120	38.9	1.0	276
E	22	110	70.9	0.463	108
G	112	197	70.9	0.463	167
J	112	400	74.9	0.045	261
K	22	296	74.9	0.045	209
Q	112	286	42.9	0.215	204
W	112	---	3.5	0.68	222
C	22	110	38.9	1.0	587
G	112	197	42.3	0.981	641

External Heat Transfer, Btu/h

Absorber	7,300
Generator	11,000
Condenser + rectifier	15,700
Evaporator	12,000

Internal Heat Transfer, Btu/h

Abs. heat exch.	4,200
Gen. heat exch.	3,900
Abs./Gen. heat exch.	10,500
Vapor/liquid heat exch.	900
Abs. recycle heat exch.	2,000

COP (thermodynamic), heating 2.09

D. COMBINATIONS ABS6A AND ABS6B

Combinations ABS6A and ABS6B employ generator heat exchange/absorber heat exchange and absorber/generator heat exchange as in Section B, but in these combinations the concept of regeneration is added in order to increase absorber/generator heat exchange. The combination ABS6B employs $\text{NH}_3/\text{H}_2\text{O}$ and is the simpler of the two, as is shown in Figure 12. This combination uses one stage of regeneration (F-N), and the regenerated vapor is absorbed at R-S. The net effect is to increase the overlap for absorber/generator heat exchange, increasing the COP from 1.74 to 1.94 (Table 14).

The combination ABS6A employs R22/DMETEG and two stages of regeneration (Figure 13). Two stages of regeneration were selected because there is very little temperature overlap between the absorber and generator with this fluid. This small overlap is evident because adding absorber/generator heat exchange (ABS5) to the generator heat exchange/absorber heat exchange cycle (ABS2) increases the COP from 1.77 to only 1.81. Adding regeneration in this case, however, actually results in a lower COP (Table 15), because the effective temperature overlap actually decreases when the temperature differences for the two additional heat exchanges are included. Thus, it has been concluded that neither absorber/generator heat exchange nor regeneration are effective cycle concepts to use with R22/DMETEG.

E. COMBINATIONS ABS14 AND ABS17

Combinations ABS14 and ABS17 were used to evaluate the concept of adding regeneration to the generator heat exchange/absorber heat exchange, absorber/generator heat exchange, and absorbent recirculation cycles of ABS13 and ABS16. The fluids employed for combinations ABS14 and ABS17 are $\text{NH}_3/\text{H}_2\text{O}/\text{LiBr}$ and $\text{CH}_3\text{NH}_2/\text{H}_2\text{O}/\text{LiBr}$, respectively.

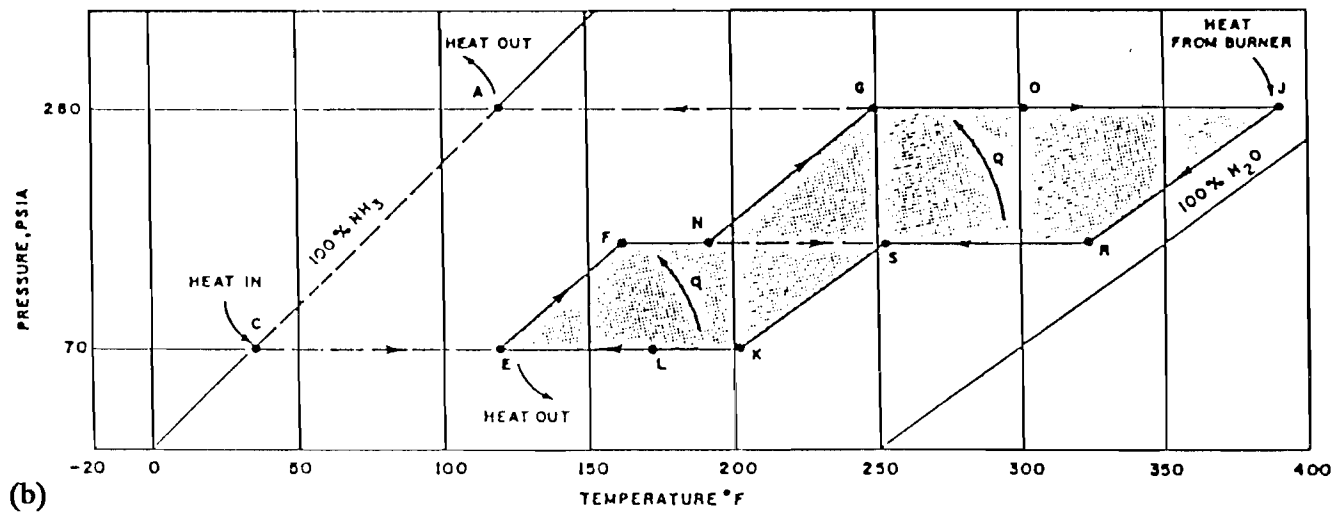
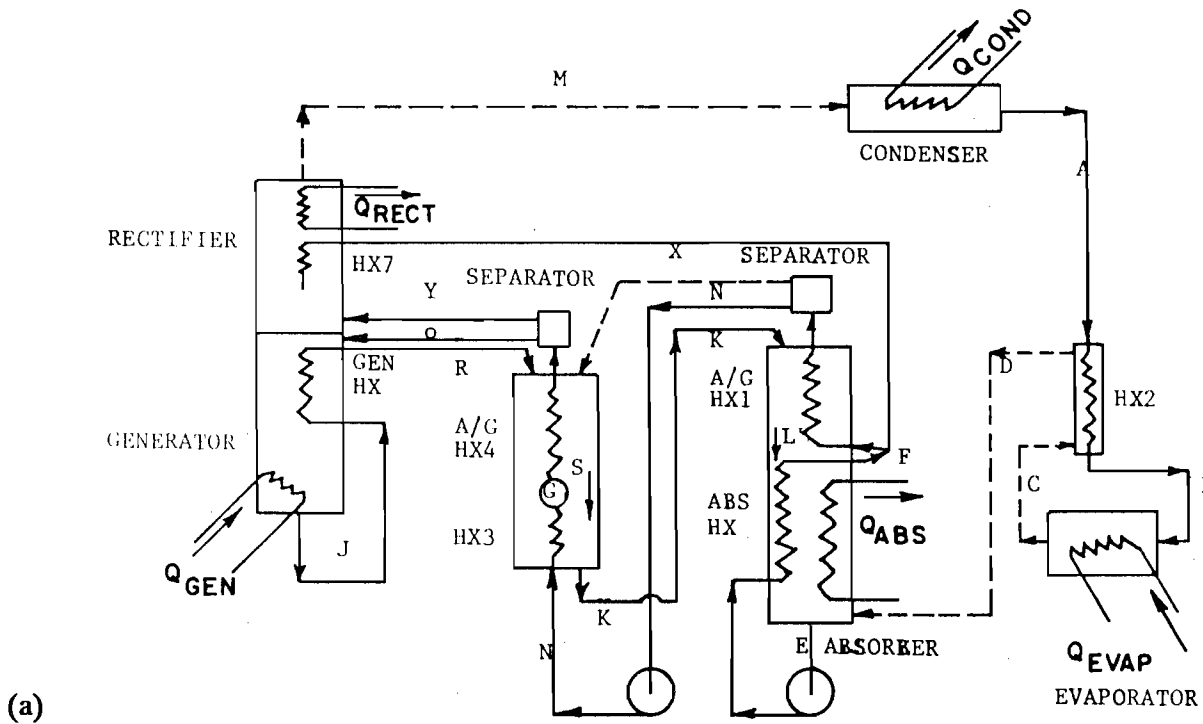


Fig. 12. (a) Circuit schematic and (b) pressure-temperature-composition chart of generator heat exchange/absorber heat exchange, absorber/generator heat exchange, and regeneration (1-stage).

Table 14. Computer model output for ABS6B (refer to Fig. 13)

Fluid: NH₃/H₂O
 Basis: 12,000 Btu/h evaporator input

Point	Pressure (psia)	Temp. (°F)	Flow (lbm/h)	Concen. (NH ₃ /mix)	H (Btu/lb)
A	286.5	120.0	24.9	0.998	101.0
B	286.5	89.2	24.9	0.998	64.5
C	68.9	37.0	24.9	0.998	546.1
D	68.9	110.0	24.9	0.998	582.6
E	68.9	110.0	79.7	0.449	-24.5
F	135.0	155.9	79.7	0.449	27.6
G	286.5	242.4	53.3	0.361	131.5
H	286.5	294.5	27.1	0.952	683.9
I	286.5	209.7	2.2	0.455	88.5
J	286.5	390.0	45.6	0.046	363.3
K	68.9	204.4	54.8	0.198	121.3
L	68.9	165.9	62.2	0.295	56.0
M	286.5	160.0	24.9	0.998	579.0
N	135.0	186.0	53.3	0.361	67.9
O	286.5	290.3	42.8	0.248	204.7
P	286.5	197.1	42.8	0.361	80.4
R	135.0	325.8	45.6	0.046	289.0
S	135.0	252.4	54.8	0.198	173.6
X	135.0	170.9	9.0	0.970	626.3
Y	286.5	285.3	10.5	0.820	721.9

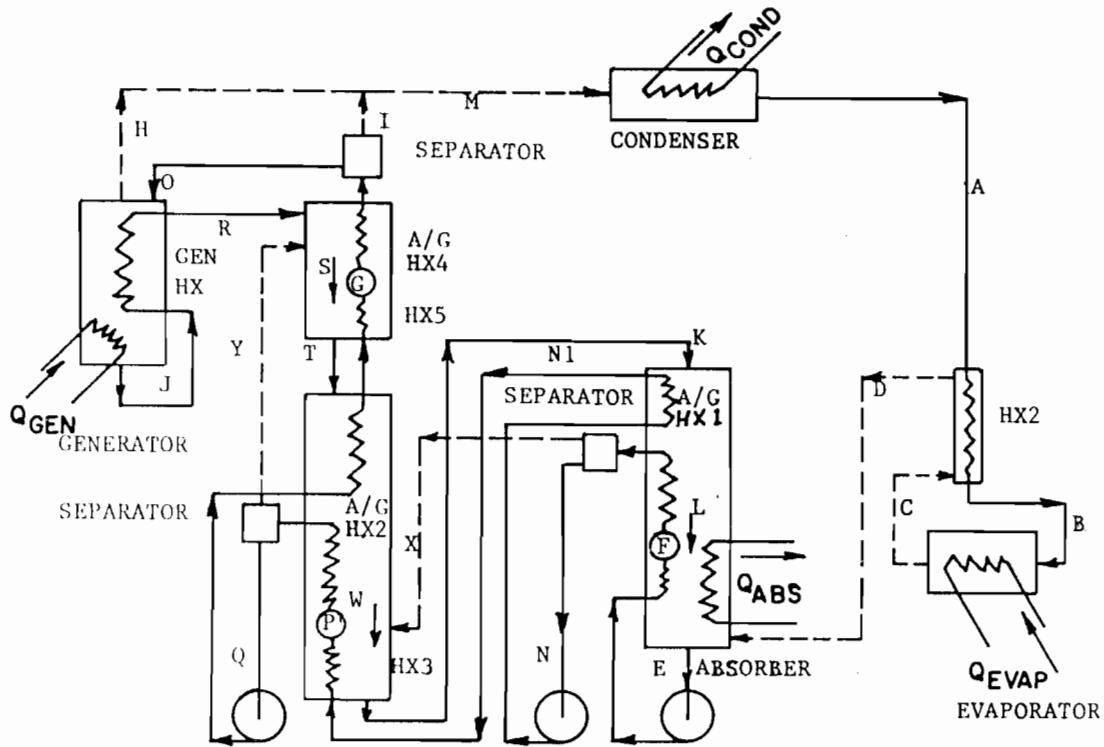
External Heat Transfer, Btu/h

Absorber	11,400
Generator	12,800
Rectifier	1,600
Condenser	11,900
Evaporator	12,000

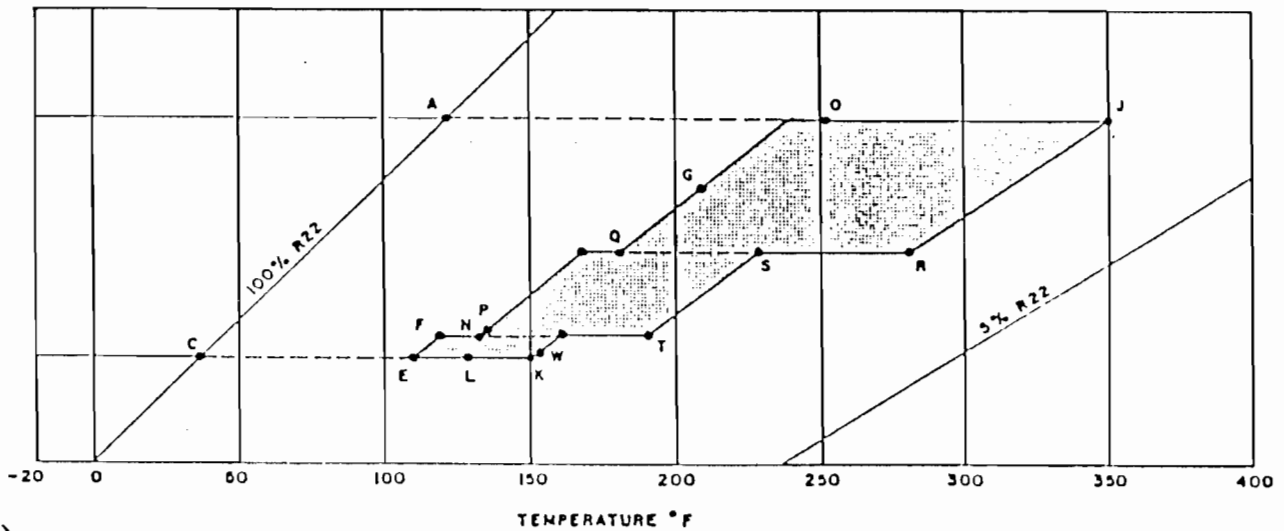
Internal Heat Transfer, Btu/h

Abs. heat exch.	4,100
Gen. heat exch.	3,400
Abs./Gen. HX1	7,500

COP (thermodynamic), heating 1.94



(a)



(b)

Fig. 13. (a) Circuit schematic and (b) pressure-temperature-composition chart of generator heat exchange/absorber heat exchange, absorber/generator heat exchange, and regeneration (2-stage).

Table 15. Computer model output for ABS6A (refer to Fig. 13)

Fluid: R22/DMETEG
 Basis: 12,000 Btu/h evaporator input

Point	Pressure (psia)	Temp. (°F)	Flow (lbm/h)	Concen. (R22/mix)	H (Btu/lb)
A	276.4	120.0	160	1.000	14.4
B	276.4	78.8	160	1.000	1.4
C	78.8	37.0	160	1.000	76.5
D	78.8	111.7	160	1.000	89.5
E	78.8	110.0	746	0.437	-4.9
F	85.0	119.4	746	0.437	-1.0
G	276.4	209.1	632	0.336	40.4
H	276.4	261.1	125	1.000	111.9
I	276.4	246.1	35	1.000	108.8
J	276.4	350.0	472	0.111	114.5
K	78.8	150.8	586	0.282	16.5
L	78.8	129.4	645	0.349	5.3
M	276.4	257.7	160	1.000	111.2
N	85.0	133.4	674	0.376	6.2
O	276.4	251.1	597	0.296	61.0
P	140.0	133.8	674	0.376	6.4
Q	140.0	179.7	632	0.336	27.2
R	140.0	281.6	472	0.111	82.8
S	140.0	228.7	514	0.182	55.5
T	140.0	228.7	514	0.182	39.2
W	85.0	192.4	514	0.282	16.6
X	85.0	126.4	72	1.000	91.9
Y	140.0	174.7	42	1.000	98.7

External Heat Transfer, Btu/h	
Absorber	13,100
Generator	16,600
Condenser	15,500
Evaporator	12,000

Internal Heat Transfer, Btu/h	
Abs. heat exch. (Abs. HX)	2,900
Gen. heat exch. (Gen HX)	15,000
Abs./Gen. HX1	11,500
Abs./Gen. HX2	17,000
Abs./Gen. HX3	200
Abs./Gen. HX4	14,700
HX2	8,300
HX5	2,100

COP (thermodynamic), heating 1.72

Utilizing regeneration with absorbent recirculation is best facilitated with another version of the regeneration concept, as is indicated in Figure 14. The concept is the same in that absorber/generator heat exchange is effected between H-L and F-I, L-K and G-O, and S-M and O-V, with vapor transfer occurring between F-I and S-M. The results are shown in Tables 16 and 17 for combinations ABS14 and ABS17, respectively. Adding the regeneration feature to the $\text{NH}_3/\text{H}_2\text{O}/\text{LiBr}$ system increases the COP from 2.19 to 2.32 (Tables 12 and 16). The corresponding increase for the $\text{CH}_3\text{NH}_2/\text{H}_2\text{O}/\text{LiBr}$ system is from 2.09 to 2.18 (Tables 13 and 17).

F. COMBINATIONS ABS18, ABS19, AND ABS20

Combinations ABS18, ABS19, and ABS20 examine the effect of replacing the conventional condenser/evaporator circuit with a resorption/desorption circuit in combinations ABS12, ABS13, and ABS14, respectively. In all cases the fluid is $\text{NH}_3/\text{H}_2\text{O}/\text{LiBr}$.

The resorption/desorption circuitry is shown schematically in Figures 15, 16, and 17, along with its location on a cycle diagram for combinations ABS18, ABS19, and ABS20, respectively.

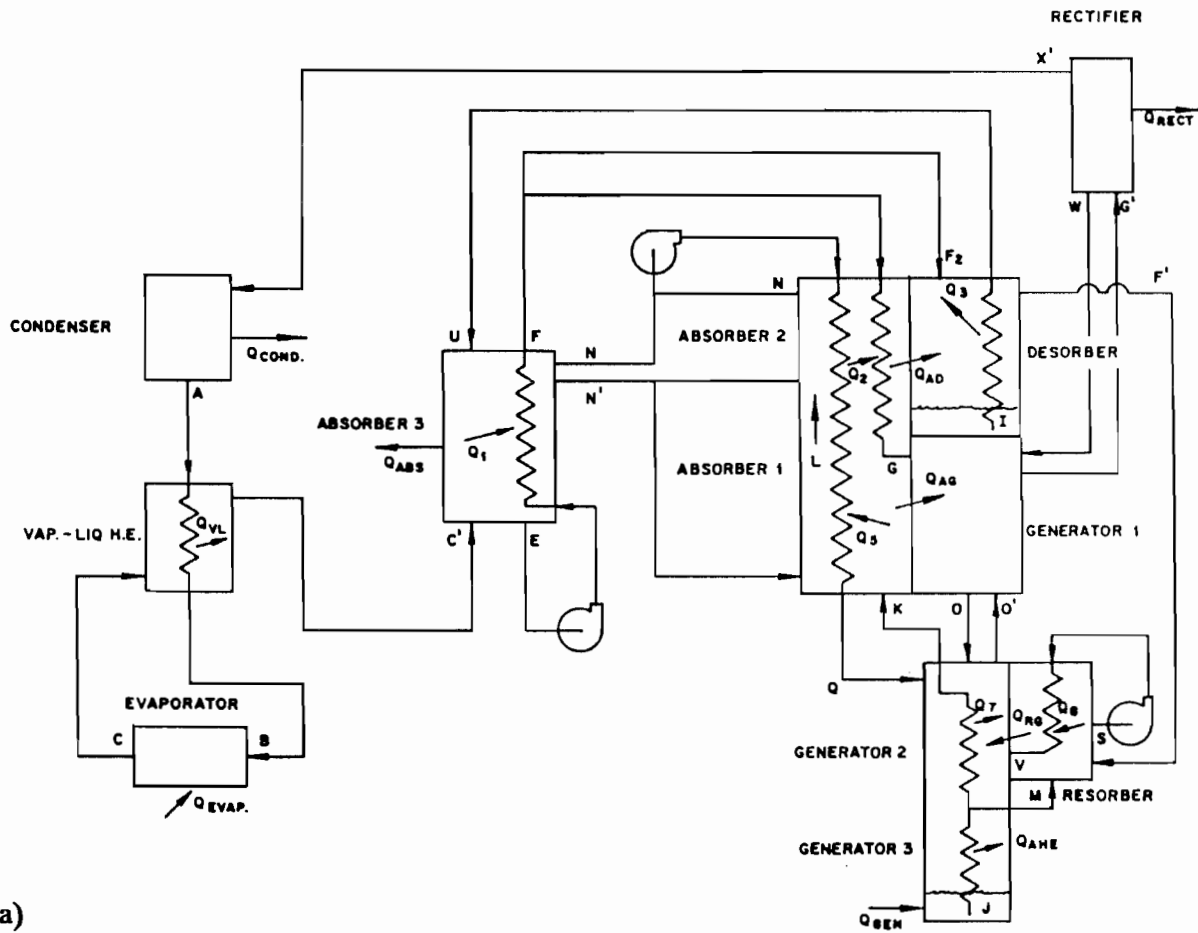
In an ideal cycle the primary effect of substituting a resorption/desorption circuit for the condenser/evaporator is to reduce the operating pressure of the system, possibly resulting in lower auxiliary power and system cost. But in a real fluid system in which the lines of constant concentration tend to diverge at higher pressures, there may be an efficiency advantage because the overlap for absorber/generator heat exchange is greater at lower operating pressures.

These effects can be observed by comparing Tables 18, 19, and 20 with Tables 10, 12, and 16, respectively.

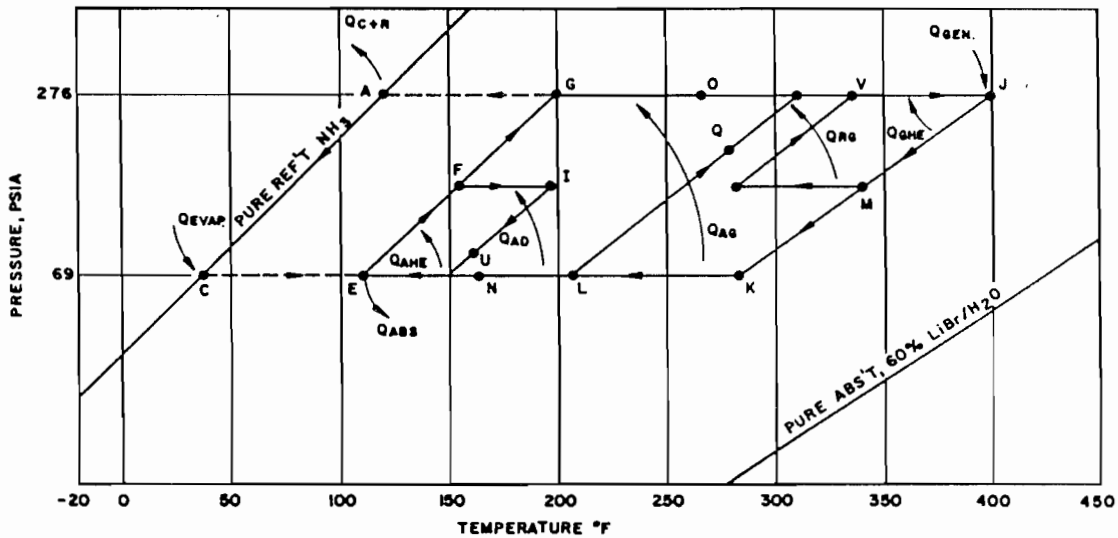
A summary of the COP values is shown below:

<u>System Features</u>	<u>COP Values</u>	
	<u>Conv. Cond./Evap.</u>	<u>Resorp./Desorp. for Cond./Evap.</u>
Gen Q-X/Abs Q-X, Abs/Gen Q-X	2.08	2.0
With Absorbent Recirculation	2.19	2.29
Plus Regeneration	2.32	2.45

The resorption/desorption circuit apparently has a negative effect in the basic absorber/generator heat exchange cycle, as indicated by the first line of the above table. This is surprising because the absorber/generator temperature overlap is about 10°F greater for the resorption/desorption system than for the conventional condenser/evaporator system. This anomaly cannot be explained at present, but it will be examined further in Phase II of the project. As expected, when absorbent recirculation and regeneration are added, the resorption/desorption system shows higher COP values than does the conventional condenser/evaporator system.



(a)



(b)

Fig. 14. (a) Circuit schematic and (b) pressure-temperature-composition chart of generator heat exchange/absorber heat exchange, absorber/generator heat exchange, absorber recirculation, and regeneration.

Table 16. Computer model output for ABS14 (refer to Fig. 14)

Fluid: NH₃/H₂O/LiBr
 Basis: 12,000 Btu/h evaporator input

Point	Pressure (psia)	Temp. (°F)	Flow (lbm/h)	Concen. (NH ₃ /mix)	Enthalpy (Btu/lb)
A	276	120	24.9	1.0	497
E	69	110	91.3	0.4	164
F	140	154	91.3	0.4	195
G	276	198	64.9	0.4	229
I	140	198	23.4	0.322	203
J	276	400	96.0	0.13	287
K	69	283	58.3	0.13	218
M	140	341	37.7	0.13	252
Q	276	273	15.2	0.225	230
S	140	283	40.7	0.195	230
U	69	164	23.4	0.322	178
V	276	331	40.7	0.195	260
W	276	---	0.6	0.60	418
C'	69	110	24.9	1.0	980
F'	140	154	3.1	0.994	973
G'	276	198	25.4	0.991	996

External Heat Transfer, Btu/h

Absorber	8,400
Generator	9,100
Condenser + rectifier	12,700
Evaporator	12,000

Internal Heat Transfer, Btu/h

Abs. & resorber heat exch.	6,900
Desorber & gen. heat exch.	5,900
Abs./Gen. heat exch.	11,500
Vapor/liquid heat exch.	900

COP (thermodynamic), heating 2.32

Table 17. Computer model output for ABS17 (refer to Fig. 14)

Fluid: CH₃NH₂/H₂O/LiBr
 Basis: 12,000 Btu/h evaporator input

Point	Pressure (psia)	Temp. (°F)	Flow (lbm/h)	Concen. (CH ₃ NH ₂ /mix)	Enthalpy (Btu/lb)
A	112	120	38.9	1.9	276
E	22	110	90.4	0.463	108
F	51	154	90.4	0.463	138
G	112	197	64.6	0.463	167
I	51	197	21.5	0.36	154
J	112	400	107.7	0.045	261
K	22	296	65.2	0.045	209
M	51	347	42.5	0.045	234
Q	112	286	35.1	0.215	204
S	51	296	46.8	0.13	210
U	22	167	21.5	0.36	137
V	112	337	46.8	0.13	231
W	112	---	3.5	0.68	222
C	22	110	38.9	1.0	587
F	51	154	4.2	0.988	613
G	112	197	42.8	0.981	641

External Heat Transfer, Btu/h

Absorber	6,400
Generator	10,200
Condenser & rectifier	15,800
Evaporator	12,000

Internal Heat Transfer, Btu/h

Abs. & resorber heat exch.	7,200
Desorber & gen. heat exch.	4,800
Abs./Gen. heat exch.	13,700
Vapor/liquid heat exch.	900

COP (thermodynamic), heating 2.18

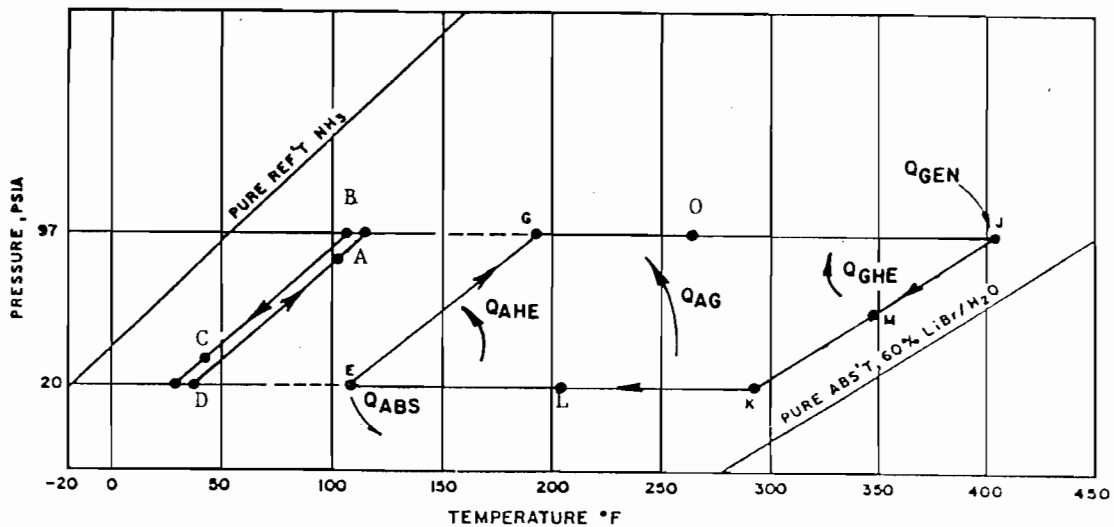
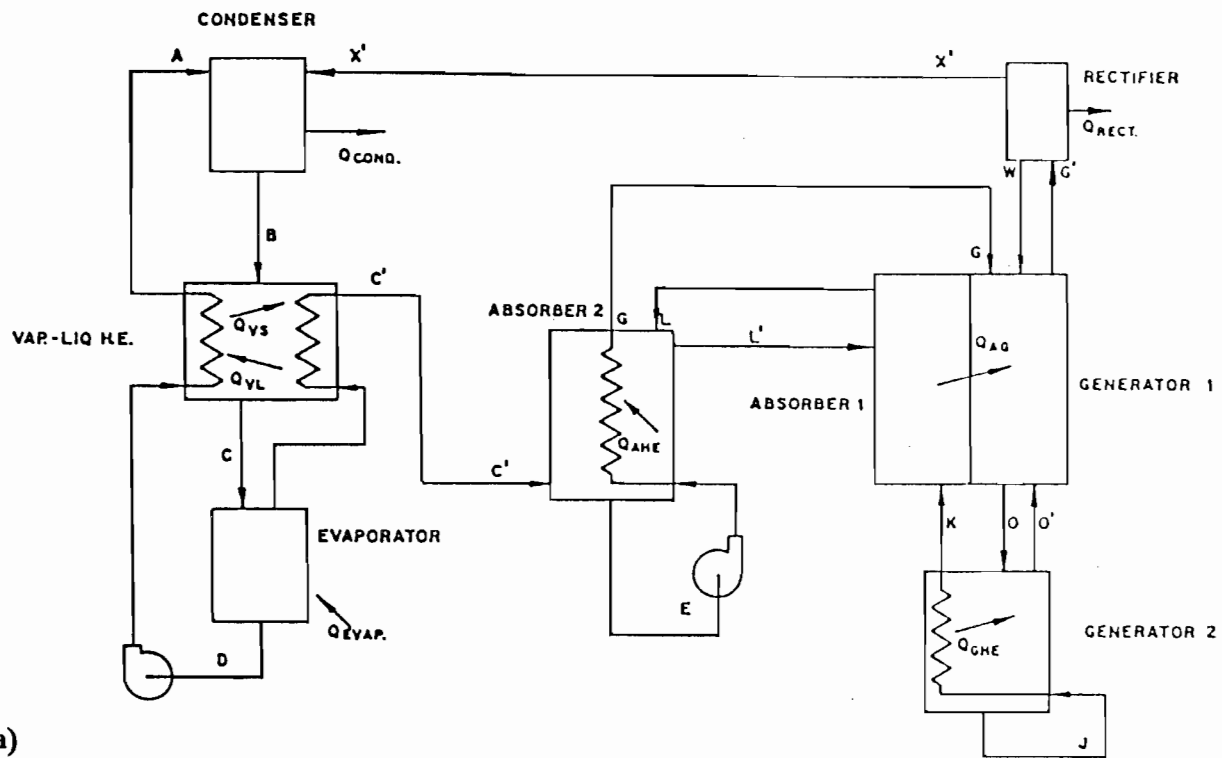
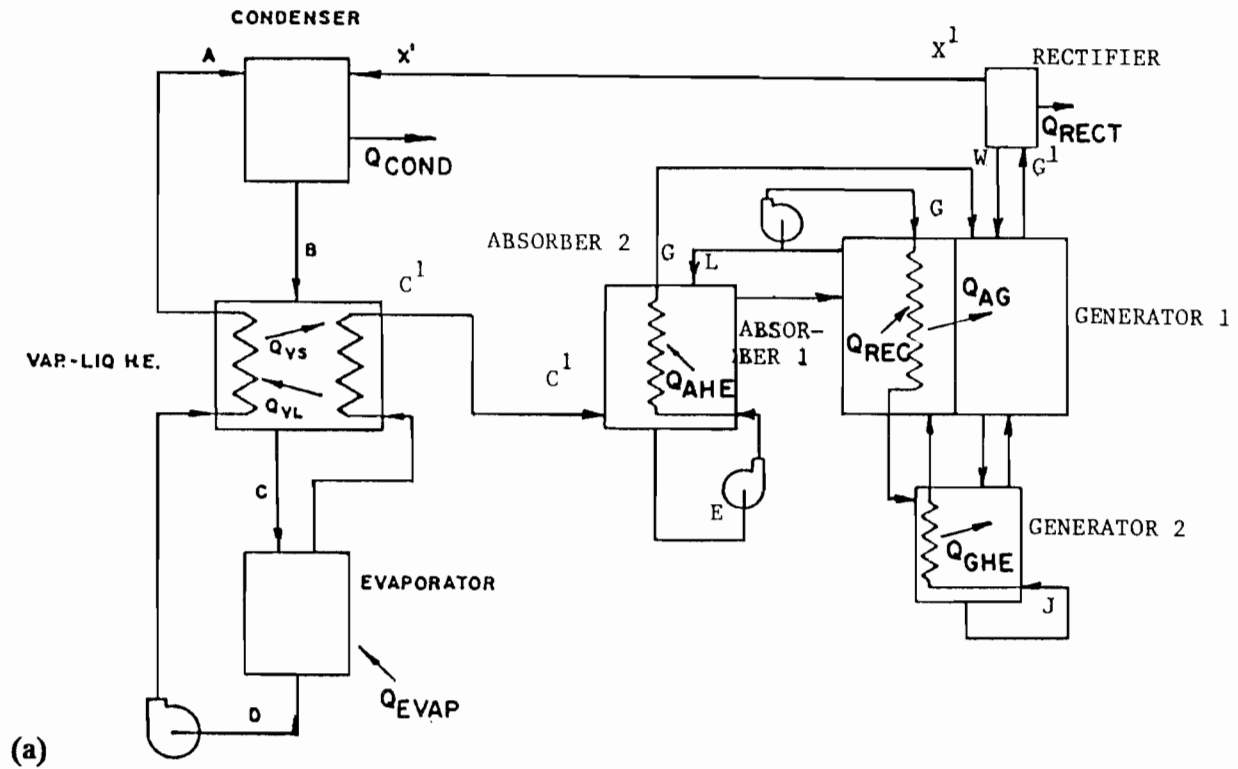
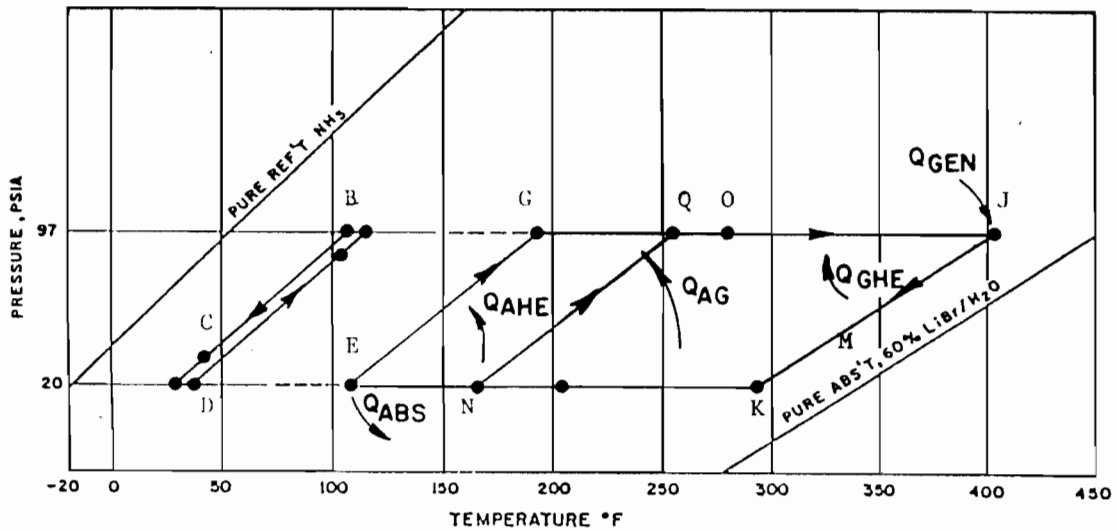


Fig. 15. (a) Circuit schematic and (b) pressure-temperature-composition chart of generator heat exchange/absorber heat exchange, absorber/generator heat exchange, and resorption/desorption circuit for evaporator/condenser.



(a)



(b)

Fig. 16. (a) Circuit schematic and (b) pressure-temperature-composition chart of generator heat exchange/absorber heat exchange, absorber/generator heat exchange, absorbent recirculation, and resorption/desorption circuit for evaporator/condenser.

Table 18. Computer model output for ABS18 (refer to Fig. 15)

Fluid: NH₃/H₂O/LiBr
 Basis: 12,000 Btu/h evaporator input

Point	Pressure (psia)	Temp. (°F)	Flow (lbm/h)	Concen. (NH ₃ /mix)	Enthalpy (Btu/lb)
A	97	105	123.0	0.46	367
B	97	110	144.6	0.54	376
C	19.5	56	144.6	0.54	316
D	19.5	45	123.0	0.46	301
E	19.5	110	87.4	0.275	135
G	97	197	87.4	0.275	190
J	97	400	66.0	0.04	264
K	19.5	292	66.0	0.04	210
I	97	120	2.1	0.5	383
D	19.5	110	21.4	1.0	989
H	97	197	23.5	0.975	1032

External Heat Transfer, Btu/h

Absorber	9,800
Generator	12,000
Condenser + rectifier	14,300
Evaporator	12,000

Internal Heat Transfer, Btu/h

Abs. heat exch.	4,900
Gen. heat exch.	3,500
Abs./Gen. heat exch.	8,700
Vapor/liquid/liquid heat exch.	8,700

COP (thermodynamic), heating 2.00

Table 19. Computer model output for ABS19 (refer to Fig. 16)

Fluid: NH₃/H₂O/LiBr
 Basis: 12,000 Btu/h evaporator input

Point	Pressure (psia)	Temp. (°F)	Flow (lbm/h)	Concen. (NH ₃ /mix)	Enthalpy (Btu/lb)
A	97	105	122.7	0.46	367
B	97	110	144.0	0.54	376
C	19.5	56	144.0	0.54	316
D	19.5	45	122.7	0.46	301
E	19.5	110	72.6	0.275	134
G	97	197	72.6	0.275	190
J	97	400	89.8	0.04	264
K	19.5	292	89.8	0.04	210
Q	97	282	38.7	0.13	218
W	97	120	2.1	0.5	383
C	19.5	110	21.4	1.0	989
G	97	197	23.5	0.975	1032

External Heat Transfer, Btu/h

Absorber	7,700
Generator	9,600
Condenser + rectifier	14,300
Evaporator	12,000

Internal Heat Transfer, Btu/h

Abs. heat exch.	4,000
Gen. heat exch.	4,800
Abs./Gen. heat exch.	10,100
Vapor/liquid/liquid heat exch.	8,700
Abs. recycle heat exch.	1,700

COP (thermodynamic), heating 2.29

Table 20. Computer model output for ABS20 (refer to Fig. 17)

Fluid: NH₃/H₂O/LiBr
 Basis: 12,000 Btu/h evaporator input

Point	Pressure (psia)	Temp. (°F)	Flow (lbm/h)	Concen. (NH ₃ /mix)	Enthalpy (Btu/lb)
A	97	105	123.0	0.46	367
B	97	110	144.4	0.54	376
C	19.5	56	144.4	0.54	316
D	19.5	45	123.0	0.46	301
E	19.5	110	111.5	0.275	134
F	46.3	153	111.5	0.275	161
G	97	197	58.4	0.275	190
I	46.3	197	48.6	0.208	178
J	97	400	115.7	0.04	264
K	19.5	292	66.1	0.04	210
M	46.3	347	49.6	0.04	237
Q	97	257	26.2	0.19	213
S	46.3	267	54.2	0.12	208
U	19.5	163	48.6	0.208	157
V	97	197	54.2	0.12	237
W	97	---	2.1	0.5	383
C	19.5	110	21.4	1.0	995
F	46.3	153	4.6	0.985	982
G	97	197	23.5	0.975	1016

External Heat Transfer, Btu/h

Absorber	6,200
Generator	8,400
Condenser + rectifier	14,300
Evaporator	12,000

Internal Heat Transfer, Btu/h

Abs. & resorber heat exch.	7,700
Desorber & gen. heat exch.	5,900
Abs./Gen. heat exch.	15,200
Vapor/liquid/liquid heat exch.	8,700

COP (thermodynamic), heating 2.45

G. COMBINATIONS ABS7A AND ABS7B

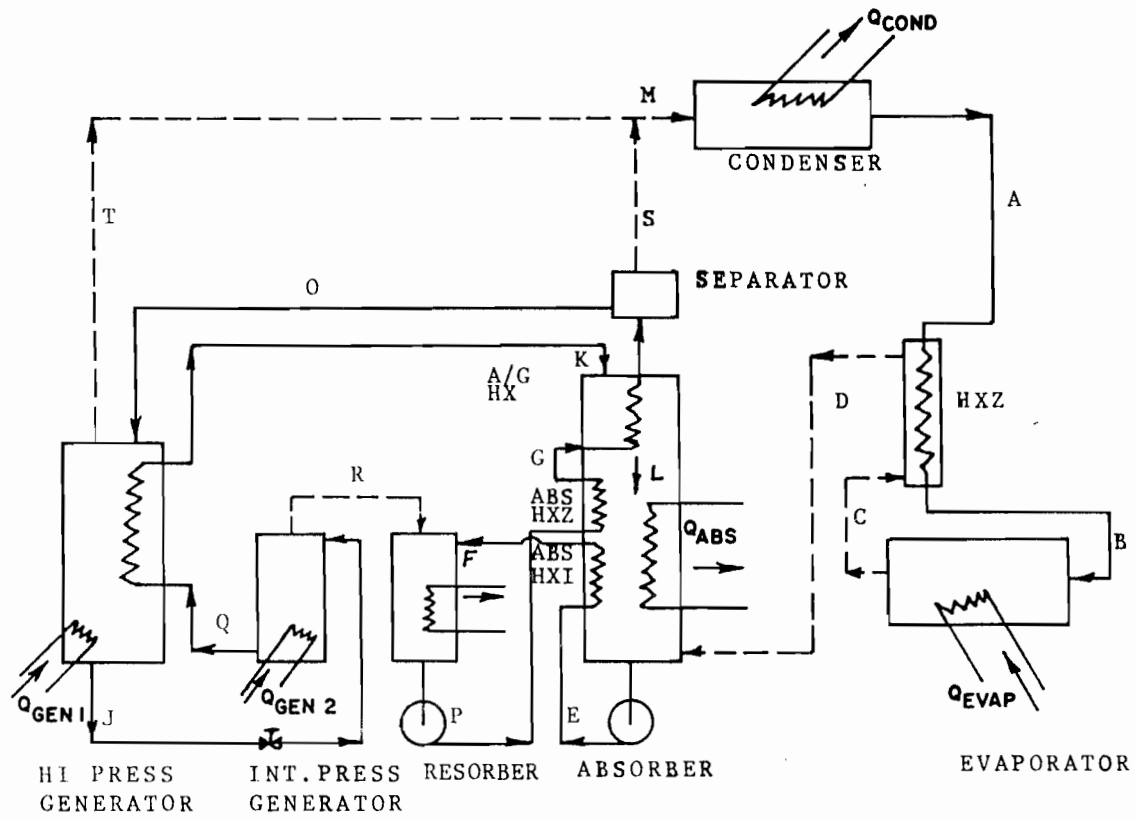
These combinations utilize generator heat exchange/absorber heat exchange, absorber/generator heat exchange, and flash regeneration. The fluids utilized for combinations ABS7A and ABS7B are R22/DMETEG and $\text{NH}_3/\text{H}_2\text{O}$, respectively.

This cycle, shown in Figure 18, is a variation of the regeneration concept designed to increase the temperature overlap for absorber/generator heat exchange. Refrigerant is boiled from solution until concentration J is reached in the generator. The solution is then flashed to an intermediate pressure, releasing additional refrigerant. Additional burner heat input may be required to reach concentration Q. The refrigerant released in the flashing process J-Q is absorbed by the solution at F-P, which widens the overlap of absorber/generator operating temperatures and increases the potential for absorber/generator heat exchange between K-L and O-G.

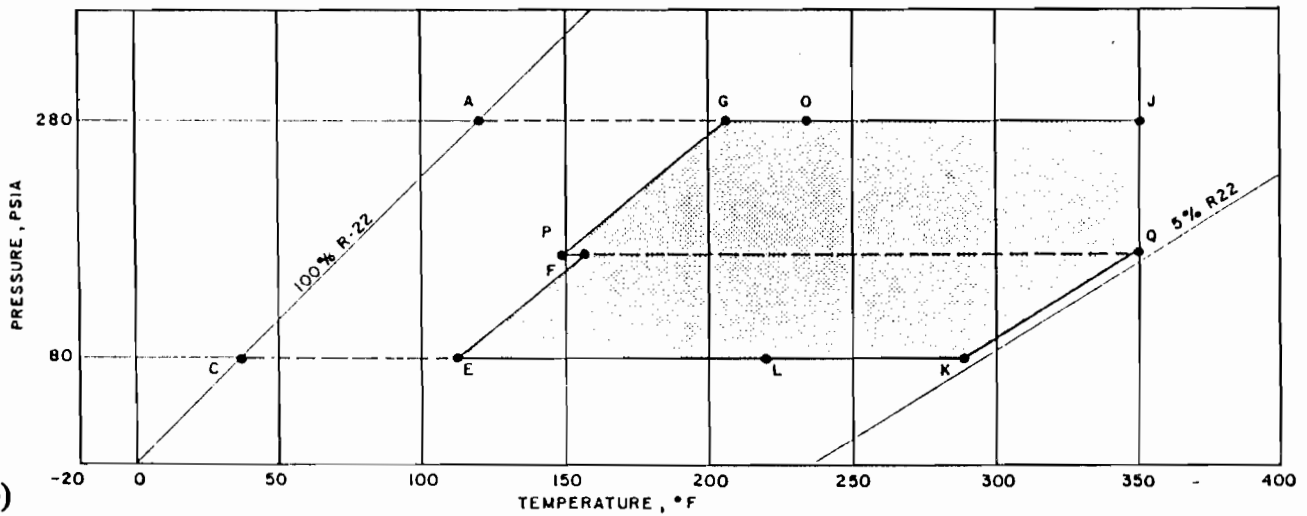
The results for ABS7A are shown in Table 21 and can be compared with the results for the conventional absorber/generator heat exchange that are shown in Table 9. The results in Table 21 indicate that the COP actually has decreased slightly from 1.81 to 1.77.

The results for ABS7B ($\text{NH}_3/\text{H}_2\text{O}$) are shown in Table 22. Figure 18 also applies to ABS7B, except that a rectifier section is required at the top of the generator. In this case, a comparison of the results with the conventional absorber/generator heat exchange cycle (Table 8) shows a larger decrease in the COP, from 1.74 to 1.59. This decrease is partly the result of not including a rectifier on the flash regenerator.

In summary, this concept is not successful in increasing cycle COP. The only real benefit is that lower maximum generator temperatures are required to reach a given solution concentration. Thus, at the expense of a slight decrease in COP, improved stability and corrosion characteristics may be achieved.



(a)



(b)

Fig. 18. (a) Circuit schematic and (b) pressure-temperature-composition chart of generator heat exchange/absorber heat exchange, absorber/generator heat exchange, and flash regeneration.

Table 21. Computer model output for ABS7A (refer to Fig. 18)

Fluid: R22/DMETEG
 Basis: 12,000 Btu/h evaporator input

Point	Pressure (psia)	Temp. (°F)	Flow (lbm/h)	Concen. (R22/mix)	H (Btu/lb)
A	276.4	120.0	160.0	1.000	14.4
B	276.4	79.7	160.0	1.000	1.7
C	78.8	37.0	160.0	1.000	76.5
D	78.8	110.0	160.0	1.000	89.2
E	78.8	110.0	408.0	0.425	-4.6
F	146.6	156.1	408.0	0.425	14.6
G	276.4	209.4	424.0	0.447	37.8
J	276.4	350.0	264.0	0.111	114.5
K	78.8	286.9	248.0	0.054	88.1
L	78.8	219.4	267.0	0.125	54.3
M	276.4	240.4	160.0	1.000	107.7
O	276.4	234.1	363.0	0.355	51.4
P	146.6	146.6	424.0	0.477	9.9
Q	146.6	350.0	248.0	0.054	115.7
R	146.6	175.0	16.0	1.000	98.5
S	276.4	234.1	61.0	1.000	106.4
T	276.4	244.1	99.0	1.000	100.4

External Heat Transfer, Btu/h

Absorber	9,300
Generator 1	15,500
Generator 2	0
Resorber	3,400
Condenser	14,900
Evaporator	12,000

Internal Heat Transfer, Btu/h

Abs. heat exch. 1	7,800
Abs. heat exch. 2	11,800
Gen. heat exch.	7,200
Abs./Gen. HX	9,100
HX2	2,100

COP (thermodynamic), heating 1.77

Table 22. Computer model output for ABS7B (refer to Fig. 18)

Fluid: NH₃/H₂O
 Basis: 12,000 Btu/h evaporator input.

Point	Pressure (psia)	Temp. (°F)	Flow (lbm/h)	Concen. (NH ₃ /mix)	H (Btu/lb)
A	286.5	120.0	24.9	0.998	101.0
B	286.5	89.2	24.9	0.998	64.5
C	68.9	37.0	24.9	0.998	546.1
D	68.9	110.0	24.9	0.998	582.6
E	68.9	110.0	62.2	0.442	-24.4
F	166.4	164.9	62.2	0.442	37.9
G	286.5	206.0	68.5	0.466	84.4
H	286.5	230.5	27.9	0.957	53.4
I	286.5	167.7	3.0	0.608	53.4
J	286.5	330.0	43.6	0.162	264.7
K	68.9	262.8	37.3	0.071	214.5
L	68.9	216.1	24.9	0.171	140.8
M	286.5	160.1	24.9	0.998	579.0
O	286.5	222.6	62.2	0.417	104.1
P	166.4	154.9	68.5	0.466	26.3
Q	166.4	330.0	37.3	0.071	286.8
R	166.4	315.4	6.2	0.707	813.7
S	286.5	222.6	6.2	0.957	646.6
T	286.5	223.6	21.7	0.957	651.6

External Heat Transfer, Btu/h

Absorber	11,400
Generator 1	16,300
Generator 2	4,200
Resorber	5,700
Rectifier	3,500
Condenser	11,900
Evaporator	12,000

Internal Heat Transfer, Btu/h

Abs. heat exch. 1	3,900
Abs. heat exch. 2	4,000
Gen. HX	3,100
Abs./Gen. HX	4,700
HX2	900

COP (thermodynamic), heating 1.59

H. COMBINATION ABS8

Combination ABS8 incorporates a double-effect generator and a cascaded evaporator/absorber with the fluid $H_2O/LiBr$. The flow chart and equilibrium diagram are shown in Figure 19.

The basic $H_2O/LiBr$ cycle cannot operate at nominal heat pump conditions because the salt is not sufficiently soluble to provide the needed vapor-pressure depression for design conditions of 37°F evaporator / 110°F absorber. In addition, pure water cannot be used as refrigerant below its 32°F freezing point, so the cycle cannot operate at the specified low outdoor temperature (17°F).

The cycle shown in Figure 19, however, will operate at the nominal heat pump conditions. This cycle includes two evaporator/absorber stages in cascade arrangement to provide the needed vapor lift, a provision for running 20% LiBr in the low-temperature evaporator to prevent freeze-up, and a double-effect generator to achieve high COP.

As shown in Figure 17, high-pressure refrigerant at V is boiled from the solution in the high-temperature, direct-fired generator at U-J. The intermediate solution is cooled in the liquid/liquid heat exchanger and then goes to the low-temperature generator.

Condensation of the refrigerant from the high-temperature generator acts as the heat source for boiling more refrigerant from the solution in the low-temperature generator at G-S. The strong solutions at S and Y are passed through the liquid/liquid heat exchangers and then to the absorbers, where vapor is absorbed at P-O and K-E. Condenser A and absorber P-O both reject heat to the conditioned space in the heat pump mode. Taking heat from the outdoor air at the low ambient condition, water evaporates from the saltwater (20% LiBr) refrigerant in the low-temperature evaporator at B-C and is absorbed in the low-temperature absorber at K-E. The heat sink for this absorber is the high-temperature evaporator Z-H, connected in cascade arrangement along with absorber P-O.

Initial computer modeling of this concept was done with an outdoor temperature condition of 47°F. Using this temperature simplified the model because a saltwater refrigerant liquid was not needed. The results are shown in Table 23. Because the calculated COP at this condition is well below the project goal, the concept was dropped from further consideration without actually modeling a saltwater refrigerant loop.

I. COMBINATION ABS9

Combination ABS9 incorporates a resorption/desorption cycle to achieve double evaporation using NH_3/H_2O . The flow chart and equilibrium diagram are shown in Figure 20.

Refrigerant is generated by direct heat input at O-J. This refrigerant is condensed at A and evaporated at C. The evaporated refrigerant is resorbed at L-R in the resorption/desorption cycle and then is desorbed at V-Y, producing double-effect evaporation. Absorption of this vapor occurs at K-E.

This combination has a reasonably high COP, as shown in Table 24.

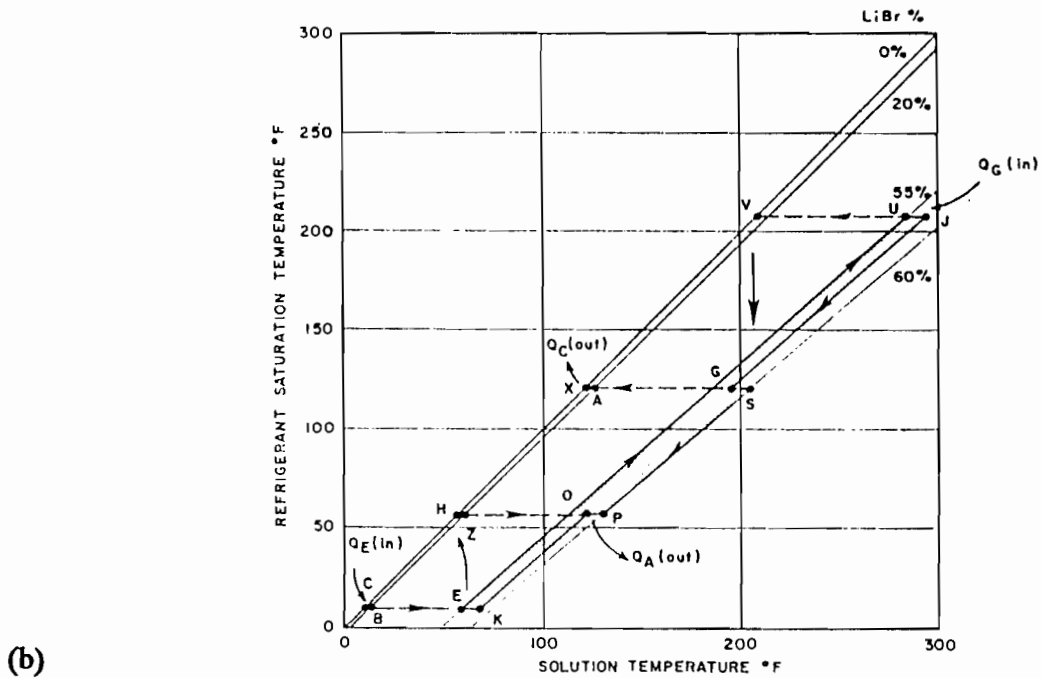
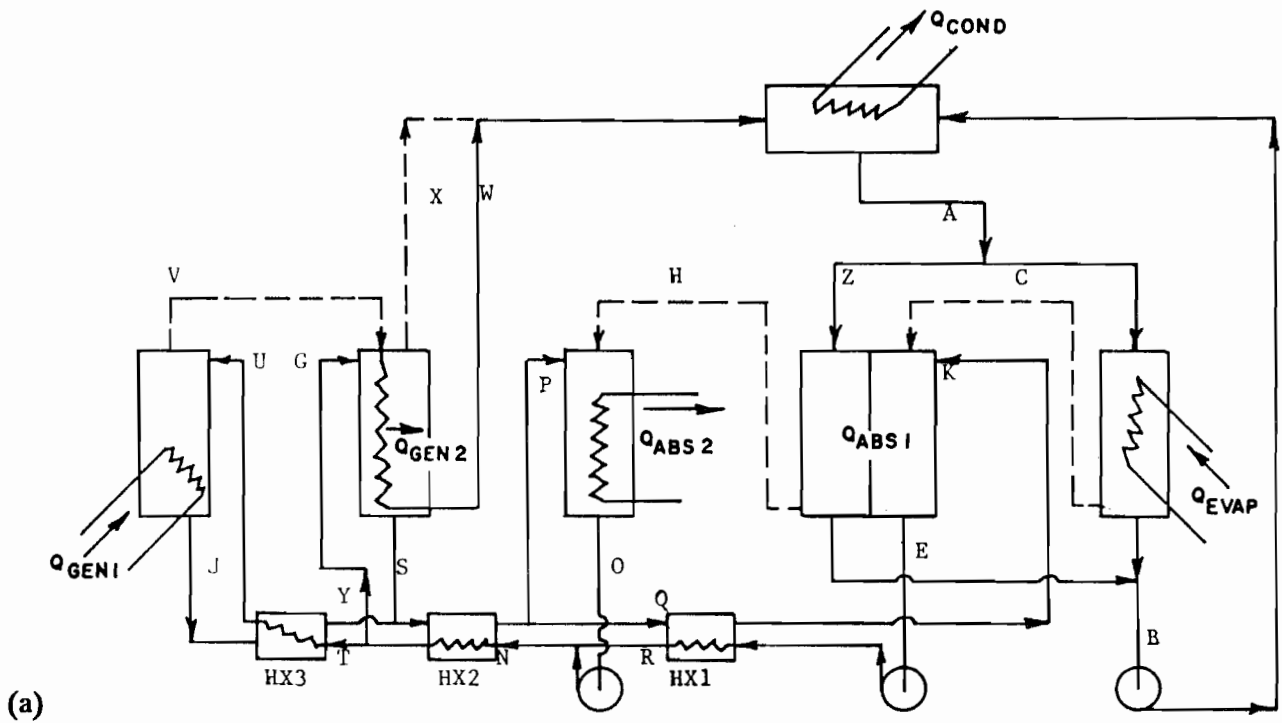


Fig. 19. (a) Circuit schematic and (b) pressure-temperature-composition chart of double-effect generator with cascaded evaporator/absorber.

Table 23. Computer model output for ABS8 (refer to Fig. 19).

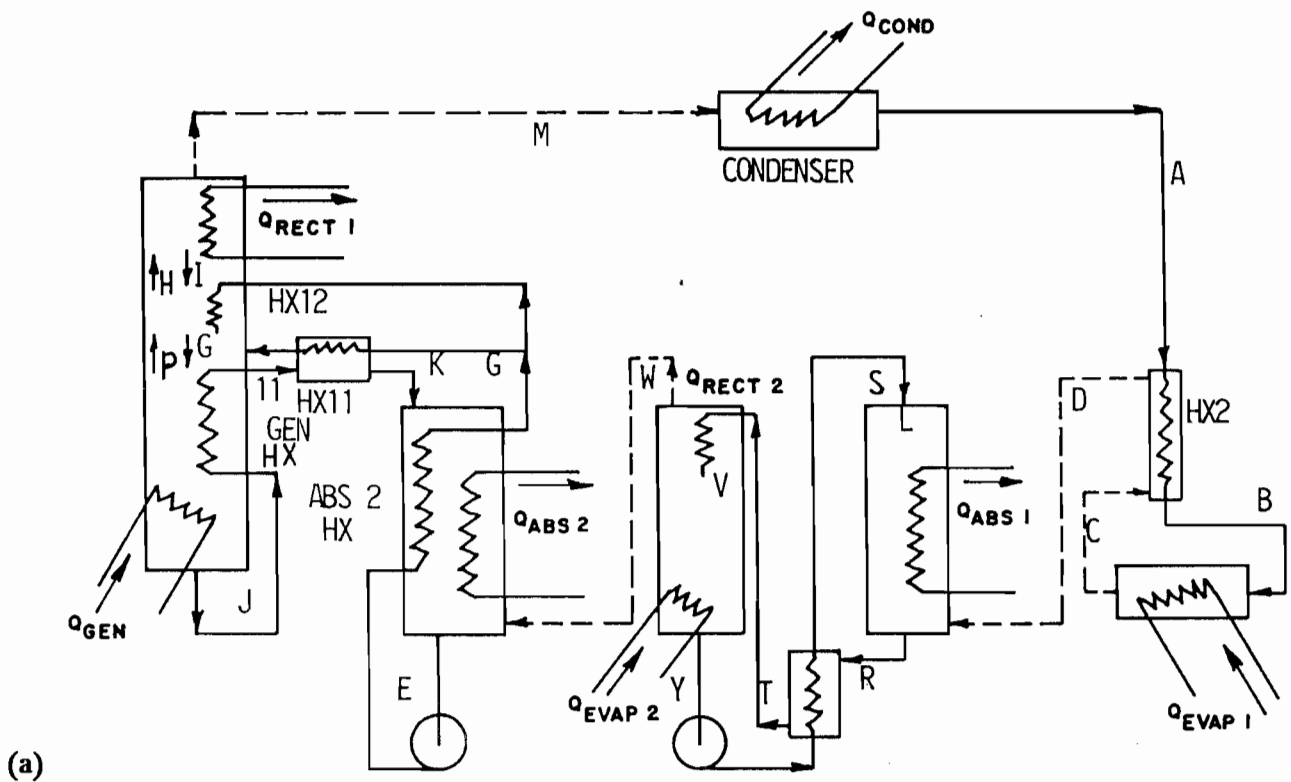
Fluid: H₂O/LiBr
 Basis: 12,000 Btu/h evaporator input

Point	Pressure (psia)	Temp. (°F)	Flow (lbm/h)	Concen. (NH ₃ /mix)	H (Btu/lb)
A	1.69	120.0	32.9	1.000	88.0
C	0.11	37.0	11.8	1.000	1077.6
E	0.11	76.0	77.6	0.489	-658.2
G	1.69	184.0	78.9	0.489	-301.5
H	0.32	97.7	21.0	1.000	1104.5
J	14.13	310.0	116.7	0.398	-22.8
K	0.11	107.8	65.8	0.398	-537.4
N	1.69	131.7	216.7	0.489	-460.7
O	0.32	110.0	139.1	0.489	-534.1
P	0.32	141.7	118.0	0.398	-424.4
Q	0.32	141.7	65.8	0.398	-424.4
R	1.69	131.7	77.6	0.489	-460.4
S	1.69	204.8	66.7	0.398	-242.7
T	1.69	184.0	137.8	0.489	-301.5
U	14.13	260.8	137.8	1.000	-115.0
V	14.13	270.8	21.0	1.000	1178.9
W	14.13	210.0	21.0	1.000	178.1
X	1.69	194.1	11.8	1.000	1147.2
Y	1.69	204.8	116.7	0.398	-242.7
Z	0.32	66.0	21.0	1.000	88.0

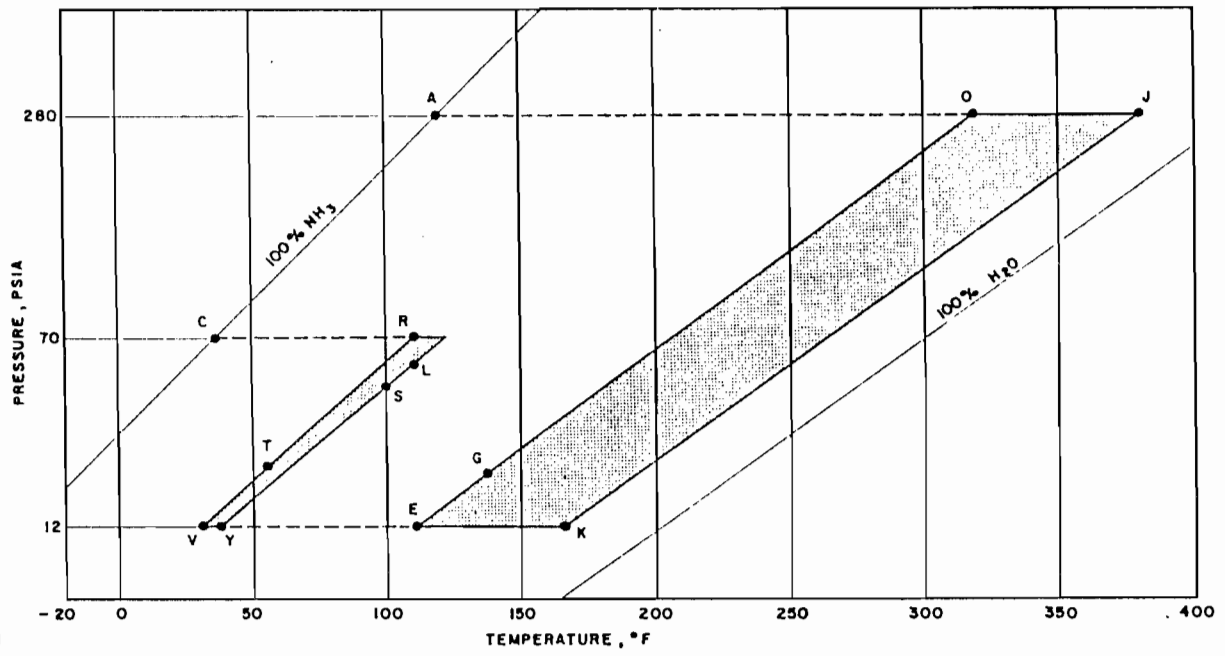
<u>External Heat Transfer, Btu/h</u>	
Absorber 2	37,300
Generator 1	37,800
Condenser	12,500
Evaporator	12,000

<u>Internal Heat Transfer, Btu/h</u>	
Abs. 1	21,400
Gen. 2	20,900
HX1	8,100
HX2	44,700
HX3	25,700

COP (thermodynamic), heating 1.32



(a)



(b)

Fig. 20. (a) Circuit schematic and (b) pressure-temperature-composition chart of double evaporator with resorption/desorption circuit.

Table 24. Computer model output for ABS9 (refer to Fig. 20)

Fluid: NH₃/H₂O
 Basis: 12,000 Btu/h evaporator inputs 1 and 2

Point	Pressure (psia)	Temp. (°F)	Flow (lbm/h)	Concen. (NH ₃ /mix)	H (Btu/lb)
A	286.5	120.0	12.4	0.998	101.0
B	286.5	88.5	12.4	0.998	63.7
C	68.9	37.0	12.4	0.998	546.1
D	68.9	111.7	12.4	0.998	583.5
E	12.3	110.0	94.2	0.188	20.9
G	286.5	137.7	93.9	0.188	51.0
H	286.5	287.9	15.7	0.857	706.8
I	296.5	262.9	3.2	0.312	161.8
J	286.5	380.0	81.5	0.065	344.9
K	12.3	165.4	81.5	0.065	114.6
L	68.9	110.0	0.3	0.188	20.9
M	286.5	160.0	12.4	0.998	579.0
N	286.5	321.1	81.5	0.065	278.8
O	286.5	318.0	93.9	0.188	246.9
P	286.5	338.2	21.2	0.659	833.6
Q	286.5	319.5	8.8	0.185	249.0
R	68.9	110.0	161.4	0.459	-24.6
S	68.9	100.0	148.9	0.415	-34.3
T	68.9	54.9	161.5	0.459	-85.5
V	12.3	30.9	161.5	0.445	-93.7
W	12.3	37.0	11.2	0.985	567.3
Y	12.3	37.0	150.3	0.420	-103.2

External Heat Transfer, Btu/h

Absorber 1	6,100
Absorber 2	11,700
Generator	15,100
Rectifier 1	3,300
Condenser	5,900
Evaporator 1	6,000
Evaporator 2	6,000

Internal Heat Transfer, Btu/h

Abs. 2 HX	2,800
Gen. HX	5,400
Rectifier 2	1,400
HX2	500
HX3	9,800
HX11	13,400
HX12	5,000

COP (thermodynamic), heating 1.80

Several disadvantages of this combination should be considered: (1) the narrow concentration spread requires a high solution-circulation rate, (2) the low refrigerant concentration in the generator feed stream requires a relatively high reflux rate, and (3) the combination cannot work in the heating mode at the low-temperature outdoor rating condition because of the narrow concentration spread. Provision would have to be made to switch to the simple single-stage absorption cycle at low-temperature outdoor conditions.

J. COMBINATIONS ABS10A AND ABS10B

Combinations ABS10A and ABS10B attempt to use R123a/ETFE in a double-effect generator cycle. Combination ABS10A utilizes a resorption/desorption cycle, and combination ABS10B utilizes regeneration. Cycle diagrams for ABS10A and ABS10B are shown in Figures 21 and 22, respectively.

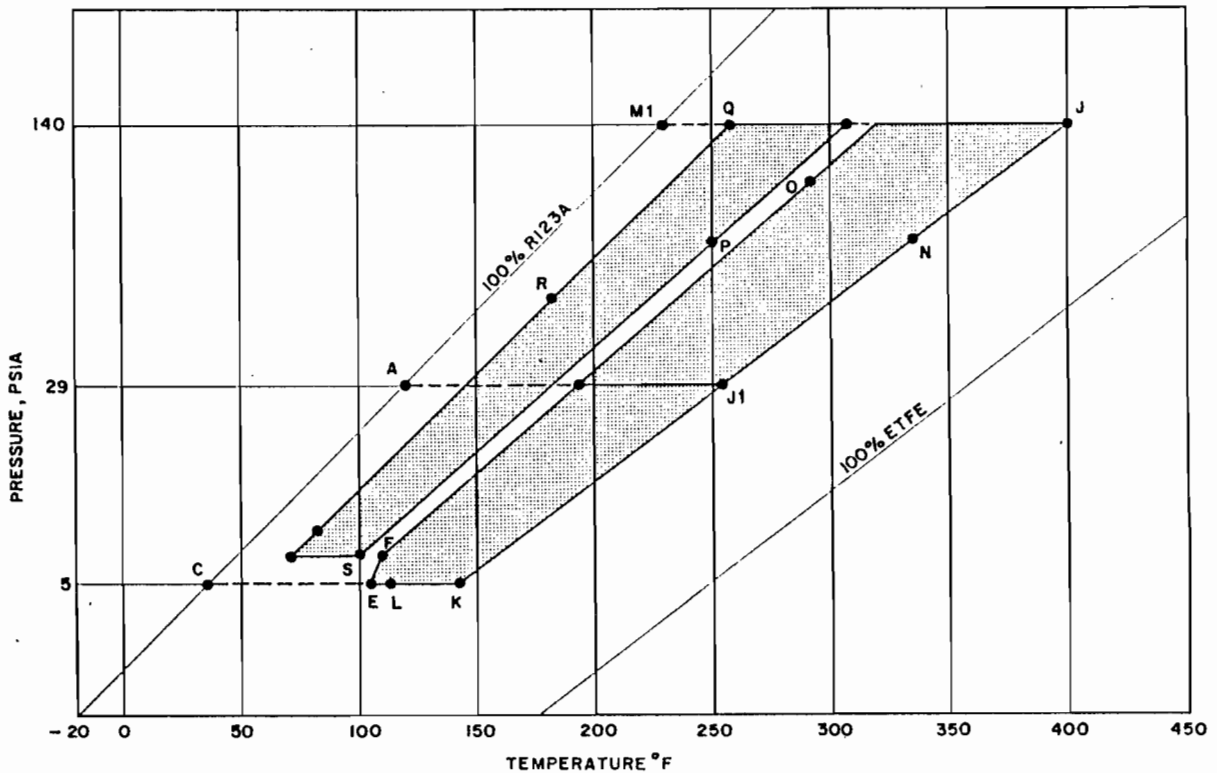


Fig. 21. Pressure-temperature-composition chart of double-effect generator with resorption/desorption circuit.

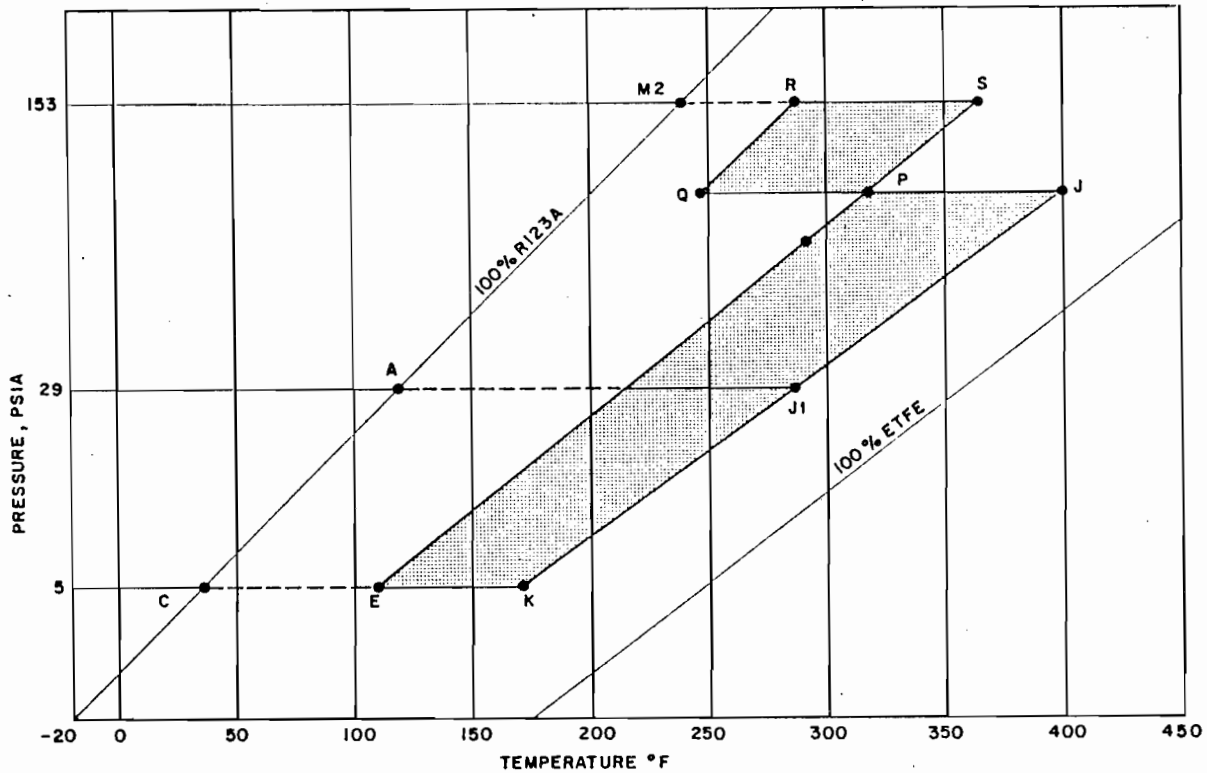


Fig. 22. Pressure-temperature-composition chart of double-effect generator with regeneration.

The conventional double-effect generator cycle (as used commercially by Trane in water-cooled LiBr machines) was considered not practical for air-cooled heat pump operation with R123a/ETFE, because first-stage generator temperatures of about 450°F would be required. Two modified versions of the double-effect concept, involving resorption/desorption and regeneration, were therefore considered. Each appeared potentially to offer the equivalent of about a 1.5-effect generator cycle.

The cycle for ABS10A is illustrated on the equilibrium diagram in Figure 21. In the high-temperature generator, refrigerant is boiled out of solution at G-J. Part of the vapor is condensed as pure refrigerant at M1, and the rest is resorbed by solution P-Q in the resorber. The heat of condensation at M1 and the heat of resorption at P-Q both are used to boil refrigerant out of solution in the low-temperature generator at G1-J1, and this refrigerant is condensed at A. Disregarding heat losses, two units of heat input to the high-temperature generator produce one unit of pure refrigerant at M1 and two units of pure refrigerant at A, thus the 1.5-effect equivalence.

To continue description of the cycle, refrigerant at C is evaporated by heat from the outdoor air and is absorbed by solution K-L-E. The heat of absorption from K-L is used to heat the conditioned air in the heating mode. The heat of absorption from L-E is transferred to the desorber component at R-S where it boils refrigerant from the solution, which in turn is absorbed at E-F. The heat of absorption evolved at E-F also goes toward heating the conditioned space.

This cycle is quite complicated, involving at least 3 solution pumps and several parallel solution-flow paths. The initial results of computer calculations reveal relatively low COPs, as shown in Table 25.

Table 25. Computer output for ABS10A (refer to Fig. 21)

Fluid: R123a/ETFE
 Basis: 12,000 Btu/h evaporator input

Point	Pressure (psia)	Temp. (°F)	Flow (lbm/h)	Concen. (NH ₃ /mix)	H (Btu/lb)
A	28.9	120.0	169.0	0.998	39.5
C	4.9	37.0	169.0	0.998	100.0
E	4.9	106.2	642.0	0.435	32.0
F	6.3	110.0	703.0	0.476	32.5
G	28.9	198.5	313.0	0.476	67.2
J	137.2	400.0	260.0	0.233	180.2
K	4.9	140.6	475.0	0.233	53.2
L	4.9	110.0	607.0	0.401	34.4
N	137.2	335.3	260.0	0.233	144.6
O	137.2	291.8	390.0	0.476	105.2
P	137.2	250.0	49.0	0.531	84.8
Q	137.2	260.0	108.0	0.743	78.8
R	137.2	180.3	108.0	0.743	53.4
S	6.3	100.0	49.0	0.531	27.6
J ₁	28.9	252.6	215.0	0.233	103.8
M ₁	137.2	230.0	69.0	0.998	65.2

External Heat Transfer, Btu/h

Absorber	17,700
Generator	16,400
Rectifier	3,000
Condenser	7,800
Evaporator	12,000

Internal Heat Transfer, Btu/h

Q1	4,700
Q2	4,500
Other exchangers	60,200

COP (thermodynamic), heating 1.73

The addition of more heat recovery schemes to improve COP makes the cycle so complex that the system is impractical. Preparation of a schematic diagram of the cycle for this report was not considered justified because of the cycle's complexity and the lack of further interest in the cycle.

The cycle for ABS10B is illustrated on the equilibrium diagram in Figure 22. At the high temperature, intermediate-pressure refrigerant is regenerated by direct heat input at conditions O-J, and this regenerated refrigerant is absorbed at P-Q. Solution Q is pumped to the first-stage generator where refrigerant is boiled out of the solution by direct heat input at conditions R-S, and this refrigerant is condensed as pure refrigerant in the high-temperature condenser at M2. The heat of absorption evolved at P-Q and the heat of condensation evolved at M2 are used to produce more pure refrigerant from the low-temperature generator at G-J1. Thus, if heat losses are disregarded, one unit of burner heat input at O-J and one unit of burner heat input at R-S combine to produce one unit of refrigerant at M2 and two units at A, hence the 1.5-effect equivalence.

To continue the cycle description, refrigerant is evaporated at C and is absorbed by solution at K-E. The solution K comes from both the first-stage generator R-S and the second-stage generator G-J1.

The computed results are shown in Table 26. Like the preceding example, this cycle is quite complicated, especially when several heat exchangers are added to raise the COP to a reasonable value. It was concluded that this cycle also is too complicated to be practical and that preparation of a schematic diagram was not justified.

Table 26. Computer output for ABS10B (refer to Fig. 22)

Fluid: R123a/ETFE
 Basis: 12,000 Btu/h evaporator input

Point	Pressure (psia)	Temp. (°F)	Flow (lbm/h)	Concen. (NH ₃ /mix)	H (Btu/lb)
A	28.9	120.0	169.0	0.998	39.5
C	4.9	37.0	169.0	0.998	100.0
E	4.9	110.0	548.0	0.395	34.5
G	28.9	203.3	308.0	0.395	72.7
J	95.8	400.0	166.0	0.126	190.7
K	4.9	171.4	213.0	0.126	190.7
O	95.8	291.1	238.0	0.395	110.4
P	95.8	317.8	91.0	0.383	123.6
Q	95.8	241.3	166.0	0.657	75.8
R	153.0	288.8	166.0	0.657	92.9
S	153.0	363.9	91.0	0.383	146.3
J ₁	28.9	287.8	213.0	0.126	129.0
M ₂	153.0	240.0	74.0	0.998	67.6

External Heat Transfer, Btu/h

Absorber	15,500
Generator 1	10,800
Generator 2	8,100
Rectifier 1	3,700
Rectifier 2	1,700
Rectifier 3	1,900
Condenser	8,100
Evaporator	12,000

Internal Heat Transfer, Btu/h

Q1	4,700
Q2	5,900
Other exchangers	48,800

COP (thermodynamic), heating 1.63

K. COMBINATION ABS11

Combination ABS11 incorporates a double-effect generator, common-condenser cycle with generator heat exchange/absorber heat exchange. The fluid employed is $\text{NH}_3/\text{H}_2\text{O}$.

The flow schematic and equilibrium diagram are shown in Figure 23. Refrigerant is generated at O1-J1 by direct heat addition and at O-J by heat Q2 from the high-temperature absorption process at E1-K1 and by heat Q1 from the high temperature rectifier. All the refrigerant is condensed at A and is evaporated at C, with some of it going to the high-temperature absorber at E1-K1 and some to the low-temperature absorber at E-K.

Table 27 shows computer model calculations for ABS11. The COP is the highest of any of the binary fluid systems investigated, but this concept has the same disadvantages as combination ABS9: (1) the narrow concentration spread requires a high solution-circulation rate, (2) the low refrigerant concentration in the generator feed stream requires a relatively high reflux rate, and (3) the combination cannot work in the heating mode at the low-temperature outdoor heating condition because of the narrow concentration spread. Provision would have to be made to switch to the simple single-stage absorption cycle at low-temperature outdoor conditions.

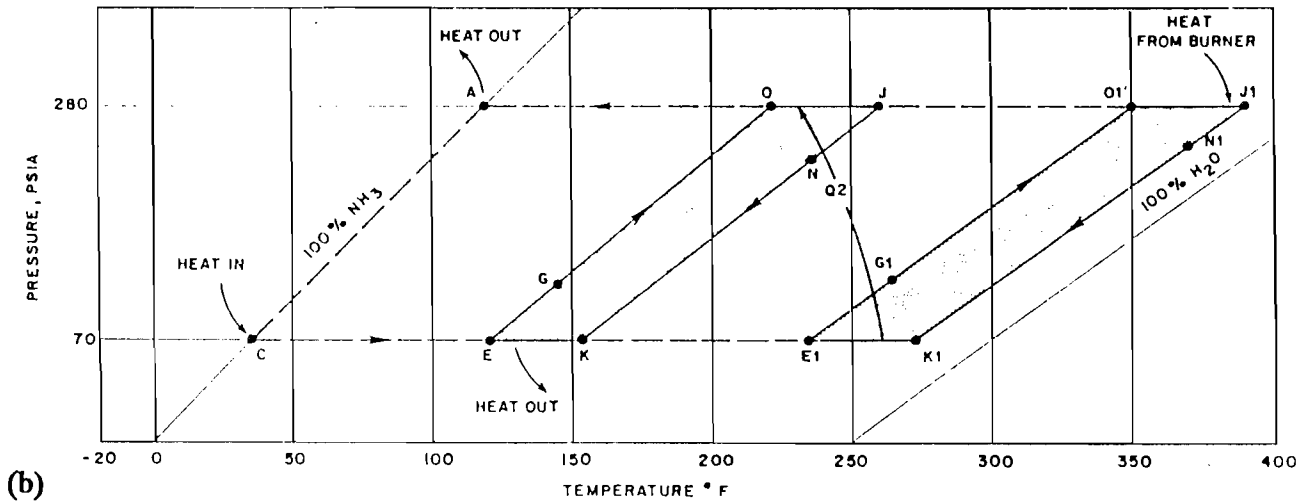
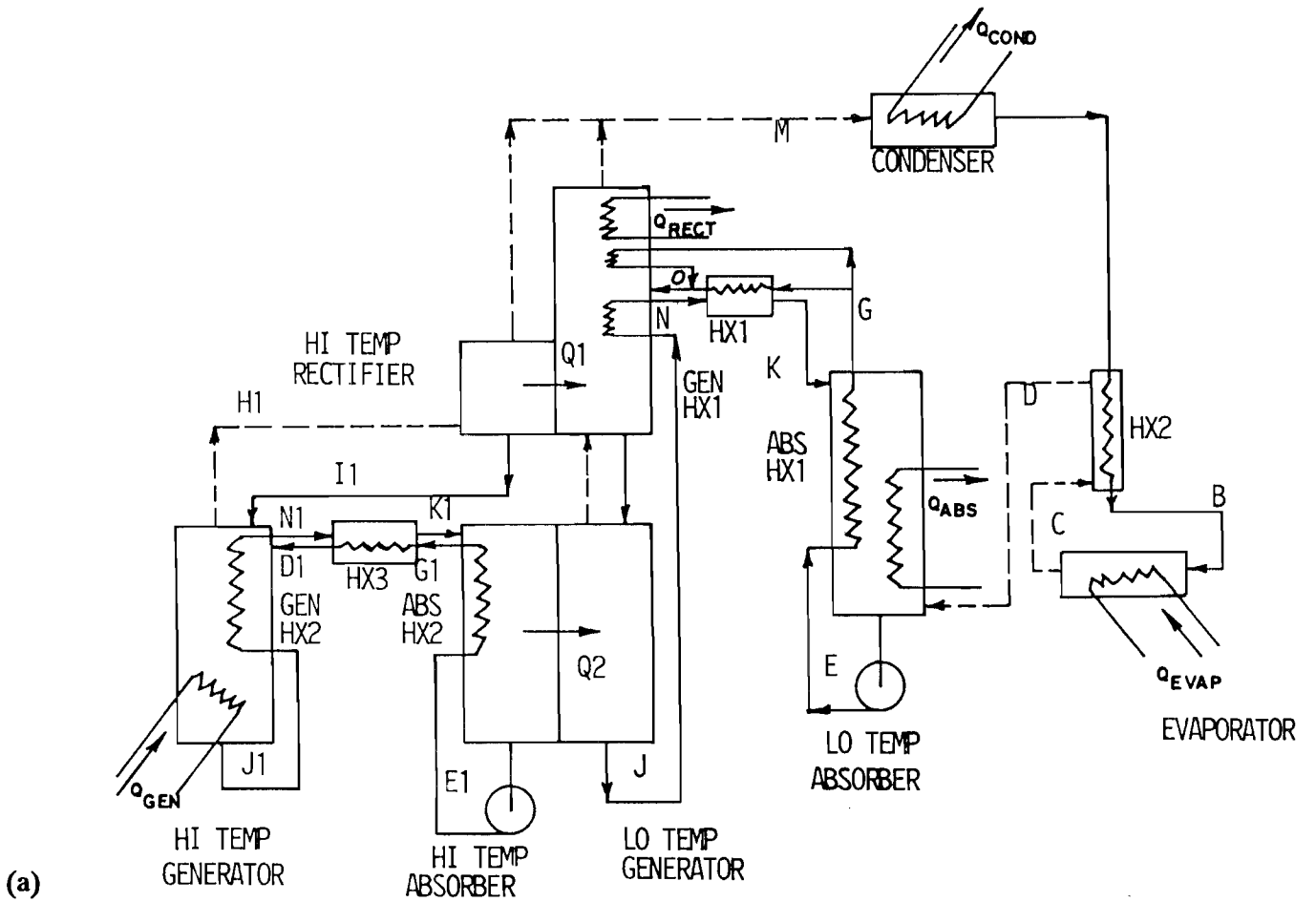


Fig. 23. (a) Circuit schematic and (b) pressure-temperature-composition chart of double-effect generator with generator heat exchange/absorber heat exchange.

Table 27. Computer output for ABS11 (refer to Fig. 23)

Fluid: NH₃/H₂O
 Basis: 12,000 Btu/h evaporator input

Point	Pressure (psia)	Temp. (°F)	Flow (lbm/h)	Concen. (NH ₃ /mix)	H (Btu/lb)
A	286.5	120.0	24.9	0.998	101.0
B	286.5	89.2	24.9	0.998	64.5
C	68.9	37.0	24.9	0.998	546.1
D	68.9	110.0	24.9	0.998	582.6
E	68.9	110.0	99.5	0.456	-24.6
G	286.5	137.9	99.5	0.456	7.0
J	286.5	250.0	82.6	0.345	142.0
K	68.9	147.7	82.6	0.345	26.7
M	286.5	160.0	24.9	0.998	579.0
N	286.5	223.5	82.6	0.345	112.3
O	286.5	209.3	99.5	0.456	88.1
E ₁	68.9	220.0	81.6	0.157	148.5
G ₁	286.5	254.2	81.6	0.157	185.1
H	286.5	344.2	14.9	0.627	854.4
I	286.5	315.9	6.9	0.193	243.7
J ₁	286.5	380.0	73.5	0.065	344.9
K ₁	68.9	266.2	73.5	0.065	219.7
N ₁	286.5	333.0	81.6	0.065	312.6
O ₁	286.5	333.0	81.6	0.157	268.8

External Heat Transfer, Btu/h

Absorber	11,300
Generator	12,100
Rectifier	900
Condenser	11,900
Evaporator	12,000

Internal Heat Transfer, Btu/h

Abs. HX1	3,100
Abs. HX2	3,000
Gen. HX1	2,500
Gen. HX2	2,400
HX1	7,100
HX2	900
HX3	6,800
Q1	6,400
Q2	5,700

COP (thermodynamic), heating 1.99

VI. SELECTION OF PREFERRED CYCLE/FLUID COMBINATIONS

A summary of the cycle/fluid combinations described in the previous section is provided in Table 28. Table 29 shows the primary outputs that are of interest from the computer model calculations, namely, heating COP, theoretical pump power, and internal heat transfer. Basically, heating COP and theoretical pump power affect operating cost, while internal heat transfer influences the first cost of the system.

To make a rigorous comparison of the various systems including the effects of the three parameters, a rating procedure was developed based on penalty points. The method of assigning penalty points is shown in Table 30. The ranking of the systems according to this procedure is shown in Table 31. The following are some observations concerning the rankings:

1. The nine highest-ranking cycle/fluid combinations are ternary fluid systems.
2. The four highest-ranking systems utilize the ternary mixture $\text{NH}_3/\text{H}_2\text{O}/\text{LiBr}$.
3. The three highest-ranking binary mixture systems utilize the mixture $\text{NH}_3/\text{H}_2\text{O}$.
4. The highest-ranking binary system utilizes regeneration, absorber/generator heat exchange, and generator heat exchange/absorber heat exchange.
5. The second highest-ranking binary system is a double-effect generator, common-condenser system with generator heat exchange/absorber heat exchange. Nevertheless, while the system looks good at the 47/43/70 rating condition, operation would not be possible in the double-effect mode at the 17/15/70 condition.
6. The third highest-ranking binary system is a somewhat simpler system utilizing both absorber/generator heat exchange and generator heat exchange/absorber heat exchange.

Table 28. Cycle/fluid combinations

Cycle/Fluid Designation	Fluid	Cycle
ABS1	NH ₃ /H ₂ O	Generator heat exchange/absorber heat exchange
ABS2	R22/DMETEG	Generator heat exchange/absorber heat exchange
ABS3	R123a/ETFE	Generator heat exchange/absorber heat exchange
ABS4	NH ₃ /H ₂ O	Absorber/generator heat exchange, generator heat exchange/absorber heat exchange
ABS5	R22/DMETEG	Absorber/generator heat exchange, generator heat exchange/absorber heat exchange
ABS6A	R22/DMETEG	Regeneration, absorber/generator heat exchange, generator heat exchange/absorber heat exchange
ABS6B	NH ₃ /H ₂ O	Regeneration, absorber/generator heat exchange, generator heat exchange/absorber heat exchange
ABS7A	R22/DMETEG	Two-stage absorption, flash regeneration abs./gen. heat exch., gen. heat exch./abs. heat exch.
ABS7B	NH ₃ /H ₂ O	Two-stage absorption, flash regeneration abs./gen. heat exch., gen. heat exch./abs. heat exch.
ABS8	LiBr/H ₂ O	Double-effect generator, cascaded evaporator/absorber
ABS9	NH ₃ /H ₂ O	Use of resorption/desorption cycle to achieve double effect evaporation
ABS10A	R123a/ETFE	Double-effect generator with resorp./desorp. cycle
ABS10B	R123a/ETFE	Double-effect generator with regeneration
ABS11	NH ₃ /H ₂ O	Double-effect generator, common condenser, generator heat exchange/absorber heat exchange
ABS12	NH ₃ /H ₂ O/LiBr	Abs./gen. heat exch., gen. heat exch./abs. heat exch.
ABS13	NH ₃ /H ₂ O/LiBr	Same as ABS12 plus absorbent recirculation
ABS14	NH ₃ /H ₂ O/LiBr	Same as ABS13 plus regeneration
ABS15	CH ₃ NH ₂ /H ₂ O/LiBr	Same as ABS12
ABS16	CH ₃ NH ₂ /H ₂ O/LiBr	Same as ABS13
ABS17	CH ₃ NH ₂ /H ₂ O/LiBr	Same as ABS14
ABS18	NH ₃ /H ₂ O/LiBr	Same as ABS12 except resorption/desorption cycle substituted for conventional evaporator/condensor
ABS19	NH ₃ /H ₂ O/LiBr	Same as ABS13 except resorption/desorption cycle substituted for conventional evaporator/condensor
ABS20	NH ₃ /H ₂ O/LiBr	Same as ABS14 except resorption/desorption cycle substituted for conventional evaporator/condensor
ABS21	CH ₃ OH/LiBr/ZnBr	Generator heat exchange/absorber heat exchange

Table 29. Computer model results

Cycle/Fluid Designation	COP _H *	Theoretical Pump Power, W**	Internal Heat Transfer, Btu/h**
ABS1	1.67	6.5	6,000
ABS2	1.77	33.3	16,200
ABS3	1.75	3.9	15,300
ABS4	1.74	5.9	7,200
ABS5	1.81	32.4	18,600
ABS6A	1.72	54.6	30,100
ABS6B	1.94	8.3	14,000
ABS7A	1.77	33.0	16,600
ABS7B	1.59	6.0	6,100
ABS8	1.32	0.3	29,100
ABS9	1.80	14.7	17,000
ABS10A	1.73	21.0	29,300
ABS10B	1.63	12.0	23,100
ABS11	1.99	20.1	18,900
ABS12	2.08	6.6	9,100
ABS13	2.19	7.8	10,800
ABS14	2.32	10.0	14,300
ABS15	1.87	2.9	8,000
ABS16	2.09	3.9	11,200
ABS17	2.18	3.9	14,400
ABS18	2.00	7.2	12,800
ABS19	2.29	8.5	16,000
ABS20	2.45	9.9	22,000
ABS21	1.58	2.8	10,900

* Neglecting flue losses.

** Per 12,000 Btu/h Heating.

Table 30. Definition of penalty points

Penalty Points	COP _H	Theoretical Pump Power, W*	Internal Heat Transfer, MBH*†
-5	2.5	---	---
-4	2.4	---	---
-3	2.3	---	---
-2	2.2	---	---
-1	2.1	---	---
0	2.0	0	0
1	1.9	10	12
2	1.8	20	24
3	1.7	30	36
4	1.6	40	48
etc.	etc.	etc.	etc.

* per 12,000 Btu/h heating

† MBH = million Btu/h

Table 31. Ranking of cycle/fluid combinations

Rank	Cycle/Fluid Designation	COP	Penalty Points Pump Power	IHE	Total	Sensitivity Analysis
**1	ABS20	-4.5	1.0	1.8	-1.7	0.1
2	ABS14	-3.2	1.0	1.2	-1.0	0.2
3	ABS19	-2.9	0.8	1.3	-0.8	0.5
4	ABS13	-1.9	0.8	0.9	-0.2	0.7
5	ABS17	-1.8	0.5	1.2	-0.1	1.1
6	ABS16	-0.9	0.4	1.0	0.5	1.5
7	ABS12	-0.8	0.7	0.8	0.7	1.5
8	ABS18	0	0.7	1.1	1.8	2.9
9	ABS15	1.3	0.3	0.7	2.3	3.0
**10	ABS6B	0.6	0.8	1.2	2.6	3.8
11	ABS11	0.1	2.0	1.6	3.7	5.3
**12	ABS4	2.6	0.6	0.6	3.8	4.4
**13	ABS3	2.5	0.4	1.3	4.2	5.5
**14	ABS1	3.3	0.7	0.5	4.5	5.0
15	ABS9	2.0	1.5	1.4	4.9	6.3
16	ABS7B	4.1	0.6	0.5	5.2	5.7
17	ABS21	4.2	0.3	0.9	5.4	6.3
18	ABS5	1.9	3.2	1.6	6.7	8.3
19	ABS10B	3.7	1.2	1.9	6.8	8.7
20	ABS2	2.3	3.3	1.4	7.0	8.4
21	ABS7A	2.3	3.3	1.4	7.0	8.4
22	ABS10A	2.7	2.1	2.4	7.2	9.6
23	ABS8	6.8	0	2.4	9.2	11.6
24	ABS6A	2.8	5.5	2.5	10.8	13.3

* Total with double penalty points for Internal Heat Exchange.

** Selected for more detailed economic analysis.

SENSITIVITY ANALYSIS

Questions might be raised about the validity of the penalty point method of ranking systems as defined in Table 30. Concerning the relative importance of heating COP and theoretical pump power, however, it can be shown that a 1-penalty-point differential translates into approximately the

same operating-cost differential for gas and electricity usage when burner efficiency, pump efficiency, motor efficiency, and typical electricity and gas prices are used. The biggest question is how the penalty points assigned to operating cost (COP and pump power) compare with the penalty points assigned to first cost (internal heat transfer).

A first-order analysis shows that a 1-penalty-point differential in internal heat transfer will give a 5- to 10-year payback if an efficiency improvement can be achieved comparable to a 1-penalty-point differential in heating COP and pump power. Because this payback is longer than is generally accepted in commercial and residential products, the ranking is repeated with the penalty points for internal heat transfer doubled. This would translate into a 2.5- to 5-year payback. The results are shown in the far right column of Table 31.

Doubling the penalty points for internal heat transfer has no effect on the ranking of the top ten cycle/fluid combinations. Nevertheless, it does affect the relative ranking of the second through the fifth highest-ranking binary fluid systems, with the double-effect system moving from the second to the fourth highest-ranking binary fluid system.

The five systems selected for further economic analysis are identified in Table 31. Four of these were selected from the top five binary fluid systems, primarily because this work was done before the scope of the project was expanded to include ternary fluids. The other system chosen was the highest ranking ternary fluid system. The second-ranking binary system, the double-effect generator, was dropped from consideration because of its operational problems at low ambient temperatures and because the sensitivity analysis showed a lower ranking when more emphasis was placed on first cost in the ranking procedure.

VII. PRELIMINARY SYSTEM DESIGNS AND INSTALLED COST ESTIMATES

Preliminary system designs were developed for each of the five systems selected for further economic analysis. The design concept selected would use a secondary fluid loop for both the indoor and outdoor coils. System reversal was accomplished by switching secondary fluid flows. Parametric studies were conducted using the computer models to investigate efficiency/cost trade-offs for each design. Designing the ABS1 and ABS3 systems to meet or exceed project COP goals was determined to be impractical, so designs were selected that did not meet the goals. The other three systems met or exceeded project COP goals, although ABS4 required very small approach temperatures for the solution-side heat exchanger and relatively large air-side heat exchangers. Cost estimates were developed for a 100-ton unit of each of the five preliminary designs. In most cases, cost estimates were based on the fabrication costs of similar equipment in this size range. Thus, heat exchanger designs and materials were not specified, but costs were assumed to be similar to the costs of two-stage absorption chillers with comparable heat transfer requirements.

A summary of the performance and installed-cost estimates of the five preliminary designs are given in Table 32. The high installed cost of the ABS3 system should be noted; it is caused in large part by an attempt to utilize brazed aluminum construction in the design. It was found, however, that large-frontal-area brazed exchangers were required to avoid flooding in the rectifier and absorber sections, resulting in higher-than-expected exchanger costs. Although the costs of a more conventional design were not estimated, they would be higher than those of the ABS4 or ABS6B designs because of lower heat and mass transfer coefficients for the R123a/ETFE vs. NH₃/H₂O and because of higher internal heat transfer requirements. Thus, the ABS3 was dropped from further consideration.

Table 32. Summary of preliminary system performance and installed cost

(Size basis for all systems is 100-ton cooling capacity @ 95°F.)

Characteristic	Cycle Designation				
	ABS1	ABS3	ABS4	ABS6B	ABS20
<i>Cooling (45°F glycol solution circulated to conditioned space)</i>					
Capacity (MBH) @ 95°F	1200	1200	1200	1200	1200
(MBH) @ 115°F	1060	--	960	1020	9000
COP (incl. 85% @ 95°F comb. eff.)	0.56	0.65	0.80	0.91	1.21
@115°F	0.51	--	0.64	0.78	0.90
<i>Heating (120°F glycol solution circulated to conditioned space)</i>					
Capacity (MBH) @47°F	2880	2880	2380	2170	2050
@ 17°F	2740	--	2060	1870	1570
COP (incl. 85% @ 47°F comb. eff.)	1.35	1.55	1.61	1.65	2.08
@ 17°F	1.29	--	1.40	1.41	1.59
<i>Parasitic power</i>					
Fanpower, outdoor (kW)	15	15	15	15	15
indoor (kW)	13	13	13	13	13
Glycol sol'n pump, outdoor, kW	4	4	4	4	4
indoor, kW	4	4	4	4	4
Solution pump, kW	6	3.5	5.3	7.4	9
<i>Cost</i>					
Installed cost	\$60,900	\$143,200	\$78,500	\$79,500	\$90,500

VIII. USER ECONOMICS

The parameters used in examining the economic feasibility of the absorption heat pump systems were simple payback (SPB) period and after-tax internal rate of return (IRR). The following assumptions were used in computing these parameters:

● Equipment Life	20 years
● Tax Rate	48%
● Investment Tax Credit	10%
● Property Tax	1%
● Insurance	0.5%
● Inflation Rate	7%
● Energy Cost Escalation Rate (including inflation)	
Gas: 1984, 1985	12%
after 1985	9%
Electricity: 1984, 1985	10%
after 1985	7%

TRACE, Trane's computer program for building-system energy and economic analysis, was used to compare the various system alternatives. An apartment building with a design cooling load of 155 tons was used. System alternatives were compared to a reference system that included an air-cooled reciprocating water chiller and a gas-fired boiler. The primary analysis was conducted using Chicago weather data, 1983 Commonwealth Edison electricity prices, and \$0.55/therm gas prices. In addition, the effects of geographic region and electricity prices were investigated by including weather data from New York and Atlanta and electricity prices of Con-Edison and Georgia Power.

Typical results from the TRACE program are shown in Table 33 for the Chicago location. SPB and IRR values look quite good for the ABS4, ABS6B, and ABS20 systems when compared with the reference system. There is not a great deal of difference among the three systems, but ABS4 is best. System ABS3 was discarded previously, and System ABS1 is not shown in Table 33 because it has a negative payback (i.e., operating costs are higher than those of the reference system). This is not surprising because neither of these systems met project design goals for efficiency.

Table 33. Results of user economics analysis

Basis: Apartment building in Chicago climate with Commonwealth Edison rate structure. All costs in 1983 dollars.

Parameters		System			
		Conventional	ABS4	ABS20	ABS6B
Input	Size, tons cooling	155	155	155	155
	Installed cost, \$/ton	490	678	780	687
	Heating COP, 47°F	0.8	1.61	2.08	1.65
	Heating COP, 17°F	0.8	1.37	1.59	1.41
	Cooling COP, 95°F	3.0	0.80	1.21	0.91
	Cooling COP, 115°F	--	0.64	0.90	0.78
	Parasitic power, kW/ton	0.18	0.283	0.319	0.304
Output	Ann. elec. consump., kW/h	1022	1017	1074	1044
	Ann. gas consump., therms	83.1	64.5	48.1	63.7
	Elect. cost, energy	50.5	49.3	51.5	50.5
	Elect. cost, demand, \$	15.0	12.9	13.3	13.1
	Gas cost, \$	45.7	35.5	27.7	35.0
	Total utility cost, \$	111.2	97.7	91.7	98.7
	SPB, years	--	2.2	2.3	2.5
	IRR, %	--	37	30	34.2

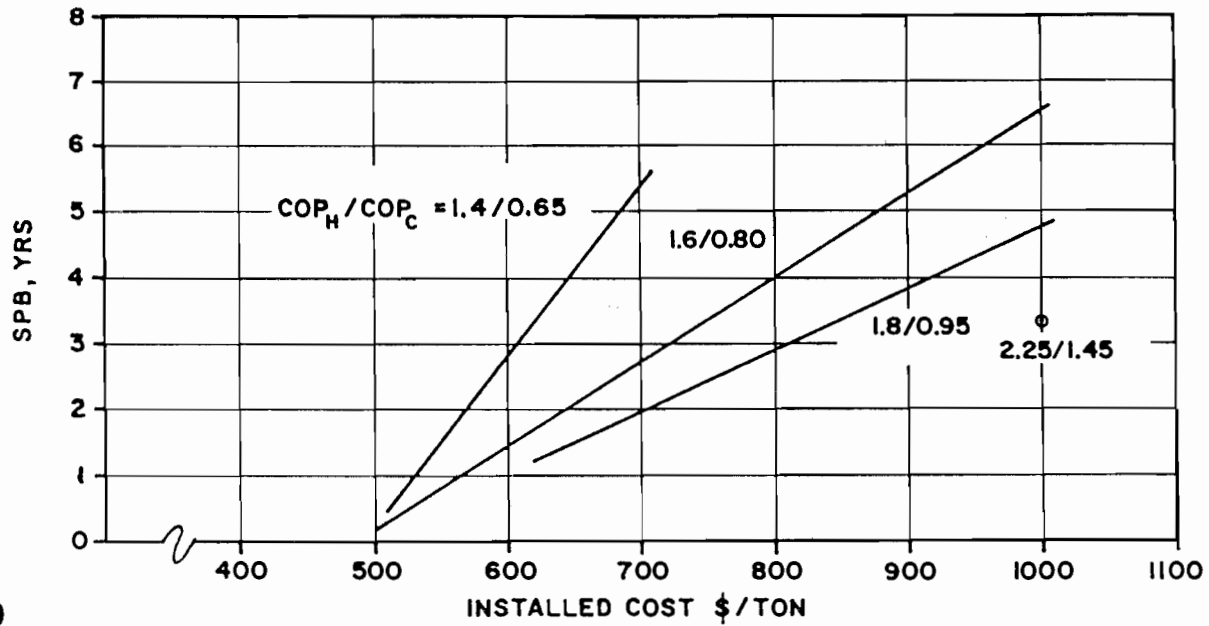
Other points to be noted concerning Table 33 are as follows:

- The installed cost figures do not agree with those in Table 32 because \$/ton decreases with increasing tons.
- The annual electric consumption numbers include everything for the building, not just HVAC equipment.
- Two of the three absorption systems require more annual electrical energy than does the conventional system, because the absorption system pumps were assumed to run continuously while gas flow was modulated.
- The absorption systems all show slightly lower electric energy costs because of lower demand charges. Demand charges are higher today than in 1983 and are on an increasing trend.

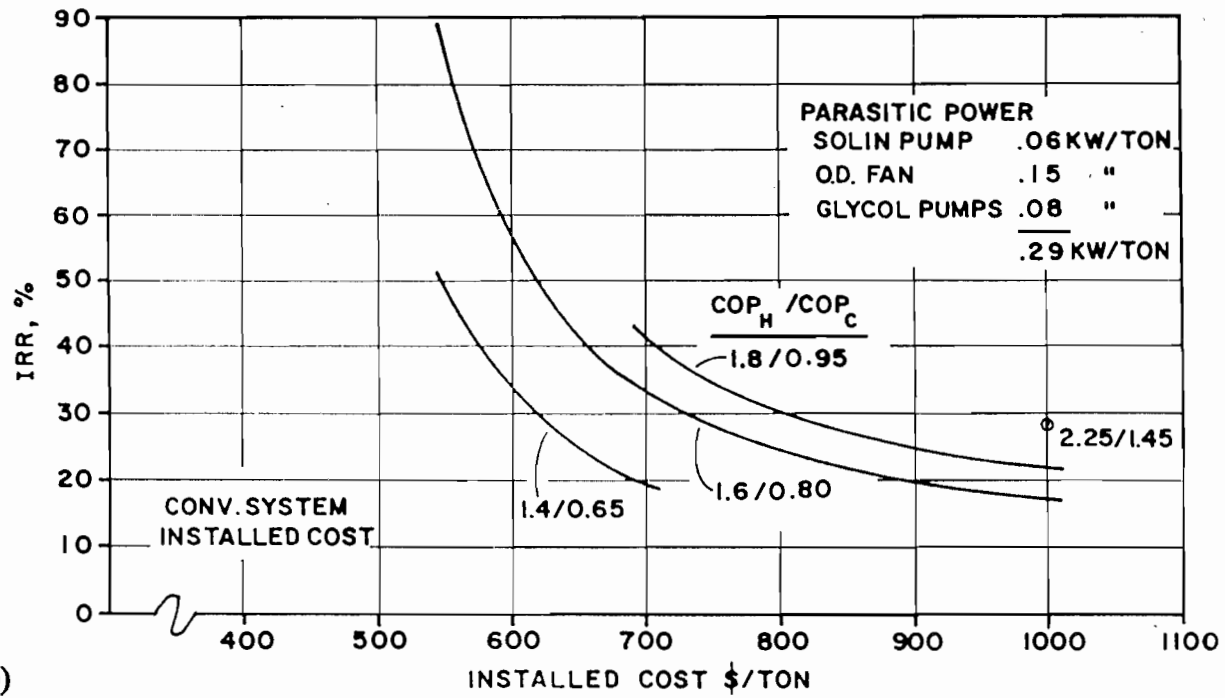
- The primary operating-cost savings result from less gas consumption by absorption heat pumps during the heating season. Thus, the economics of absorption heat pumps will improve as the cost of gas increases and will be related primarily to the cost of gas rather than to the relative cost of gas and electricity.

The results of a parametric study for the Chicago location are shown in Figure 24. SPB and IRR are plotted vs. installed cost in \$/ton for various efficiency levels. These curves can be used to set cost goals for a given efficiency level.

The effects of geographic location on the economics of the ABS4 system are illustrated in Table 34, which shows that the economics are marginal in New York and probably are not widely acceptable in Atlanta. The reason for this is that in warmer climates more gas is burned during the summer, and less gas is saved during the winter, which suggests that a system with a higher cooling COP likely will be required in warmer climates. Although a TRACE run was not made for the ABS20 system in Atlanta, an approximate calculation indicates that the SPB for the ABS20 system would be less than 5 years there.



(a)



(b)

Fig. 24. (a) Simple payback period and (b) internal rate of return obtained from parametric study.

Table 34. Summary of trace runs

Basis: Apartment building in various locations, all having the same (Commonwealth Edison) energy price structure.

Parameters		Run No.					
		9-1	9-2	10-1	10-2	11-1	11-2
Input Data	Weather (location)	Chicago	Chicago	New York	New York	Atlanta	Atlanta
	System	conv.	ABS4	conv.	ABS4	conv.	ABS4
	Heating COP, 47°F	0.8	1.61	---	1.61	---	1.61
	Heating COP, 17°F	0.8	1.37	---	1.37	---	1.37
	Cooling COP, 95°F	3.0	0.80	---	0.80	---	0.80
	Cooling COP, 115°F	---	0.64	---	0.64	---	0.64
	Cost, \$/ton	490	678	490	678	490	678
	Parasitic power, kW	---	0.283	---	0.283	---	0.283
	sol'n pump	---	0.053	---	0.053	---	0.053
	O.D. fan	0.14	0.15	---	0.15	---	0.15
	glycol pumps	0.04	0.08	---	0.08	---	0.08
size, tons cooling	155	155	163	163	161	161	
Output Data	Ann. elec. consump., 103 kW/h	1022	1017	1045	1029	1071	1021
	Ann. gas consump., 103 therms	83.1	64.5	66.6	56.3	52.2	52.3
	Elec. cost, energy, 103 \$	50.5	49.3	51.5	49.8	52.6	49.5
	Elec. cost, demand 103 \$	15.0	12.9	14.4	13.0	15.7	12.8
	Gas cost, 103 \$	45.7	35.5	36.6	31.0	28.7	28.8
	Total utility cost, 103 \$	111.2	97.7	102.5	93.8	97.1	91.2
	SPB, years	---	2.2	---	4.3	---	6.5
	IRR, %	---	37.2	---	22.6	---	15.2

IX. CONCLUSIONS

The primary conclusions of this program to date are as follows:

1. The gas-fired absorption heat pump can be an attractive heating/cooling alternative in the commercial market. The economics look best in areas that have high heating loads.
2. The economics of the commercial gas-fired absorption heat pump will improve as the cost of gas increases, at least to the point at which an all-electric system shows lower operating costs in northern climates.
3. Compared to the conventional electric chiller/gas boiler system used as the reference system in this study, the gas-fired absorption heat pump accomplishes the DOE's goal of conserving energy, and it provides much more balanced loads for both electric and gas utilities.
4. The preferred absorption cycle for commercial gas-fired heat pumps contains the following efficiency enhancement features:
 - generator heat exchange/absorber generator heat exchange,
 - absorber/generator heat exchange,
 - regeneration, and
 - a resorption/desorption circuit to replace the conventional condenser/evaporator circuit.
5. The preferred fluid at this point appears to be the ternary mixture $\text{NH}_3/\text{H}_2\text{O}/\text{LiBr}$, with $\text{CH}_3\text{NH}_2/\text{H}_2\text{O}/\text{LiBr}$ as a possible alternative. The preferred binary mixture is $\text{NH}_3/\text{H}_2\text{O}$.

INTERNAL DISTRIBUTION

- | | | | |
|-----|-----------------|--------|-------------------------------|
| 1. | V. D. Baxter | 17. | R. W. Murphy |
| 2. | R. S. Carlsmith | 18. | D. E. Reichle |
| 3. | F. C. Chen | 19. | C. K. Rice |
| 4. | G. E. Courville | 20. | M. W. Rosenthal |
| 5. | F. A. Creswick | 21. | J. R. Sand |
| 6. | R. C. DeVault | 22. | R. B. Shelton |
| 7. | P. D. Fairchild | 23. | J. A. Shonder |
| 8. | S. K. Fischer | 24. | J. N. Stone |
| 9. | W. Fulkerson | 25. | T. A. Stone |
| 10. | M. A. Hensley | 26. | E. A. Vineyard |
| 11. | P. J. Hughes | 27. | A. Zaltash |
| 12. | M. A. Kuliasha | 28-29. | Laboratory Records Department |
| 13. | W. P. Levins | 30. | Laboratory Records-RC |
| 14. | V. C. Mei | 31. | ORNL Patent Office |
| 15. | W. A. Miller | 32-33. | Central Research Library |
| 16. | W. R. Mixon | 34. | Document Reference Section |

EXTERNAL DISTRIBUTION

- 35-36. M. Aizawa, Refrigerating-Heating Equipment and System, Design Department, Tsuchiura Works, Hitachi, Ltd., 603, Kandatsumachi, Tsuchiura-shi, Ibaraki-ken, 300 Japan
- 37-38. K. Akagi, Research Center, Osaka Gas Company, Ltd., 6-19-9, Torishima, Konohana-Ku, Osaka, 554 Japan
39. L. F. Albright, School of Chemical Engineering, Purdue University, Chemical and Metallurgical Engineering Building, West Lafayette, IN 47907
40. G. Alefeld, Physik-Department, Technische Universitat Munchen, James-Frank-Strasse, D-8046 Garching b. Munchen, Federal Republic of Germany
41. D. A. Ball, Battelle Columbus Laboratories, 505 King Avenue, Columbus, OH 43201-2693
42. J. Bassols, Rendamax BV, Hamstraat 76, P.O. Box 1035, 6460 BA Kerkrade, The Netherlands
43. F. Bawel, Dometic, P.O. Box 3792, Evansville, IN 47736
44. M. Behar, Agence Francaise pour la Maitrise, de l'Energie, Route des Lucioles, 06565 Valbonne Cedex, France
45. J. Berghmans, Universiteit Leuven, Instituut Mechanica, Celestynen Laan 300A, B-3030 Heverlee, Belgium

46. T. Berntsson, Chalmers University of Technology, S-41296 Gothenburg, Sweden
47. W. J. Biermann, 45 Foxcroft Drive, Fayetteville, NY 13066
48. H. Bjurstrom, Studsvik AB, S-61182 Nykoping, Sweden
49. H. Bokelmann, GEA GmbH, R&D Department, Reisingstrasse 9, D-4630 Bochum, Federal Republic of Germany
50. U. Bonne, Honeywell Corporate Technology Center, 10701 Lyndale Avenue South, Boomington, MN 55420
51. I. Borde, The Institutes for Applied Research, Ben-Gurion University of the Negev, P.O. Box 1025, Beer-Sheva 84110, Israel
52. M. Boulanger, Centre de Recherche Industrielle du Quebec, 333, rue Franquet, Case postale 9038, Sainte-Foy (Quebec) Canada G1V 4C7
53. J. W. J. Bouma, Novem, Postbus 17, 6130 AA Sittard The Netherlands
54. B. G. Buchanan, Computer Science Department, University of Pittsburgh, 206 Mineral Industries Building, Pittsburgh, PA 15260
55. R. Bugarel, Institut de Genie Chimique, Chemin de la Loge, Toulouse Cedex, France
56. J. M. Calm, P. O. Box 12014, Arlington, VA 22209-0014
57. J. Cheron, Direction de Recherche, Physico-chimie appliquee et analyse, Institut Francais du Petrole, 1 and 4 avenue de Bois-Preau BP 311, 92506 Rueil Malmaison Cedex, France
58. R. Cohen, Ray W. Herrick Laboratories, Purdue University, West Lafayette, IN 47907
59. D. D. Colosimo, Mechanical Technology, Inc., 968 Albany-Shaker Road, Latham, NY 12110
60. P. O. Danig, Technical University of Denmark, Refrigeration Laboratory, DTH 402B, DK-2800 Lyngby, Denmark
61. K. Davidson, Gas Research Institute, 8600 West Bryn Mawr Avenue, Chicago, IL 60631
62. A. C. DeVuono, Battelle, Columbus Division, 505 King Avenue, Columbus, OH 43201-2693
63. D. A. Didion, National Institute of Standards & Technology, CBT, Gaithersburg, MD 20899
64. W. Dolan, Gas Research Institute, 8600 West Bryn Mawr Avenue, Chicago, IL 60631

65. D. C. D'Zurko, Research, Development and Demonstration, Suite 428, 500 Fifth Avenue, New York, NY 10110
66. J. Engelhard, M.A.N., Neue Technologie, Dachauer Strasse 667, 8000 München 50, Federal Republic of Germany
67. D. C. Erickson, Energy Concepts Co., 627 Ridgely Ave., Annapolis, MD 21401
68. M. Falek, Gas Energy Inc., 166 Montague Street, Brooklyn, NY 11201
69. R. J. Fiskum, CE-422, 5H-048/FORS, U.S. Department of Energy, Washington, DC 20585
70. S. Freedman, Gas Research Institute, 8600 West Bryn Mawr Avenue, Chicago, IL 60631
71. C. E. French, Gas Research Institute, 8600 West Bryn Mawr Avenue, Chicago, IL 60631
72. P. E. Frivik, SINTEF-N.TH., Division Refr. Eng., N-7034 Trondheim, Norway
73. A. Gac, Institute International du Froid, 177, Boulevard Malesherbes, F 75017 Paris, France
74. B. Genest, Direction des Etudes et de Recherches Nouvelles, Centre D'Essais et des Recherches sur les Utilisations du Gaz, Gaz de France, 361 Avenue du President Wilson BP 33, 93211 LaPlaine Saint-Denis Cedex, France
75. P. V. Gilli, Technische Hochschule in Graz, Inffeldgasse 25, A-8010 Graz, Austria
76. T. Gilles, Lennox Industries Incorporated, P.O. Box 799900, Dallas, TX 75379-9900
77. J. C. Goldsmith, CE-332, 5H-041/FORS, U.S. Department of Energy, Washington, DC 20585
78. E. Granryd, Royal Institute of Technology, Department of Applied Thermodynamics and Refrigeration, S-100-44 Stockholm, Sweden
79. G. Grossman, Technion Institute of Technology, Faculty of Mechanical Engineering, Haifa 32000, Israel
80. M. E. Gunn, U.S. Department of Energy, CE-12/FORS, Washington, DC 20585
81. H. Halozan, Graz University of Technology, Inffeldgasse 25, A-8010 Graz, Austria
82. W. T. Hanna, Battelle Columbus Laboratories, 505 King Avenue, Columbus, OH 43201-2693

83. J. R. Harnish, Central Environmental Systems, York International Corporation, P.O. Box 1592-191B, York, PA 17405-1592
84. P. Hay, PLE-PBE, KFA-Julich GmbH, Postfach 1913, D-5170 Jülich, Federal Republic of Germany
85. K. E. Herold, Department of Mechanical Engineering, University of Maryland, College Park, MD 20742
86. K. E. Hickman, York International Corporation, P.O. Box 1592-191A, York, PA 17405-1592
87. A. Hirsch, Midwest Research Institute, 5109 Leesburg Pike, Suite 414, Falls Church, VA 22041
88. D. L. Hodgett, Chemical & Process Industries Division, Electricity Research & Development Centre, Capenhurst Chester, UK CH1 6ES
89. K. Holzapfel, Joseph Haydn Str. 29, D-7524 Ostringen, Federal Republic of Germany
90. P. Iedema, FDO Technische Adviseurs, P.O. Box 194, 7550 AD Hengelo, The Netherlands
91. Y. Igarashi, Heat Pump Technology Center of Japan, Asuma-Shurui Bldg. 2-9-11, Kanda-Awajicho, Chiyoda-ku, Tokyo 100, Japan
92. H. M. Ingram, Udall Center for Studies in Public Policy, The University of Arizona, 803/811 East First Street, Tucson, AZ 85719
93. N. Inoue, Ebara Corporation, Refrigeration Products & Systems Division, 2-1 Hon Fujisawa 4-chome, Fujisawa-shi 251, Japan
94. N. Isshiki, Nihon University, Koriyama 963, Japan
95. P. Joyner, Electric Power Research Institute, P.O. Box 10412, Palo Alto, CA 94303
96. T. Kapus, Building Equipment Division, CE-422, 5H-048/FORS, U.S. Department of Energy, Washington, DC 20585
97. T. Kashiwagi, Dept. of Mech. Systems Engrg., Tokyo University of Agriculture & Technology, 24-16, Nakamachi 2-chome, Koganei, Tokyo 184, Japan
98. H. Kawamoto, Gas Utilization Development Center, Osaka Gas Company Ltd., 3-2-95 Chiyosaki, Nishi-Ku, Osaka 550, Japan
99. A. Kawata, Takasago Research & Development Center, Mitsubishi Heavy Industries, Ltd., 2-1-1, Shinhama, Arai-Cho, Takasago, Hyogo Pref. 676 Japan

100. K. Kazmer, Gas Research Institute, 8600 West Bryn Mawr Avenue, Chicago, IL 60631
101. J. U. Keller, Institut für Fluid-und-Thermodynamik, Universität Siegen, Postfach 101240, 5900 Siegen, Federal Republic of Germany
102. S. A. Klein, University of Wisconsin, Mechanical Engineering Department, Madison, WI 53706
103. G. Knobbout, TNO-MT, Laan van Westenenk 501, 7334 DT Apeldoorn, Netherlands
104. K. F. Knoche, Lehrstuhl für Technische Thermodynamik, RWTH Aachen, Schinkelstrasse 8, 5100 Aachen, Federal Republic of Germany
105. S. Kurosawa, Research Department, Advanced Cogeneration Technology Research Association, 9-6 Shinbashi 6 Chome, Minato-Ku, Tokyo, Japan
106. A. Lannus, Electric Power Research Institute, P.O. Box 10412, Palo Alto, CA 94303
107. Z. Lavan, Department of Mechanical Engineering, Illinois Institute of Technology, Chicago, IL 60616
108. P. LeGoff, Laboratoire des Sciences du Génie Chimique, CNRS-ENSIC-INPL-Nancy, France
109. T. A. Lott, Research and Development Department, Electric Power Research Institute, 3400 Crow Canyon Road, San Ramon, CA 94583
110. I. R. G. Lowe, NRC-Canada, Bldg. R.105, Montreal Rd., Ottawa K1A 0R6 Canada
111. B. Lundquist, Swedish Council for Building Research, St. Goransgatan 66, S-11233 Stockholm, Sweden
112. C. D. MacCracken, Calmac Manufacturing Corporation, 101 West Sheffield Avenue, P. O. Box 710, Englewood, NJ 07631
113. R. A. Macriss, Phillips Engineering Company, 721 Pleasant Street, St. Joseph, MI 49085
114. W. Malewski, Borsig GmbH, Berlinerstr. 27/33, D-1000 Berlin, Federal Republic of Germany
115. A. Manago, Research Center, Osaka Gas Company, Ltd., 6-19-9, Torishima, Konohana-Ku, Osaka, 554 Japan
116. J. Marsala, Gas Research Institute, 8600 West Bryn Mawr Ave., Chicago, IL 60631
117. K. Mashimo, Sanyo Electric Company, Ltd., 180 Sakata Oizumi, Ora Gunma 370-05, Japan

118. K. Matsuo, Mechanical Engineering Research Laboratory, Hitachi, Ltd., Tsuchiura, Japan
119. L. A. McNeely, 7310 Steinmeier Drive, Indianapolis, IN 46250
120. B. Meckel, Westfälische Ferngas - AG, Kampstr. 49, Postfach 495, 4600 Dortmund 1, Federal Republic of Germany
121. G. Melikian, United Technology Research Center, East Hartford, CT 06108
122. M. S. Menzer, Air Conditioning and Refrigeration Institute, 1501 Wilson Boulevard, Arlington, VA 22209
123. F. Meunier, Laboratoire de Thermodynamique des Fluides, CNRS, Campus Universitaire-Bat 502 Ter., 91405 Orsay Cedex, France
124. J. Mezon, Direction des Etudes et de Recherches Nouvelles, Centre d'Essais et des Recherches sur les Utilisations du Gaz, Gaz de France, 361 Avenue du President Wilson BP 33, 93211 LaPlaine Saint-Denis Cedex, France
125. J. P. Millhone, U.S. Department of Energy, CE-13, 6A-081/FORS, Washington, DC 20585
126. J. M. Miriam, Utilization Efficiency Division, Watson House, British Gas Corporation, Peterborough Road, London, SWG 3HN, England
127. E. Miura, Heat Pump Technology Center of Japan, Azuma Shurui Bldg., 9-11, Kandaawaji-cho 2-chome, Chiyoda-ku, Tokyo 101, Japan
128. H. Moriyama, Agency of Industrial Science & Technology/MITI, 1-3-1 Kasumigaseki, Chiyoda-ku, Tokyo 100, Japan
129. F. Moser, Institut für Verfahrenstechnik, Technische Universität Graz, Inffeldgasse 25, A-8010 Graz, Austria
130. H. P. Muhlmann, Ruhrgas AG, Halterner Strasse 125, 427 Dorsten, Federal Republic of Germany
131. K. P. Murphy, Allied-Signal, P.O. Box 1087 R, Morristown, NJ 07960
132. G. H. Myers, Gas Research Institute, 8600 West Bryn Mawr Avenue, Chicago, IL 60631
133. S. Nagamatsu, Agency of Industrial Science & Technology, M.I.T.I., 1-3-1, Kasumigaseki, Chiyoda-Ku, Tokyo, Japan
134. Y. Nagaoka, Manager, Heat Pump Systems, Gas Utilization Group, Research and Development Institute, 16-25 Shiobaura, 1-chome, Minato-Ku, Tokyo, 105, Japan

135. S. I. Nakatsugawa, Air Conditioning Research and Development Laboratories, Yazaki Corporation, 1370 Koyasu-Cho Hamamatsu-Shi, Shizuoka-PRF Japan
136. S. Nakayama, AIST Ministry of International Trade & Industry, 1-3-1 Kasumigaseki, Chiyoda-ku, Tokyo, Japan
137. T. Nakayama, Air Conditioning Headquarters, Sanyo Electric Co., Ltd., 180, Sakata Oizumi-Machi, Ora-Gun, Gunma, Japan
138. M. Naradoslawsky, Institut fur Verfahrenstechnik, A-8010 Graz, Inffeldgasse 25, 9ustria
139. N. Nishiyama, Research and Development Institute, 16-25, Shibaura, 1-Chome, Minato-Ku, Tokyo, 105, Japan
140. D. L. Noreen, Research, Development and Demonstration, Brooklyn Union gas, One MetroTech Center, Brooklyn, NY 11201
141. U. Nowaczyk, Institut fur Angewandte, Universitat Essen, Universitat Strasse 15, Postfach 6843, D-4300 Essen 1, Federal Republic of Germany
142. A. J. Occhionero, American Gas Cooling Center, 1515 Wilson Boulevard, Arlington, VA 22209
143. T. Ohuchi, Mechanical Engineering Research Laboratory, Hitachi, Ltd., 502, Kandatsu-machi, Tsuchiura-shi, Ibaraki-ken, 300 Japan
144. K. Ooka, Engineering Department-I, Kawasaki Heavy Industries, Ltd., 1-1, Higashikawasaki-Cho 3-Chome, Chuo-Ku, Kobe 650-91 Japan
145. M. Otake, Takasago Research & Development Center, Mitsubishi Heavy Industries, Ltd., 2-1-1, Shinhama, Arai-Cho, Takasago, Hyogo Pref. 676 Japan
146. E. Ozaki, Central Research Laboratory, Mitsubishi Electric Corporation, 1-1, Tsukaguchi-Honmachi 8-Chome, Amagasaki, Hyogo, 661 Japan
147. D. Pellish, CE-332, 5H-041/FORS, U.S. Department of Energy, Washington, DC 20585
148. H. Perez-Blanco, 314 Mechanical Engineering Building, Pennsylvania State University, University Park, PA 16802
149. S. Petty, Columbia Gas System Service Corporation, 1600 Dublin Road, P.O. Box 2318, Columbus, OH 43215
150. B. A. Phillips, Phillips Engineering Company, 721 Pleasant Street, St. Joseph, MI 49085
151. B. Plzak, Refrigeration Systems Division, The Trane Company, 3600 Pammel Creek Road, LaCrosse, WI 54601-7599

152. R. Radermacher, University of Maryland, Mechanical Engineering Department, College Park, MD 20742
153. W. Raldow, Swedish National Board for Technical Development, Box 43200, 100 72 Stockholm, Sweden
154. J. Rasson, Lawrence Berkeley Laboratory, 1 Cyclotron Road, Berkeley, CA 94720
155. V. Recchi, National Research Council-PFE 2, c/o O.T.B., P.O. Box 330, I-70100 Bari, Italy
156. R. C. Reimann, Carrier Corporation, 6304 Carrier Parkway, P.O. Box 4800, Syracuse, NY 13221
157. G. M. Reistad, Department of Mechanical Engineering, Oregon State University, Corvallis, OR 97331
158. H. H. Rhea, Lennox Industries, Inc., P.O. Box 877, Carrollton, TX 75006
159. U. Rockenfeller, Rocky Research, 674 Wells Road, Boulder City, NV 89005
160. A. Rojey, Direction de Recherche, Physico-chimie appliquee et analyse, Institut Francais du Pétrole, 1 and 4 avenue de Bois-Preau BP 311, 92506 Rueil Malmaison Cedex, France
161. J. D. Ryan, CE-422, 5H-048/FORS, U.S. Department of Energy, Washington, DC 20585
162. W. A. Ryan, Gas Research Institute, 8600 West Bryn Mawr Avenue, Chicago, IL 60631
163. T. Saito, The University of Toyko, Department of Mechanical Engineering, 7-3-1 Hongo, Bunkyo, Tokyo 114, Japan
164. N. Sawada, Sanyo, 180, Sakata Oizumi-Machi, Ora-Gun, Gunma, Japan
165. U. Schaerer, Swiss Federal Office of Energy, CH-3003 Bern, Switzerland
166. J. Scharfe, Physik Dept. E19, T.U. Muenchen-Garching, D.-8046 Muenchen Garching, Federal Republic of Germany
167. P. Scheihing, CE-141, 5G-067/FORS, U.S. Department of Energy, Washington, DC 20585
168. E. L. Schmidt, Institut für Angewandte, Thermodynamik und Klimatechnik, Universität Essen, Universität Strasse 15, Postfach 6843, D-4300 Essen 1, Federal Republic of Germany
169. T. Setoguchi, 107 Mechanical Engineering Building, Pennsylvania State University, University Park, PA 16802

170. F. Setterwall, The Royal Institute of Technology, Department of Chemical Engineering, S-100 44 Stockholm, Sweden
171. S. V. Shelton, Thermax, Inc., 296 14th Street NW, Atlanta, GA 30318
172. J. B. Shrago, Office of Technology Transfer, 405 Kirkland Hall, Vanderbilt University, Nashville, TN 37240
173. I. Smith, Applied Energy Group, School of Mechanical Engineering, Cranfield Institute of Technology, England
174. K. Snelson, National Research Council Canada, Div. of Mechanical Engineering, Montreal Road, Ottawa, Ontario K1A 0R6, Canada
175. H. O. Spauschus, Georgia Institute of Technology, Energy and Materials Sciences Laboratory, Atlanta, GA 30332
176. W. R. Staats, Gas Research Institute, 8600 West Bryn Mawr Avenue, Chicago, IL 60631
177. T. Statt, CE-422, 5H-048/FORS, U.S. Department of Energy, Washington, DC 20585
178. F. Steimle, Institut für Angewandte, Thermodynamik und Klimatechnik, Universität Essen, Universität Strasse 15, Postfach 6843, D-4300 Essen 1, Federal Republic of Germany
- 179-180. K. Stephan, Institut für Technische Thermodynamik und Thermische Verfahrenstechnik, Universität Stuttgart, Pfaffenwaldring 9, FA 1705, Postfach 1140, 7000 Stuttgart 80, Federal Republic of Germany
181. H. Stierlin, Sibir AG, Munohwiesen 5, Postfach 362, CH-8952 Schlieren, Switzerland
182. Y. Sumida, Energy Science & Technology Department, Central Research Laboratory, Mitsubishi Electric Corporation, 1-1, Tsukaguchi-Honmachi 8-Chome, Amagasaki, Hyogo, 661 Japan
183. P. Swenson, Consolidated Natural Gas, CNG Tower, Pittsburgh, PA 15222-3199
184. H. Takenouchi, Technology Research Association of Super Heat Pump Energy Accumulation System, Takara Bldg., 1-6 Kanda-Ogawamachi, Chiyodaku, Toyko, Japan
185. W. E. Tomala, Research, Development, and Demonstration, Brooklyn Union Gas, One MetroTech Center, Brooklyn, NY 11201
186. C. Trepp, Eidgenössische Technische Hochschule, Institut für Verfahrens und Kaltechnik, ETH-Zentrum, 8092 Zurich, Switzerland

187. T. Uemura, Kansai University, Faculty of Engineering, Senriyama, Suita, Osaka, 564 Japan
188. D. Uselton, Lennox Industries, Inc., P.O. Box 877, Carrollton, TX 75011-0877
189. H. van der Ree, TNO-MT, Laan van Westenenk 501, NL-7334 DT Apeldoorn, The Netherlands
190. S. A. Vitale, Research, Development and Demonstration, Brooklyn Union Gas, One MetroTech Center, Brooklyn, NY 11201
191. G. C. Vliet, Taylor Hall 116, The University of Texas, Austin, TX 78712
192. M. Wahlig, Lawrence Berkeley Laboratory, 1 Cyclotron Road, Berkeley, CA 94720
193. K. Watanabe, Department of Mechanical Engineering, Keio University, 3-14-1, Hiyoshi, Kohoku-Ku, Yokohama 223, Japan
194. W. H. Wilkinson, Battelle Columbus Laboratories, 505 King Avenue, Columbus, OH 43201-2693
195. M. Williams, Department of Economics, Northern Illinois University, DeKalb, IL 60115
196. B. D. Wood, College of Engineering and Applied Science, Arizona State University, Tempe, AZ 85281
197. W. M. Worek, Department of Mechanical Engineering (M/C 251), 2055 Engineering Research Facility, Box 4348, Chicago, IL 60680
198. T. Yoshie, Appliance and Installation R&D Dept., Tokyo Gas Co., Ltd., 5-20 Kaigan 1-Chome, Minato-Ku, Tokyo 105, Japan
199. T. Yoshii, Mitsubishi Heavy Industries, Ltd., 5-1, Marunouchi 2-chome, Chiyoda-ku, Tokyo, Japan
200. T. Zawacki, Phillips Engineering Company, 721 Pleasant Street, St. Joseph, MI 48095
201. P. Zegers, Commission of the European Communities, Directorate General XII, Wetstraat 200, B-1049 Brussel, Belgium
202. Office of the Assistant Manager for Energy R&D, U.S. Department of Energy, Oak Ridge Operations, Oak Ridge, TN 37831
- 203-212. Technical Information Center, Department of Energy, P.O. Box 62, Oak Ridge, TN 37831